AD-A045 511 NAVAL WEAPONS CENTER CHINA LAKE CALIF F/G 11/6
COSO GEOTHERMAL CORROSION STUDIES.(U)
OCT 77 S A FINNEGAN
UNCLASSIFIED NWC-TP-5974 NL

1 OF 1
ADA045511

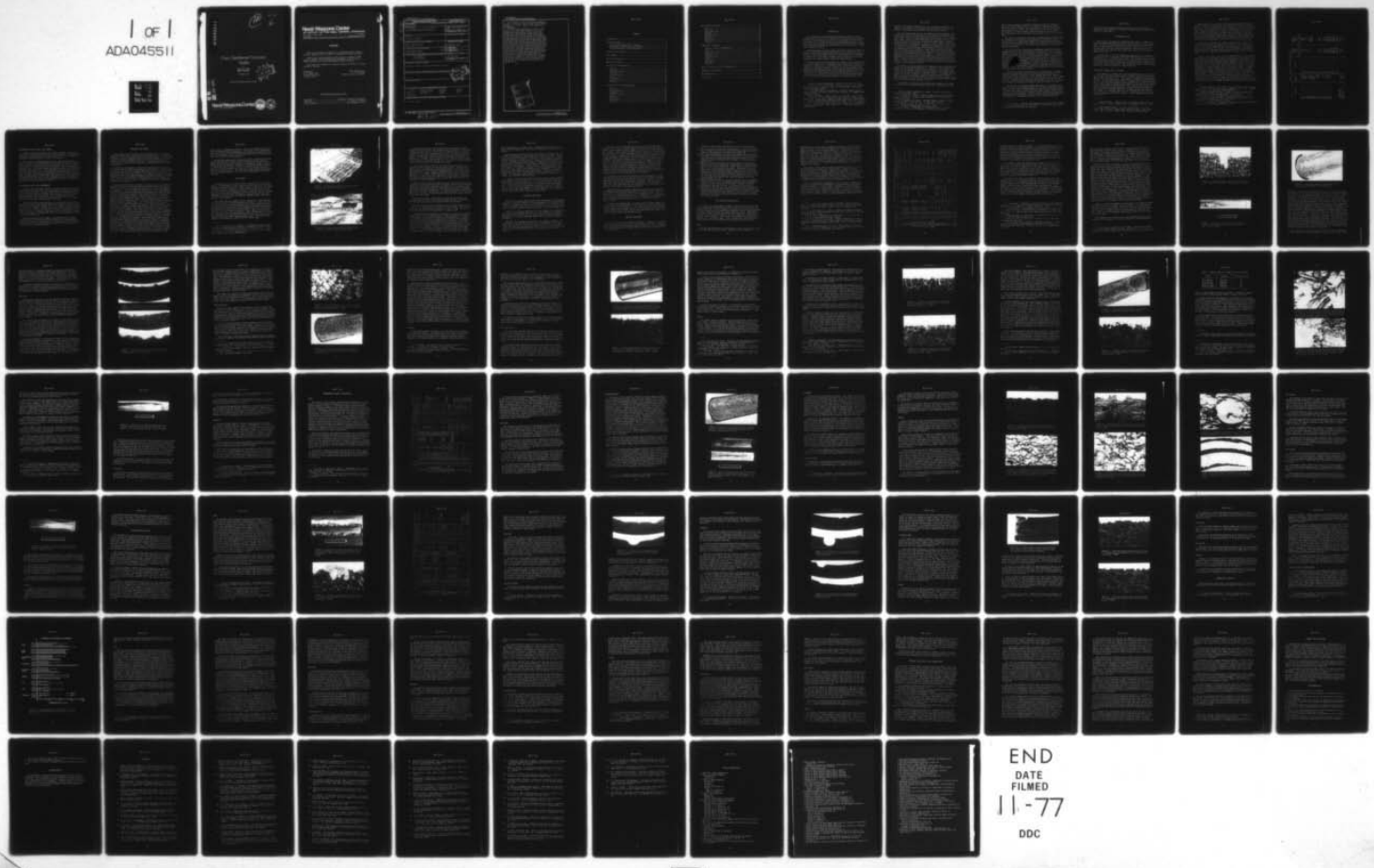

END
DATE FILMED
11-77
DDC

NWC TP 5974

Coso Geothermal Corrosion Studies

by
Stephen A. Finnegan
Research Department

OCTOBER 1977

Naval Weapons Center
CHINA LAKE, CALIFORNIA 93555

Naval Weapons Center

AN ACTIVITY OF THE NAVAL MATERIAL COMMAND

W. L. Harris, Jr., RAdm., USN ..... Commander
R. M. Hillyer ..... Technical Director (Acting)

FOREWORD

This report documents one phase of a continuing research program at the Naval Weapons Center in support of geothermal corrosion problems.

These studies were supported by Work Request No. N68305-77-70029 from Pt. Hueneme, and were conducted by personnel of the Detonation Physics Division and the Navy Postgraduate School, Monterey.

This report was reviewed for technical accuracy by Gilbert F. Kinney and Carl F. Austin.

Released by
E. B. ROYCE, *Head*
Research Department
1 October 1977

Under authority of
R. M. HILLYER
Technical Director (Acting)

NWC Technical Publication 5974

Published by.....Technical Information Department
Collation.....Cover, 44 leaves
First printing.....160 unnumbered copies

UNCLASSIFIED

SECURITY CLASSIFICATION OF THIS PAGE (When Data Entered)

REPORT DOCUMENTATION PAGE

READ INSTRUCTIONS BEFORE COMPLETING FORM

1. REPORT NUMBER: NWC-TP-5974	2. GOVT ACCESSION NO.
3. RECIPIENT'S CATALOG NUMBER	
4. TITLE (and Subtitle): COSO GEOTHERMAL CORROSION STUDIES.	5. TYPE OF REPORT & PERIOD COVERED: Final report.
6. PERFORMING ORG. REPORT NUMBER	
7. AUTHOR(s): Stephen A. Finnegan	8. CONTRACT OR GRANT NUMBER(s)
9. PERFORMING ORGANIZATION NAME AND ADDRESS: Naval Weapons Center, China Lake, CA 93555	10. PROGRAM ELEMENT, PROJECT, TASK AREA & WORK UNIT NUMBERS: WR N68305-77-70029
11. CONTROLLING OFFICE NAME AND ADDRESS: Naval Weapons Center, China Lake, CA 93555	12. REPORT DATE: October 1977
	13. NUMBER OF PAGES: 86
14. MONITORING AGENCY NAME & ADDRESS (if different from Controlling Office): 89p.	15. SECURITY CLASS. (of this report): UNCLASSIFIED
	15a. DECLASSIFICATION/DOWNGRADING SCHEDULE

16. DISTRIBUTION STATEMENT (of this Report)

Approved for public release; distribution unlimited.

17. DISTRIBUTION STATEMENT (of the abstract entered in Block 20, if different from Report)

18. SUPPLEMENTARY NOTES

19. KEY WORDS (Continue on reverse side if necessary and identify by block number)

Corrosion	Hydrogen sulfide	Cast iron	Plastics
Geothermal	Stainless steel	Aluminum	Steam
Steel	Hot water	Copper	Zinc
Acid sulfate			

20. ABSTRACT (Continue on reverse side if necessary and identify by block number)

See back of form.

DD FORM 1 JAN 73 1473 EDITION OF 1 NOV 65 IS OBSOLETE
S/N 0102-014-6601

UNCLASSIFIED
SECURITY CLASSIFICATION OF THIS PAGE (When Data Entered)

403 019

LB

Coso Geothermal Corrosion Studies by Stephen A. Finnegan. China Lake, Calif., Naval Weapons Center, October 1977. 86 pp. (NWC TP 5974, publication UNCLASSIFIED.)

(U) This report documents the results of geothermal corrosion studies conducted at the Coso Thermal Area, Naval Weapons Center, China Lake, California. Nine different common construction-grade piping materials were tested for periods up to about one year in three distinctive low-pressure, medium temperature environments (acid-sulfate steam, groundwater-diluted steam, and hot mineralized alkaline water) under anaerobic and aerobic conditions. Exposed specimens were analyzed principally by optical microscopy and X-ray diffraction techniques, and selectively by scanning electron microscopy, X-ray fluorescence, and atomic absorption spectroscopy. Corrosion/erosion modes, rates, and principal insoluble corrosion products were established and mechanisms based on established theory proposed to account for the modes of deterioration. Corrosion results were compared for the three fluid systems, and specific materials were then recommended for use in each of the fluid types found at the Coso Thermal Area.

CONTENTS

INTRODUCTION

Large quantities of heat energy are known to be stored in near-surface regions of the earth's crust where recent volcanism or intrusive activity has taken place. In view of the increasing costs and demand for energy, and in consideration for the nonrenewable nature of fossil fuels, an increasing level of interest has been shown recently in using these geothermal resources for such purposes as the production of power and for municipal heating.

Geothermal energy is often found in the form of medium-to-high temperature, pressurized fluids contaminated with a wide variety of entrapped, dissolved and undissolved, solid and gaseous matter—depending on the geologic environment. Different kinds and levels of contamination result in a wide range of highly acidic to highly alkaline fluid conditions that differ greatly in chemical aggressiveness.

As these fluids cool and pressures are reduced, the precipitation of dissolved solids occurs. The agglomeration of these often results in the formation of complex scale. Utilizing these fluids then creates some complex, interrelated corrosion, erosion, and scaling problems within gathering, distributing, storage, and energy conversion installations depending on the chemistry of the fluids and the characteristics of the installation.[1-4] The condensation of corrosive vapors previously released into the atmosphere as a by-product of these processes results in the deterioration of external surfaces of the installation, plus

---

[1] Lawrence Livermore Laboratory. *Possibilities for Controlling Heavy Metal Sulfides in Scale From Geothermal Brines*, by D. D. Jackson and John H. Hill. Livermore, Calif., 19 January 1976. (UCRL-51977, publication UNCLASSIFIED.)

[2] T. Marshall and W. R. Braithwaite. "Corrosion Control in Geothermal Systems," *Geothermal Energy (Earth Sciences, 12)*, UNESCO, Paris (1973), pp. 151-60.

[3] Bureau of Mines. *Corrosion Resistance of Metals in Hot Brines: A Literature Review*, by Lloyd H. Banning and Laurance L. Oden. Washington, D.C., August 1973. (BuMines IC 8601, publication UNCLASSIFIED.)

[4] Idaho National Engineering Laboratory, ERDA. *Corrosion Engineering in the Utilization of the Raft River Geothermal Resource*, by Richard L. Miller. Idaho Falls, Idaho, August 1976. (ANCR-1342, publication UNCLASSIFIED.)

possible environmental degradation of the surrounding landscape. In addition, the presence of toxic metals such as arsenic, antimony, and mercury in geothermal fluids present added disposal problems.

In view of the limited use of and experience with geothermal fluids to date, the selection of materials for use in these environments has been largely based on results obtained in handling other types of aggressive fluids. This selection approach may not be valid, even for chemically similar fluids, as small differences in temperature, pressure, levels and kinds of impurities, coupled with small changes in material parameters and flow conditions can result in large changes in the rate of deterioration of materials. Temperatures and pressure changes result in changes in solubilities and flow velocities that in turn can alter corrosion/erosion rates and modes. Quantities of undissolved solids carried in high-velocity fluids can cause serious erosion and erosion/corrosion problems depending on their numbers, sizes, shapes, mechanical properties, velocities, and angles of impact.[4] Pitting erosion due to impingement by water droplets in the steam varies with velocity and is enhanced by the presence of undissolved solids and gas bubbles in the fluid.[5] Changes in flow conditions can result in turbulent rather than lamellar fluid flow and in cavitation of the fluid, both of which should increase corrosion/erosion rates.[5]

The addition of minute quantities of impurities such as chloride and copper ions or hydrogen sulfide gas in a fluid can cause catastrophic failure of some materials under certain conditions. For example, only about 5 ppm of chloride ions in an aerated fluid at 50°C causes stress corrosion cracking of austenitic stainless steels.[6] A hydrogen sulfide content of 0.1 ppm can result in sulfide stress cracking of steel.[7] Small quantities of more noble metals in solution, such as copper, will initiate pitting corrosion of more active metals like aluminum by plating out on its surface to form galvanic cells.[8]

A geothermal fluid may provide one additional complication in that its characteristics might alter appreciably over long periods of time[9]

---

[5] Mars D. Fontana and Norbert D. Greene. *Corrosion Engineering*. New York, McGraw-Hill, 1967.

[6] J. A. Collins. "Effect of Design, Fabrication, and Installation on the Performance of Stainless Steel Equipment," *Corrosion*, Vol. 11 (1955), pp. 11t-18t.

[7] C. M. Hudgins, and others. "Hydrogen Sulfide Cracking of Carbon and Alloy Steels," *Corrosion*, Vol. 22 (Aug. 1966), p. 238.

[8] G. Butler and H. C. K. Ison. *Corrosion and Its Prevention in Waters*. New York, Reinhold Publishing Corp., 1966.

[9] R. S. Bolton. "Management of a Geothermal Field," *Geothermal Energy (Earth Sciences, 12)*, UNESCO, Paris (1973), pp. 175-84.

due to gradual changes in reservoir conditions under the influence of reinjection and recharge effects. For example, assuming geothermal waters are largely meteoric, the recharge rate could alter with long-term changes in the level of the water table as a result of changes in the usage rate, or else changes in weather patterns. Reinjection of waste fluids back into the reservoir may eventually alter the fluid chemistry.

The selection of materials for use in a geothermal environment, based on information established in other aggressive environments such as sea or mine water, or in processing industries or desalinization plants, should be done with great care. Similar care should be taken even when the selection process is to be based on prior experience in other geothermal environments.

In view of the wide variations in geothermal reservoir conditions, perhaps a better way to choose materials initially for use in a given installation would be to run extensive corrosion tests on all candidate materials using the same fluid condition that is expected to be encountered later on.[10] Even then, some materials selected on the basis of corrosion tests will prove unsatisfactory when used in a full-scale installation because of changes in flow conditions, fluid chemistry, design, or fabrication procedures that lead to excessive deterioration of the materials in that circumstance. However, building the installation without any prior screening of construction materials based on actual exposure to the fluid to be handled would be expected to result generally in a more protracted break-in period.

This report describes the results of a corrosion study of common, construction grade pipe materials exposed to medium-temperature, low-pressure geothermal fluids at the Coso Thermal Area, Naval Weapons Center, China Lake, California. Nine different materials, plus a sample made up of combinations of these nine were exposed to three different kinds of geothermal fluids and under oxygen-poor (anaerobic) and oxygenated (aerobic) conditions for periods of time up to about one year.

The analyses of corrosion specimens were done as a cooperative program between the Naval Weapons Center and the Naval Postgraduate School, Monterey, The former was responsible for identifying corrosion modes, for measuring corrosion rates, for identifying corrosion products principally by x-ray diffraction analyses, and for analyzing microstructures using optical metallography. The latter made detailed high-magnification analyses of topographic features found on selected corrosion

---

[10] E. Tolivia. "Corrosion Measurements in a Geothermal Environment," *Geothermics*, Special Issue 2, Vol. 2, Part 2, Pisa, Italy (Sept. 1970). United Nations, New York, pp. 1596-1601.

specimens using scanning electron microscopy and x-ray fluorescence techniques, plus analyses for mercury in corrosion deposits using atomic absorption spectrometry.

GEOTHERMAL FLUIDS

Each material was exposed to three different kinds of common low-pressure, medium-temperature geothermal fluids found at the Coso Thermal Area. Two were acid steam conditions, exhibiting different degrees of chemical aggressiveness. Both were extracted from near-surface layers located within the zone of surface oxidation. The third fluid was a medium-temperature alkaline water taken from a well drilled below the zone of oxidation.

A recent model of the Coso Thermal Area postulates the existence of a steam reservoir in the Sugarloaf Mountain-Devil's Kitchen area that is capped by a zone of altered granitic rock. The steam reservoir is shown to be bounded on the east by the major north-south trending normal fault at the Coso Resort and to the west by an unknown boundary somewhere near the eastern edge of Rose Valley. Two hot water reservoirs are postulated directly to the east and west of these boundaries.

ACID SULFATE STEAM, DEVIL'S KITCHEN

This example of a common, very corrosive geothermal steam condition[11] is located in the Devil's Kitchen Area, a highly fractured acid-sulfate/hydrothermal alteration zone.[12] This locality is topographically high, and well above the water table. The absence of recharge from underground aquifers and atmospheric precipitation, combined with a high evaporation rate in this desert environment, have resulted in the near-surface layers of the ground becoming saturated with highly acid sulfate waters from the mixing of geothermal fluids venting to the surface along fissures and oxidizing hydrogen sulfide emissions. Hydrogen sulfide and carbon dioxide gases have both been identified in steam emissions which have a pH of about 4.5. Standing pools of water or materials soaked with condensate eventually reach a pH of about 1.5, after additional oxidation takes place.[12]

---

[11] Donald E. White. "Thermal Waters of Volcanic Origin," *Bulletin of the Geologic Society of America*, Vol. 68 (December 1957), pp. 1637-57.

[12] Naval Weapons Center. *Geologic Investigations at the Coso Thermal Area*, by Carl F. Austin and J. Kenneth Pringle. China Lake, Calif., NWC, June 1970. (NWC TP 4879, publication UNCLASSIFIED.)

Surface water in this locality contains approximately 2500 ppm of dissolved solids,[12] of which silicon constitutes the major portion (see Table 1). Deposits of amorphous silica (opal) found in the Coso Thermal Area attest to its presence. The major remaining cations include aluminum, calcium, potassium, boron, magnesium and sodium, in that order. These dissolved solids mainly represent the dissolution of common minerals within the alteration zone. Mercury has also been identified in black coatings formed on copper plates exposed to fumarolic gases[13] and is expected to be present in fluids also, although the species present (elemental sulfide compound, etc.) has not been clearly established.

Acid-sulfate conditions are common in thermal areas. However, the oxidation reactions do not appear to be completely established in all cases. Recent work[14] suggests that bacterial action is a significant factor in the production of sulfuric acid in geothermal environments. The appearance of large quantities of aggressive ferric ions in these waters can also be explained principally as a result of bacterial activity.[15]

Sulfuric acid, ferric ions, plus hydrogen sulfide and carbon dioxide gases appear to be principal factors in determining the corrosiveness of this acid-sulfate environment along with temperature and pressure. As reactions can take place between oxidizing agents (ferric ions and perhaps hot sulfuric acid) and the reducing (hydrogen sulfide) gas, other oxidation states of the sulfur species may also be found in the fluid. The amount of oxygen dissolved in the fluid may be reduced or completely eliminated as it readily reacts with the hydrogen sulfide. Hydrogen sulfide can be a major problem as it causes sulfide stress cracking, hydrogen embrittlement, and delayed fracture of steel in anaerobic acid environments.[2] Mercury, if present, may be a significant factor in initiating corrosion, particularly in aluminum alloys, depending on its oxidation state.[16] Traces of copper have also been found in water samples from this area,[12] which may lead to localized corrosion of more active metals, such as aluminum, depending on the copper species present.[8]

---

[13] Bureau of Mines. *Bucket-Drilling the Coso Mercury Deposit, Inyo County, California*, by Leon W. Dupuy. Washington, D.C., 1948. (BuMines Report Invest. 4201, publication UNCLASSIFIED.)

[14] Thomas D. Brock, and Jerry L. Mosser. "Rate of Sulfuric-Acid Production in Yellowstone National Park," *Bulletin of the Geological Society of America*, Vol. 86 (February 1975), pp. 194-8.

[15] Thomas D. Brock and others. "Biogeochemistry and Bacteriology of Ferrous Iron Oxidation in Geothermal Habits," *Geochimica et Cosmochimica Acta*, Vol. 40 (1976), pp. 493-500.

[16] R. J. H. Wanhill. "Cleavage of Aluminum Alloys in Liquid Mercury," *Corrosion*, Vol. 30 (October 1974), pp. 371-8.

TABLE 1. Analyses of Typical Geothermal Fluids

Constituent	Coso water, ppm	Constituent	Devil's Kitchen, clear pool	Resort, shallow steam well
			% Residue on evaporation to dryness	
Ca	359.0	Si	10-100	10-100
Mg	0.6	Fe	...	3-30
Na	2,808.0	Al	1-10	1-10
K	172.0	Ca	.3-3	.1-1
Co_3	50.4	Mg	.1-1	.3-3
HCO_3	0.0	Na	.03-.3	.3-3
SO_4	216.0	K	.3-3	.1-1
Cl	3,681.0	Mo	...	.0003-.003
NO_3	trace	Zn	...	.003-.03
NO_2	negative	Sn	...	...
SiO_2	27.0	Co	...	...
F	1.60	Sc	...	...
B	57.42	Y	...	...
Fe	...	B	.3-3	.03-.3
Mn	...	Mn	.003-.03	.03-.3
PO_4	0.23	Ag	...	...
Cu	...	Cu	.003-.03	.01-.1
OH	76.2	Ti	.03-.3	.1-1
Br	4.67	Sr	.01-.1	.003-.03
As	0.94	Ni	.003-.03	.0003-.003
NH_4	trace	V	.001-.01	.001-.01
Hg	1.4	Pb	.001-.01	.001-.01
		Ba	.003-.03	.01-.1
		Ga	.001-.01	.001-.01
		Cr	.0003-.003	.0003-.003
		Zr	.0003-.003	.003-.03
		Be	.0003-.003	.001-.01
Total dissolved solids, ppm.	6,894.0		2,500	2,800
pH	9.8		1.5	4.5
Temp., °C	142		80	95

GROUNDWATER-DILUTED STEAM, COSO SURFACE

A mildly acid steam condition was located alongside a long, major north-south trending fault zone at the Coso Resort Area. This fault zone contains an extensive network of fractures that serves as a conduit for geothermal fluids and gases to ascend to the surface.

This locality is topographically low and, consequently, meteoric water is found at relatively shallow depths below the surface. As water moves through the Coso Resort Area in an eastward direction toward the valley floor, it dilutes and partially transports away ascending geothermal fluids. As a result, those reaching the surface are only slightly acid with a pH of about 5.[12] Steam emissions along the fault contain about the same amount and kind of dissolved solids as emissions at the Devil's Kitchen. No analyses of gas emissions in this locality have been made, although hydrogen sulfide and carbon dioxide levels are expected to be significantly lower than at Devil's Kitchen due to the influence of the migrating meteoric waters. Trace amounts of mercury were found in water samples from the Coso Resort Area.[12]

HOT ALKALINE WATER, COSO UNDERGROUND

Hot water from a 115-metre-deep well drilled in the major fault zone at the Coso Resort adjacent to the steam source described above, served as the third test fluid. This well was drilled into bedrock below the zone of surface oxidation to sample fluid conditions in the more basic environment expected at that depth. A 10-cm-diameter steel liner, slotted over its lower 15 metres was inserted into the well to insure that test fluids came from the bottom strata only.

Analyses of the well water showed it to be alkaline, with a pH of about 9.0 containing approximately 6000 ppm of dissolved solids of which 5000 ppm were sodium and chloride ions.[12] No analyses of admixed gases have been made. However, hydrogen sulfide and carbon dioxide levels are expected to be low due to dilution and transport by groundwater as discussed previously. Normally, oxygen should be virtually absent in this reducing environment, although the flow of shallow groundwater into this zone may introduce some.

Sodium-chloride brines are common in geothermal areas, are good electrolytes, and are usually fairly corrosive due to the aggressive chloride ion which is responsible for establishing localized (pitting) corrosion in many metals, plus stress corrosion cracking of austenitic stainless steel and aluminum alloys.[5]

CORROSION TEST ARRAYS

Each corrosion test facility consisted essentially of an air-tight gathering system which collected fluids and carried them to a large manifold that, in turn, distributed them to individual samples. If the fluid consisted of steam, condensate that collected on the bottom of the manifold was carried off through an air trap. Steam produced under this condition was considered to be essentially a water-saturated vapor for test purposes.

A maximum of ten samples could be tested simultaneously at each installation. Manifold ports were designed specifically for 2-inch-diameter (2 IPS) specimens of pipe, although other sizes of pipe or tubing could be attached with the aid of adapters. Each sample was connected to the manifold through an air-tight, galvanically insulated coupling, and rested horizontally on a wood-insulated V-channel supporting framework. Condensate flowed from the lower end of each sample into an open trough and from there to a storage reservoir. Figure 1 is a view of an operating corrosion test facility.

Hot water from the well was lifted to the surface using a mechanical submersible pump positioned just above the bottom, within the slotted portion of the liner. The pump was operated by a diesel-powered pump jack mounted to a steel platform at the well bore. Fluid was pumped to a 24,000-litre insulated holding tank and pressurized to about two atmospheres. The holding tank converted the uneven discharge from the well to a more uniform flow condition. This also provided for continuous flow while the pumping system was stopped for servicing or repairs in order to prevent atmospheric oxygen from entering any anaerobic test chambers from the downstream end. A series of valves between the holding tank and manifold regulated flow to the latter while a valve on each exit port of the manifold adjusted the flow to individual samples. A flow rate of 4 litres per minute per sample at a velocity of 0.3 m/s was established as optimum for this pumping system which allowed fluids to flash in the test samples. Since the test site was in a remote area, about 65 kilometres from the main laboratory, it was operated unattended most of the time requiring the pumping system to be monitored continuously. This was done with an alarm system mounted directly on the pump jack that transmitted a radio signal to a receiver located at the NWC Police Station whenever it stopped. The holding tank allowed flow to continue uninterrupted for periods up to about 24 hours while repairs were made, if it had been initially pressurized to about 2 atmospheres. Pressurizing the holding tank to significantly higher levels generally caused a runaway pressure rise in the tank, as some of the valves that were operating in a nearly closed position due to the pressure, clogged as dissolved salts precipitated on the seats due to the sudden pressure drop across them. To prevent runaway pressures, an automatic relief valve was fitted into a second exit line at the well head that would

open at about 6 atmospheres pressure. Even at two atmospheres pressure, some precipitation still took place at the control valves, lowering the flow rate, and so periodic adjustments were required to maintain uniform flow to the samples. Figure 2 is a distant view of the hot-water corrosion test facility while in operation.

The gathering systems and testing arrays were constructed of welding grade, low-carbon steel pipes, structural shapes and plate material. Junctions and joints in the flow lines were generally welded, or else flanged and bolted together. Additional flanges were welded on the lines for inserting control valves. Valves were either 300 series stainless steel or corrosion-resistant cast iron, while the holding tank was a 300 series stainless steel. The submersible pump combined 304 stainless steel, Ni-Resist austenitic iron, and corrosion/temperature-resistant fittings.

TEST SAMPLES

Test samples for the corrosion studies consisted of nine different kinds of 2-inch-diameter (2 IPS) construction grade pipe, plus a tenth "plumber's nightmare" composed of short lengths of the other nine, welded or threaded together directly or through various couplings and valves. The last specimen was designed specifically to examine galvanic corrosion and coupling effects between dissimilar materials under an anaerobic atmosphere. Pipe materials included steel and galvanized steel, 304 stainless steel, gray cast iron, 6063-T6 aluminum, copper, ABS and PVC plastics, and transite.[17]

Steel pipes were all seamless and met Schedule 40 or 80, ASTM A53/A120 specifications. The microstructure consisted of a matrix of small, equiaxed ferrite grains containing colonies of fine, lamellar pearlite. Occasional lenticular islands composed mainly of manganese sulfide and small spheroids of either silicon or aluminum oxide were found dispersed throughout the microstructure as minor phases. Both inner and outer surfaces of the pipe were covered with a thin, adherent black coating that was judged to be largely magnetite, Fe_3O_4, on the basis of its color. The hardness of the steel varied from R_B 69 to 82 in the interior while the ASTM grain size number varied between 5 and 6. The material was judged to be equivalent to SAE 1012 to 1016 carbon steel.

---

[17] C. F. Austin and J. K. Pringle. "Geothermal Corrosion Studies at the Naval Weapons Center," University of Michigan, Ann Arbor, Mich., July 1974. *Preliminary Reports, Memoranda and Technical Notes of the Materials Research Council Summer Conference, La Jolla, Calif.* (ARPA Report 005020, publication UNCLASSIFIED.)

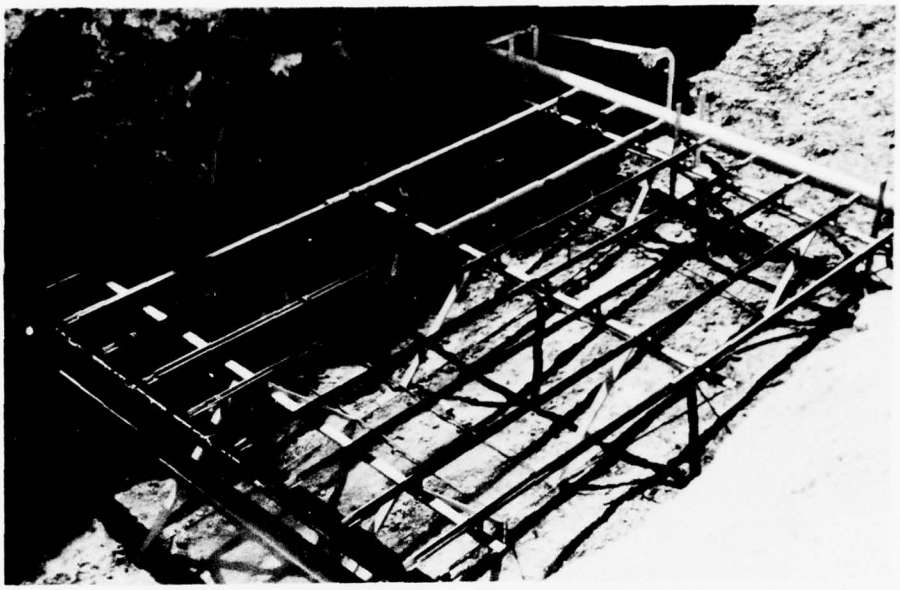

FIGURE 1. The Devil's Kitchen (Acid Sulfate Steam) Corrosion Test Facility in Operation.

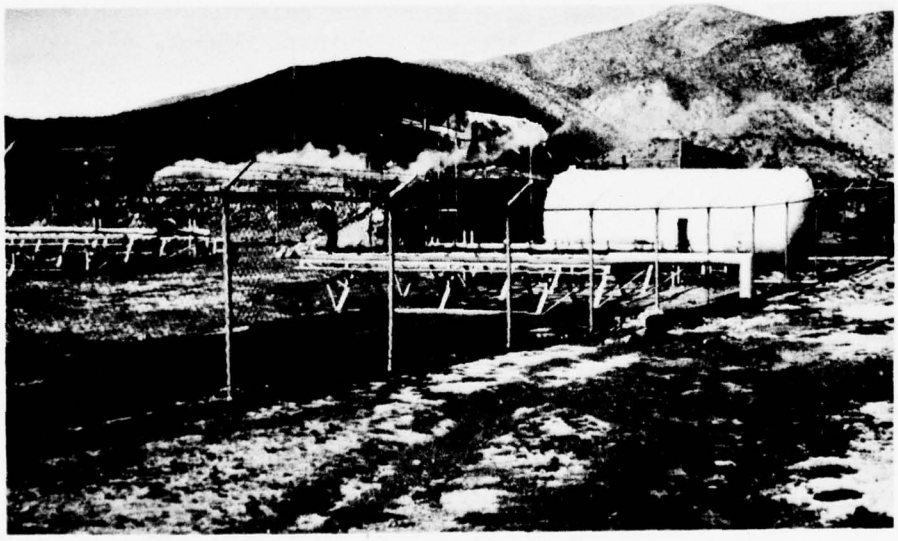

FIGURE 2. Hot-Water (Mineralized Alkaline Fluid) Corrosion Facility at the Coso Resort Area.

Galvanized steel pipes were seamless and met ASTM Grade A53/A120 Schedule 40 specifications. The microstructure consisted of fairly large, irregular-shaped grains of ferrite and fine lamellar pearlite colonies occasionally found in a Widmanstätten structure. Islands of manganese sulfide and small spheroidal precipitates were found throughout the interior. The hardness of the steel varied from R_B 58 to 68, while the ASTM grain size number varied between 4 and 5. The steel was estimated to be equivalent to SAE 1011 carbon steel. The zinc coating on both surfaces varied from 0.035 to 0.050 mm in thickness.

The microstructure of the gray cast iron consisted generally of a pearlitic-ferritic matrix and type B graphite flakes. Casting voids of various sizes and shapes were scattered throughout the microstructure. The thickness of the walls varied considerably while the surfaces were generally fairly rough. Hardness readings in the interior varied from about R_C 20 to 30, while values made on the outside surface averaged about R_B 73. These pipes were coated with a thick layer of black tar on all exposed surfaces, which was left in place when the pipes were installed for corrosion testing.

Stainless steel pipes were austenitic, AISI type 304 alloys and met Schedule 40 strength specifications. Specimens tested in the acid-sulfate steam and alkaline water appeared to be identical on a microstructural level while the ones tested in the groundwater-diluted steam contained a much finer-grained microstructure. The latter were seamless pipes while the others contained a welded seam. Interior hardness levels varied from R_B 72 to 81, with the fine-grained ones showing slightly higher average values than the others.

Aluminum pipes were wrought 6063-T6 alloys and met Schedule 40 strength specifications. This age-hardening alloy uses a precipitate of fine magnesium silicide particles to obtain its strength.

Wrought copper tubes were cold-drawn to an interior hardness level of 69 R_B. The average wall thickness was about 1.59 mm, while the average grain size generally varied between 0.15 and 0.20 mm. The microstructure contained scattered particles of cuprous oxide.

Rigid polyvinylchloride (PVC) is a member of the polyvinyl chloride resin family. It is an unplasticized (no added softener) resin with color pigments and stabilizers added in various proportions. The stabilizers are necessary in any vinyl chloride formulation to minimize heat and ultraviolet radiation degradation of the resin. Rigid PVC is relatively low in cost compared with other engineering plastics and offers flame resistance and chemical corrosion resistance to most acids, alkalies, salts, moisture, and oils. It is also tough, dimensionally stable at room temperatures, and has weatherability superior to many plastics. It is to be noted, however, that the polymer may contain a very small amount of unreacted monomer (vinyl chloride) which, among

other disadvantages, is mildly toxic. The PVC plastic pipes used in these tests met Schedule 80, PVC 1120-1220 ASTM-D-1785, 400 psi specifications.

Copolymerization of acrylonitrile, butadiene and styrene results in a family of thermoplastic resins commonly referred to as "ABS". In general, ABS plastics offer good (for plastics) tensile strength, flexural rigidity and impact resistance over a range of temperatures from -40°C to 104°C. Depending on concentration and temperature, ABS plastics are not adversely affected by most inorganic chemicals, water vapor, and many mineral acids and alkalies. Special grades of ABS are available to resist chemical environments. However, as with all thermoplastics, ABS will cold-flow or creep as the applied stress, temperature and/or time increases. ABS plastics are also sensitive to ultraviolet irradiation (photo-oxidation) which can cause embrittlement, chalking, and color change. The ABS plastic pipes used in these tests met Schedule 40, CS-270-65, TIGS ASTM-D2661 specifications.

A mixture of portland and asbestos cement is used to make a seamless pipe, commonly known as "transite". This material is characterized by its high heat resistance (up to 370°C) and its low thermal conductivity. It is fabricated into pressure pipe of four classes, with working pressures of 50 to 200 psi, in increments of 50 psi. The transite pipes used in these tests were composed of a mixed chrysolite and crocidolite asbestos filler and cement binder. The pipe used was class 50 (50 psi pressure pipe) with a wall thickness of about 9 mm.

OPERATING CONDITIONS

Each pipe was tested simultaneously under oxygen-poor and oxygenated conditions. This was achieved by dividing samples into two 3-metre-long segments. The upper one, joined to the manifold, was left whole to exclude the atmosphere from the interior portion, while the lower was split in half along its length to expose the interior to the surrounding air.

Samples of fluid were taken from each open channel at its downstream end and from each manifold air trap, after the studies were underway, and analyzed for dissolved solids. Gases were not analyzed because of inherent difficulties in obtaining samples and in getting an analysis performed.

Specimens were exposed continuously in the steam environments for approximately one year, while the hot water environment was only maintained for ten weeks due to a major mechanical failure of the diesel engine that operated the submersible pump. After testing was completed, samples were removed from the manifolds and allowed to dry under a shelter.

Some variations in steam pressure were noticed at the Coso Resort steam facility. On one occasion, after the corrosion test had been terminated and the manifold ports plugged off except for one which was used for a separate study, the air trap attached to one end of the manifold, which consisted of a steam-condensate-filled, U-shaped exit pipe designed to remove excess condensate from the manifold blew out, releasing steam to the atmosphere. This blowout was attributed to an increase in local atmospheric precipitation which could act to increase steam pressure in two ways. One would be to increase the flow of groundwater into the Coso area resulting in increased steam production. Moderate precipitation at the resort itself would partially seal the ground pores and natural steam vents causing a temporary increase in steam production through the wells instead of through the surrounding ground. An increase in steam pressure would change corrosion conditions somewhat by increasing flow velocities through the test samples and also by increasing the solubilities of gases and salts in the steam.

The steam at the Devil's Kitchen test facility appeared to contain less moisture than the one at the Coso Resort, as the amount of condensate present in the test specimens at any period of time was considerably less. However, the steam pressure appeared to remain fairly constant with time compared to the one at the resort. The constancy of this particular fluid condition was attributed to the stable water conditions in that area, as discussed previously.

Some minor pooling of steam condensate was noticed in the aerobic test samples near the downstream end at the Devil's Kitchen facility as a result of an insufficient slope of the test array itself. This condition was not considered serious as the accumulation of corrosion products, precipitation of dissolved salts and presence of wind-blown debris in the open channel would also serve to create fluid traps of similar kinds.

Although early measurements of the well water at depth showed a pH of about 9.0, measurements made of the fluids after passing through the samples showed a pH of about 7.0. The reason for the reduced alkalinity is not apparent, but might be due to increased mixing with fluids coming from shallower depths. Also, earlier tests were made under static conditions, and not while the well was flowing.

ANALYSIS PROCEDURES

In view of the lack of funding and manpower, a study of all possible corrosion conditions could not be accomplished at this time. Analyses were concentrated on the materials exposed separately, while the "plumber's nightmare" galvanic corrosion samples would be analyzed separately in a later study.

Analyses of samples were generally done in the following manner:

(1) After air-drying, samples were photographed for reference purposes and to compare major corrosion features between them, particularly identical ones exposed to different fluid conditions.
(2) After being photographed, 0.3-metre-long samples were removed from both ends of the open specimen and from the inlet (manifold) end of the closed pipe 0.3 metre downstream from the junction to avoid anomalous effects resulting from the change in flow conditions at that location.
(3) Samples of corrosion products were taken from each specimen and analyzed using a Phillips-Norelco diffractometer, vertical goniometer, and Cu or Co Kα radiation. Simple chemical tests were also made to aid in identifying the products. The copper pipes were chosen for a more detailed examination which was done at the Naval Postgraduate School, Monterey, using scanning electron microscopy, x-ray fluorescence and atomic absorption spectroscopy, the latter for analyzing corrosion products for the presence of mercury. The x-ray fluorescence technique will identify elements with atomic numbers greater than 10.
(4) The surfaces were cleaned of corrosion products and the topography observed visually with a low-magnification binocular microscope to identify the mode and extent of corrosion. Whenever feasible, measurements were made in order to calculate corrosion rates.
(5) Thin rings of material were cut from the ends of the specimens and prepared for study by optical metallographic microscopy in order to establish the microstructural condition of the pipe materials, establish corrosion modes on a microstructural level, look for evidence of damage to the interior such as cracking or blistering, and measure corrosion depths.

ACID SULFATE STEAM RESULTS

In view of the large number of samples that were analyzed, the best way to present the results seemed to be on the basis of test fluid conditions (see Table 1) with a separate discussion for each material studied. A further subdivision was made between anaerobic (closed, oxygen-poor) and aerobic (open, aerated, oxygenated) test conditions. Study was restricted to the interior surface of the test sample only, unless specifically stated otherwise. This section of the report treats material behavior for acid sulfate fluid. Later sections cover the behavior patterns associated with groundwater-diluted steam and alkaline water.

STEEL

The test specimen exposed to the anaerobic fluid condition was coated with a thin, black layer of compact adherent corrosion products.

Microstructural analysis showed localized corrosion of the steel underneath this layer. Pits up to 0.16-mm-deep were found in the condensate channel and smaller ones elsewhere (Figure 3). Occasionally, attack appeared to concentrate at pearlite colonies or ferrite grain boundaries. Iron carbide can form the cathode of a galvanic cell with iron in sulfuric acid solutions. In the present circumstance, the iron carbide platelets in the pearlite might have served as a source of galvanic corrosion. Localized corrosion has been observed at the interface between pearlite and ferrite grains in carbon steel immersed in a sulfuric acid solution with a pH of 4.[18] Surface attack in areas away from the pits appeared to be slight.

An analysis of the corrosion products showed the presence of an iron sulfide, mackinawite (Table 2), a small amount of magnetite, and at least one additional crystalline compound not identified. The magnetite, may be the remains of a coating found on the steel prior to testing, or may have been formed by the corrosion process itself. Mackinawite is a common sulfide corrosion product found on steel products used in sour oil and gas well environments[19] and is generally produced by the reaction of hydrogen sulfide with the metal in the presence of moisture.

All of the mechanisms responsible for the corrosion or passivation of metals in complex fluid environments are not completely understood in many situations.[20] In the present circumstance, a reaction should take place between iron and hydrogen sulfide.[21] Iron also reacts with dilute sulfuric acid.[8] Sulfate ions can also accelerate a corrosion reaction under cathodic control.[22] Hydrogen sulfide appears to stimulate the corrosion of steel in acid or neutral solutions, although the exact

---

[18] C. J. Cron, J. H. Payer, and R. W. Staehle. "Dissolution Behavior of Fe-Fe_3C Structures as a Function of pH, Potential, and Anion - An Electron Microscope Study," *Corrosion*, Vol. 27 (January 1971), pp. 1-25.

[19] J. S. Smith and J. D. A. Miller. "Nature of Sulphides and Their Corrosive Effect on Ferrous Metals: A Review," *Brit Corrosion J*, Vol. 10, No. 3 (1975), pp. 136-43.

[20] R. T. Foley. "Complex Ions and Corrosion," *Electrochem Soc J*, Vol. 122, No. 11 (November 1975), pp. 1493-94.

[21] E. C. Greco and J. B. Sardisco. "Reaction Mechanisms of Iron and Steel in Hydrogen Sulfide," Proceedings of the Third International Congress on Metallic Corrosion, Moscow, 1966. Vol. 1 (1969), pp. 130-138.

[22] S. E. Traubenberg and R. T. Foley. "The Influence of Chloride and Sulfate Ions on the Corrosion of Iron in Sulfuric Acid," *Electrochem Soc J*, Vol. 118, No. 7 (July 1971), pp. 1066-70.

TABLE 2. Corrosion Data from the Acid-Sulfate Steam Test Condition

Material	Aerated	Location		Precipitate	Name	Amount	Mode of attack	Maximum depth, mm	Maximum corrosion rate		Location of Maximum	Comments
									mm/yr	mpy		
Steel	No	Inlet	All	Fe_9S_8	Mackinawite	Large	Pitting	0.16	0.16	6	Bottom	
Steel	No	Inlet	All	Fe_3O_4	Magnetite	Small		...	...	...		
Steel	Yes	Inlet	Bottom	$\alpha FeOOH$	Goethite	Large		...	...	...		
Steel	Yes	Midway	Bottom	$\alpha FeOOH$		Large	Channel	1.0	1.0	40	Bottom	Steep sided
Steel	Yes	Midway	Bottom	Fe_3O_4		Large	Pitting	0.9	0.9	35	Side	
Steel	Yes	Midway	Bottom	γFe_2O_3	Maghemite	Large		...	...	...		
Steel	Yes	Midway	Bottom	αFe_2O_3	Hematite	Large		...	...	...		
Steel	Yes	Outlet					Channel	1.0	1.0	40	Bottom	Gentle sloped
Cast iron	No	Inlet	All	Fe_9S_8		Small	Uniform	0.9	0.9	35	Bottom	Rough surface
Cast iron	No	Inlet	All	Fe_3O_4		Small		...	...	...		
Cast iron	Yes	Inlet	Bottom	$\alpha FeOOH$		Medium		...	...	...		
Cast iron	Yes	Inlet	Bottom	γFe_2O_3		Medium		...	...	...		
Cast iron	Yes	Inlet	Bottom	αFe_2O_3		Medium		...	...	...		
Cast iron	Yes	Outlet	Bottom	$\alpha FeOOH$		Medium	Leaching	1.8	1.8	70	Bottom	Iron lost
Cast iron	Yes	Outlet	Bottom	γFe_2O_3		Medium		...	...	...		
Gal. steel	No	Inlet	All	βZnS	Sphalerite	Large	Uniform	0.05	0.05	2	Bottom	In zinc
Gal. steel	No	Inlet	All	ZnO	Zincite	Small		...	...	...		
Gal. steel	Yes	Inlet	Bottom	βZnS		Medium	Uniform	0.05	0.05	2	Side	In zinc
Gal. steel	Yes	Inlet	Bottom	Fe_3O_4		Medium		...	...	...		
Gal. steel	Yes	Inlet	Bottom	αFe_2O_3		Medium		...	...	...		
Gal. steel	Yes	Outlet	Bottom	ZnO		Medium	Pitting	0.7	0.7	28	Bottom	In steel
Gal. steel	Yes	Outlet	Bottom	Fe_3O_4		Medium	Uniform	0.1	0.1	4	Side	In steel
Gal. steel	Yes	Outlet	Bottom	γFe_2O_3		Medium		...	...	...		
Aluminum	No	Inlet					Pitting	0.025	0.025	1	Ceiling	Erosion
Aluminum	Yes	Outlet					Uniform	0.03	0.03	1.2	Bottom	
Aluminum	Yes	Outlet	Side	Iron oxide stain			Pitting	0.3	0.3	12	Side	
Stainless steel	No	Inlet					Grain boundary	0.02	0.02	0.8	Bottom	
Stainless steel	Yes	Outlet	Bottom	Iron oxide stain			Grain boundary	0.02	0.02	0.8	Side	
Stainless steel	Yes	Outlet					Intergranular	0.14	0.14	5.5	Side	Near weld
Copper	No	Inlet	All	$Cu_{1.96}S$	Djurleite	Large	Intergranular	0.08	0.08	3	Bottom	
Copper	No	Inlet	All	Cu_2S	Chalcocite	Medium		...	...	...		
Copper	No	Inlet	All	$Cu_{1.8}S$	Digenite	Trace		...	...	...		
Copper	Yes	Inlet	Bottom	CuS	Covellite	Medium	Pit	0.07	...	...	Bottom	Individual
Copper	Yes	Inlet	Bottom	$Cu_{1.8}S$		Medium	Pitting	0.67	0.67	26	Bottom	Total loss
Copper	Yes	Inlet					Uniform	1.6	1.6	63	Side	Perforation
Copper	Yes	Outlet	All	$Cu_4(OH)_6SO_4$	Brochantite	Large	Pit	0.22	...	...	Bottom	Individual
Copper	Yes	Outlet	All	$Cu_4(OH)_6SO_4H_2O$	Langite	Large	Pitting	0.38	0.38	15	Bottom	Total loss
Copper	Yes	Outlet					Pitting	0.52	0.52	21	Side	Total loss
Copper	Yes	Junction	top	$CuSO_4 \cdot 5H_2O$	Chalcanthite	Large		...	...	...		Exterior surface
Copper	Yes	Junction	top	$Cu_3(OH)_4SO_4$	Antlerite	Large		...	...	...		Exterior surface
PVC	No	Inlet					Void form.	2	...	...	Top	Gas form.
PVC	Yes	Inlet		Iron oxide stain			Void form.	3	...	...	Bottom	Gas form.
PVC	Yes	Inlet		FeS_2 stain	Marcasite		Warping	...	...	...	Side	Heat induced
PVC	Yes	Inlet					Cracking	...	...	...	Bottom	Heat induced
ABS	Yes	Inlet		Iron oxide stain			Warping	...	...	...	Sides	Heat induced
Transite	No	Inlet					Leaching	1	...	...		All cement gone
Transite	Yes	Inlet					Leaching	1	...	...		All cement gone

mechanism has been a subject of debate.[23] A recent publication indicates that both anodic and cathodic processes are catalyzed by the presence of hydrogen sulfide and other soluble or insoluble sulfide species.[24] Once a layer of corrosion products forms on the metal, the rate of corrosion may become controlled by diffusion rates through the layer. Sulfides contain a disordered lattice structure; consequently, diffusion rates are much higher resulting in a greater rate of corrosion. The mackinawite lattice is believed to have the most defects among the common iron sulfides and so should be the least protective.[21]

Iron sulfides, along with magnetite, are normally cathodic to iron, and so the coating itself may form a galvanic cell with the metal at areas where it is thin or broken.[19,25] The effect that the sulfide film had on the initiation of pitting corrosion in the present experiments was not established. However, the large ratio of cathode to anode areas at any small break in the sulfide film could cause localized corrosion of the metal. Pitting corrosion of steel also commonly initiates at sulfide inclusions in the metal itself.[19,24]

The corrosion of steel in an anaerobic acid environment with a pH less than about 4 is accomplished with the reduction of hydrogen ions at cathodic areas.[26] The presence of hydrogen sulfide generally results in increased diffusion of atomic hydrogen into the steel[27] causing embrittlement, delayed fracture, and sulfide stress cracking under certain conditions.[2] Since the acid sulfate steam in the present experiment was only moderately acid, with a pH of about 4.5, the amount of atomic hydrogen being generated was not expected to be significant. A careful examination of the microstructure showed no damage attributable to hydrogen infusion such as the presence of blisters next to the surface, or

---

[23] R. Bartonicek. "Corrosion of Steel in Solutions of Chlorides and Sulphides," Proceedings of the Third International Congress on Metallic Corrosion, Moscow, 1966, Vol. 1 (Moscow 1969), pp. 119-29.

[24] Gösta Wrangleń. "Electrochemical Properties of Sulfides in Steel and the Role of Sulfides in the Initiation of Corrosion," *Sulfide Inclusions in Steel*, American Society for Metals, Metals Park, Ohio (1975), pp. 361-79

[25] Gösta Wrangleń. *An Introduction to Corrosion and Protection of Metals*. New York, Halsted Press, 1972.

[26] Herbert H. Uhlig. *Corrosion and Corrosion Control*. New York, John Wiley and Sons, 1971.

[27] Asahi Kawashima, Koji Hashimoto, and Saburo Shimodaira. "Hydrogen Electrode Reaction and Hydrogen Embrittlement of Mild Steel in Hydrogen Sulfide Solutions," *Corrosion*, Vol. 32, No. 8 (August 1976), pp. 321-31.

microcracking/fracturing of the interior. Previous work[28] indicates that blistering of steel seldom occurs in geothermal fluids. Other investigators[2] have shown that the infusion of hydrogen in steel under high-temperature fluid environments may be a transient phenomenon, and that it largely diffuses out again with time. Some diffusion of hydrogen into the steel could have occurred in the present situation. However, no hydrogen probe measurements were made to verify its presence and no obvious evidence of its presence was found in the microstructure.

The open test specimen exposed to aerobic fluid conditions was covered with a thick layer of corrosion products, starting about 23 cm downstream from the junction between the aerobic and anaerobic sections (Figure 4), and continuing to the downstream end of the pipe. The products, up to about 12 mm in thickness, were identified as a layered mixture of various ferric oxides and hydrated ferric oxides (Table 2). Removal of the corrosion products showed a corrosion channel, up to 1 mm deep and 25 mm wide, cut into the floor of the pipe (Figure 5). The surface of the corrosion channel was quite smooth and was very steep-sided in the midstream portion of the pipe where the corrosion products were the thickest. Further downstream the corrosion channel gradually became more gently sloped and the covering of corrosion products began to thin, in concert. The position of the corrosion channel coincided with the drainage path for the steam condensate and was probably a consequence of its presence. This form of corrosion is fairly common in flowing acid steam condensates.[8] As the steam emerged from the anaerobic, closed pipe at high speed and pressures were suddenly reduced, a large part was lost to the atmosphere (along with all of the undissolved gases) except for a variable amount of spray and mist that condensed on the surface of the open pipe and gradually collected on the bottom. That, plus condensate from the anaerobic section upstream, constituted the major source of corrodent in the aerated test specimens.

Aeration of the fluid probably converted much of the remaining hydrogen sulfide to sulfur or higher oxidation states of the sulfur species. Dissolved oxygen also increased the corrosion rate by combining with hydrogen ions at cathodic areas. Principal corrosion reaction products due to this fluid condition would include soluble iron sulfates that are carried off in the condensate and insoluble oxides that form coatings on the steel.

Any condensation on the walls above the condensate channel quickly resulted in the formation of a layer of protective corrosion products

---

[28] P. K. Foster, T. Marshall, and A. Tombs. "Corrosion Investigations in Hydrothermal Media at Wairakei, New Zealand," *UN Conference on New Sources of Energy*, Rome, 1961. United Nations, N.Y. (E/Conf. 35G47).

FIGURE 3. A Photomicrograph Showing Pitting Corrosion in Steel Exposed to Anaerobic Acid-Sulfate Steam. (200X)

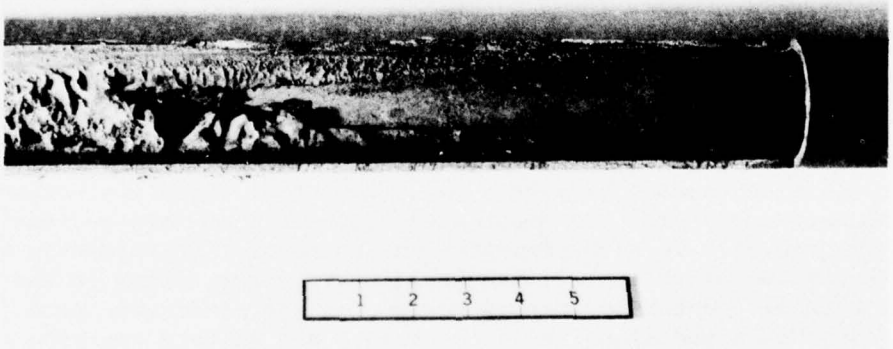

FIGURE 4. Inlet End of an Open Steel Pipe Exposed to Aerated, Acid-Sulfate Steam. Flow is from right to left. Scale in inches.

FIGURE 5. A Corrosion Channel in the Bottom of the Pipe Described in Figure 4, After Cleaning.

adjacent to the metal. This passivating layer plus the limited amount of moisture that collected on the walls resulted in a reduced corrosion rate relative to the condensate channel, which was well soaked with acid condensate. The presence of added moisture in this latter area also resulted in the formation of a thick, loose layer of hydrated ferric oxides next to the metal which were less protective and allowed corrosion to continue relatively unencumbered. The corrosion channel was filled entirely with this corrosion product. Above it was a very thick, loose, highly porous layer composed of a mixture of magnetite and maghemite, which in turn was capped with a coherent thin coating of hematite. This layering sequence resulted from differences in oxidation conditions, each layer reflecting the amount of moisture and oxygen present in that zone. The layer adjacent to the metal formed in a wet atmosphere containing a limited amount of oxygen while the outer layer was formed in a well aerated atmosphere. The magnetite represents an intermediate oxide, and forms generally in an oxygen-poor environment. The formation of large quantities of relatively insoluble corrosion products in the condensate channel eventually trapped and pooled the condensate plus all of the various solid and dissolved contaminants and soluble reaction products which resulted in a more concentrated acid environment (probably a more defective coating of oxidation products) and, consequently, more extensive corrosion of the floor of the channel

The walls above the water line, particularly within the midstream portion of the pipe, contained numerous large pits, up to about 0.9 mm

in depth (Figure 5). Oxidation products in these areas consisted of a thin, multilayered film with about the same composition as the layer covering the corrosion channel, only without its porosity. Pitting appeared to be located at areas where the film was broken and moisture was able to reach the surface of the metal. Corrosion may have been aided by the oxide film itself as magnetite is normally cathodic to iron, as mentioned before, and can form a galvanic cell with it.

No evidence of hydrogen infusion was found in the aerated steel. The diffusion of hydrogen into steel is not expected to occur in a well-oxygenated environment, as any hydrogen readily combines with the dissolved oxygen as does the hydrogen sulfide which would ordinarily serve to stimulate the diffusion process.

CAST IRON

A preliminary inspection of the pipe exposed to anaerobic fluid conditions showed the coating of protective tar to be essentially gone except for a brittle residue on the bottom of the condensate channel. A very thin coating of corrosion products was found on the surface of the iron that consisted of a mixture of mackinawite and magnetite. Identification of these compounds was difficult due to the small amount of product present. Magnetite was identified by its color, streak, and magnetic property while mackinawite was tentatively identified by x-ray diffraction analysis. In addition, a standard chemical test was run on a small sample of corrosion products that confirmed the presence of a metal sulfide.

The corrosion rate was judged to be similar to that observed for the steel pipe, although the surface was so uneven primarily as a result of the casting process, that the corrosion rate and mode were difficult to establish (Figure 6). The corrosion process appeared to cut numerous shallow grooves into the surface of the iron, in the direction of fluid flow, possibly following surface irregularities. A microstructural examination showed no leaching (graphitization) of the iron phase. The maximum corrosion rate, assuming all surface irregularities were due to fluid attack, was estimated at 0.9 mm/year (35 mils/year). This value is probably much too large.

The aerated specimen was covered with a layer of ferric oxides and hydrated oxides identical in appearance to those found on the steel pipe, only considerably thinner in depth. Corrosion of the cast iron underneath was low and quite uniform within the condensate channel. No corrosion channel was formed on the bottom as on the steel pipe although the normally rough cast iron surface was leveled and smoothed by the corrosion process. A possible graphite-rich zone about 1.8 mm deep was found next to the surface in the cast iron on the bottom of the condensate channel near the downstream end (Figure 7). An analysis of the

FIGURE 6. A Section View of Gray Cast Iron Exposed to Anaerobic, Acid-Sulfate Steam, Showing Surface Irregularities.

FIGURE 7. A Section View of Gray Cast Iron Exposed to Aerated, Acid-Sulfate Steam, Showing a Zone of Possible Graphitization Next to the Surface.

microstructure did not reveal whether the zone was due to corrosion of the iron phase (graphitization) or simply an agglomeration of graphite particles. A sample of wall material was analyzed with x-ray fluorescence which discovered an excess of silicon in these soft black-colored areas. The presence of carbon could not be verified with this method. Adjacent microstructure contained predominantly type D graphite flakes (Figure 8) which would indicate some degree of undercooling.[29] The material at the surface also showed evidence of possible chilling. This specimen clearly needs additional study. The graphitization of gray cast iron in a dilute sulfuric acid solution has been observed previously[26] and appears to proceed if the graphite phase remains exposed to the attacking fluid. Attack generally stops or slows once the graphite becomes covered with corrosion products.

Some large, very shallow pits were observed on the walls above the water line that were identical in appearance to those found on the steel pipe, except for the greatly reduced depth. These pits were probably formed in the same fashion, i.e., by the presence of small breaks in the oxide coating where aggressive fluids could reach the bare metal.

GALVANIZED STEEL

The test specimen exposed to the anaerobic fluid environment was covered with a loose, flaky coating of white corrosion products. Analyses showed these to be a mixture of β-zinc sulfide, sphalerite, and zinc oxide (zincite), with the former constituting the bulk of the products. An examination of the microstructure showed the zinc coating to be nearly completely and uniformly corroded away. The steel underneath, however, remained virtually unattacked. Zinc readily reacts with hydrogen sulfide to form zinc sulfide.[30, v.4]

The zinc corrosion products normally produced in an acid fluid of this pH, at ambient temperatures, are soluble in the acid[31] and corrosion continues unchecked. The sulfide product resulting from this acid sulfate fluid environment appeared to be insoluble in the fluid and may have served to retard the corrosion rate although, like the sulfide films discussed earlier, it was probably less protective than other kinds of insoluble coatings, like oxides.

The aerated pipe, after being cleaned, showed extensive pitting of the steel to a depth of 0.7 mm within the condensate channel (Figure 9),

---

[29] *Gray and Ductile Iron Castings Handbook*, ed. by C. F. Walton. Cleveland, Ohio, The Gray and Ductile Iron Founders' Soc., Inc., 1971.

[30] J. W. Mellor. *A Comprehensive Treatise on Inorganic and Theoretical Chemistry* (16 volumes). New York, Longmans Green and Company, published 1922-1937.

[31] Marcel Pourbaix. *Atlas of Electrochemical Equibria in Aqueous Solutions*. New York, Pergamon Press, 1966.

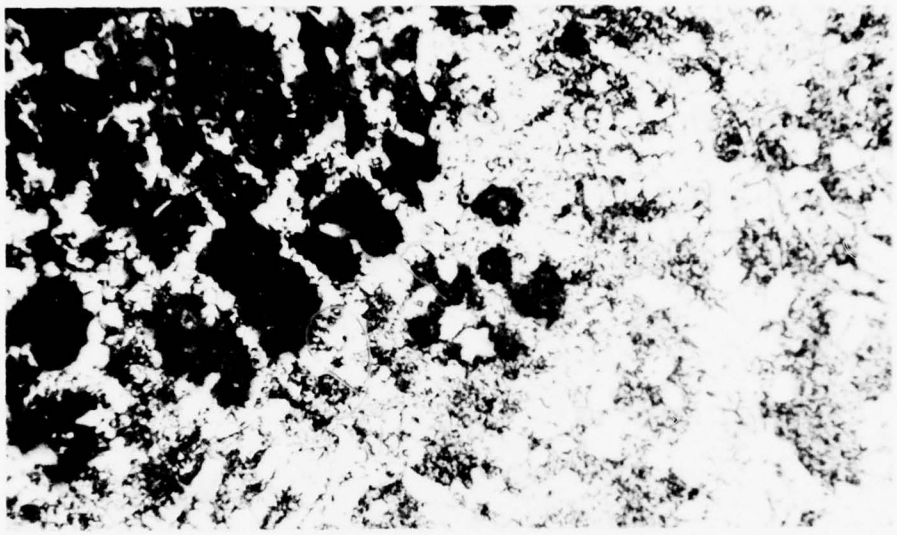

FIGURE 8. A Photomicrograph of the Specimen Shown in Figure 7, Indicating Possible Graphitized Areas (dark) and Adjacent Microstructure. (100X)

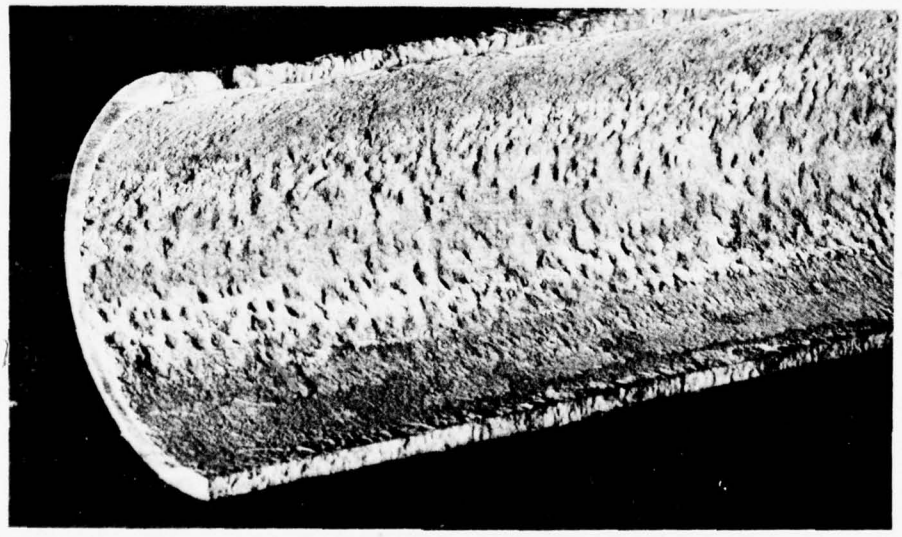

FIGURE 9. Outlet End of an Open, Galvanized Steel Pipe Exposed to Aerated Acid-Sulfate Steam, Showing Pitting Corrosion.

particularly in the downstream portion. On the walls above the water line, corrosion was generally uniform although a few large, very shallow pits up to 0.1 mm deep were observed near the top of the walls. Prior to cleaning, the surfaces (particularly within the condensate channel) were covered with an extensive coating of ferric oxides plus some β-zinc sulfide and zinc oxide directly covering the bare zinc at the upstream and downstream ends, respectively.

Evidence exists[26] that zinc becomes noble with respect to iron in aerated fluids at temperatures above about 60°C, which often results in pitting of the iron. This reversal in polarity is apparently due to the formation of a zinc oxide coating on the zinc rather than the coating that normally occurs at lower temperatures.[32] The zinc oxide formed at these elevated temperatures, where pitting occurs, is described as granular, flaky, and nonadherent.[8] Stress corrosion cracking of zinc in hot potable water has also been observed[33] which could result in separation of the zinc plating from the steel substrate. The presence of a nonuniform coating of corrosion products that is also cathodic to the metal underneath would readily explain the pitting corrosion observed in the present case. The absence of pitting on the walls above the water line could be explained as a result of a lower corrosion rate of the zinc in the areas. The walls should be much drier as the only electrolyte present would be irregular condensation of steam vapor. This should result also in the corrosion products remaining more intact, and consequently more protective. Also, the surface temperatures should be lower as these areas are more exposed to the atmosphere. In contrast, the continuous flow conditions present in the condensate channel should serve to carry off some of the more loosely adhering corrosion products and also to soak the remaining material with fluids. In addition, temperatures should remain higher within the channel, as the thick covering of poorly conducting corrosion products would serve as a good insulating blanket.

ALUMINUM

The specimen exposed to anaerobic fluid conditions did not appear to be attacked significantly. An examination of the microstructure showed very slight, occasional pitting of the surface to a depth of about 0.025 mm. Studying the surface with a low-power binocular microscope revealed that the pits, which were concentrated along the upper part of

---

[32] P. T. Gilbert. "The Nature of Zinc Corrosion Products," *Electrochem Soc, J*, Vol. 99, No. 1 (January 1952), pp. 16-19.

[33] G. R. Foster, S. G. Lee, and J. R. Myers. "Stress Corrosion of Eta-Phase, Hot-Dip-Zinc Alloy in Potable Hot Water," *Corrosion*, Vol. 30, No. 7 (July 1974), pp. 239-41.

the pipe, were elongated in the direction of flow and were clean and shiny on the inside. This meant that they were not corrosion features but were probably caused either by the impingement of water droplets in the steam or else by the impact of solid particles.

The aerated specimen (particularly at the downstream end) was coated along the sides, above the condensate channel, with a thin uneven film of brown precipitates. An x-ray diffraction pattern of the coating could not be identified. From the color, however, it appeared to contain some iron oxides and may have precipitated out of the steam vapor condensing on the walls. Pitting of the aluminum was observed underneath this coating (Figure 10) whose presence may have enhanced the formation of simple, differential aeration cells at the surface of the aluminum. The potential of the film with respect to the metal underneath was not determined, and so the possibility of galvanic corrosion could not be estimated.

Pitting was also found in the condensate channel which seemed to be related to the presence of solid debris, perhaps windblown, that collected on the bottom and created differential aeration conditions in this location. A careful examination of the microstructure showed no correlation between initiation sites and the presence of secondary phases or grain boundaries within the aluminum. The maximum pitting depth in the aerated sample was measured as 0.3 mm.

In addition to the pitting corrosion found in the condensate channel, this region was also subject to a slight amount of uniform corrosion. A rate of about 0.030 mm/year (1.2 mils/year) was measured at the downstream end, at the bottom of the channel.

STAINLESS STEEL

The closed pipe contained some small pits that were elongated in the flow direction and were shiny and clean on the inside like the ones observed on the aluminum pipe. Their cause would be the same as discussed for the aluminum. A study of the microstructure showed very minor corrosion of the surface, with attack concentrated at the grain boundaries. Damage was no more than 0.02 mm deep, which was not considered significant.

The aerated sample showed minor pitting of the surface to a depth of about 0.03 mm. The largest concentration of pits was found in the condensate channel, at the downstream end. The surface of the pipe was generally covered with a very thin, uneven film of brown precipitates that were not identified but were probably iron oxides that precipitated out of the steam as a result of aeration. The pitting may have been related to the presence of this film which could cause an uneven flow of

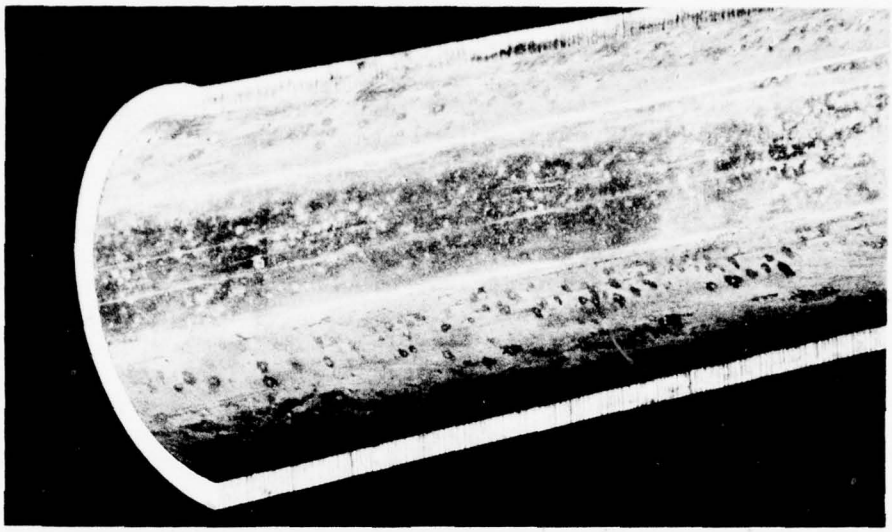

FIGURE 10. Outlet End of an Open Aluminum Pipe Exposed to Aerated Acid-Sulfate Steam, Showing Pitting Corrosion on the Walls Under a Thin Film of Brown Precipitates.

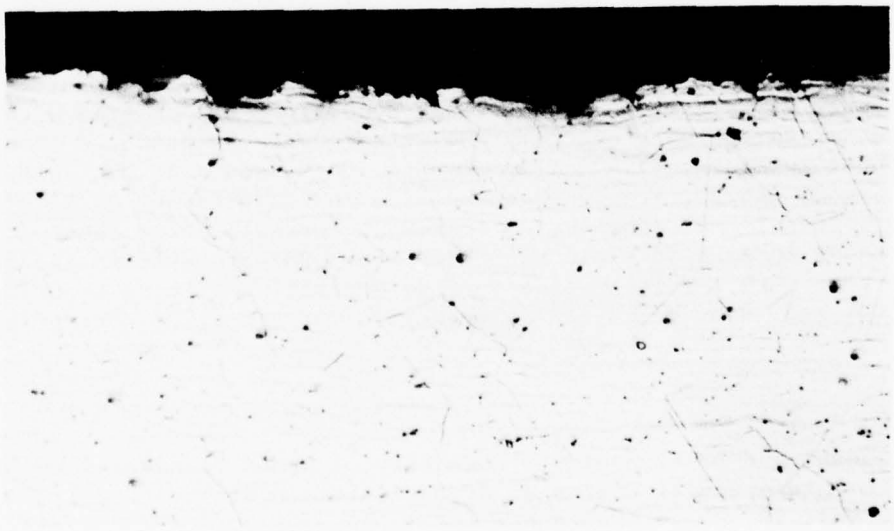

FIGURE 11. A Photomicrograph Showing Minor Pitting Corrosion and Grain Boundary Attack of a Stainless Steel Pipe Exposed to Aerated, Acid-Sulfate Steam. (200X)

oxygen to the surface of the metal. In addition to pitting, the surface showed minor attack to grain boundaries (Figure 11).

A study of the microstructure showed intergranular corrosion at the surface adjacent to a longitudinal welded seam in the pipe, located near the downstream end and on the upper wall above the condensate channel (Figure 12). This form of corrosion is believed to result from the material becoming sensitized during the welding process.[26] Heating of the alloy within a temperature range of 400 to 850°C causes precipitation of chromium carbides along grain boundaries, hence these areas become depleted of chromium and lose passivity. Loss of passivity along the boundaries can result in these areas becoming anodic with respect to the interior of the grain, and due to an unfavorable areal ratio (large cathode/small anode) corrosion of the boundaries would take place in the presence of an electrolyte. The severity of the attack is expected to depend on the degree of chromium depletion and the aggressiveness of the electrolyte.[26] In the present case, the maximum depth of penetration was about 0.14 mm.

Alternate explanations (strain, electrochemical, or segregation theories) have also been advanced to account for intergranular corrosion of stainless steel. In many instances, that also might account for the grain boundary attack, as occurred in the present circumstance.[34] Additional study is clearly needed.

COPPER

The sample exposed to anaerobic fluid conditions was covered with a black layer of corrosion products. Analysis showed the products to be mainly copper sulfides, principally $Cu_{1.96}S$, Cu_2S, and also possibly $Cu_{1.8}S$. Copper reacts with hydrogen sulfide in the presence of moisture to form sulfides.[35] At equilibrium (constant current) below about 70°C, a copper anode in an acid fluid saturated with hydrogen sulfide should become covered with a multilayered sulfide deposit consisting of Cu_2S, $Cu_{1.96}S$, $Cu_{1.75}S$, CuS, and S—in an outward direction.[36-38] Pulverization

---

[34] A. Joshi and D. F. Stein. "Chemistry of Grain Boundaries and Its Relation to Intergranular Corrosion of Austenitic Stainless Steel," *Corrosion*, Vol. 28, No. 9 (September 1972), pp. 321-30.

[35] Per Backlund. "The Influence of Oxygen Pressure on the Reaction of Hydrogen Sulphide With Copper," *Acta Chemica Scandinavica*, Vol. 23, No. 5 (1969), pp. 1541-52.

[36] A. Etienne. "Electrochemical Method to Measure the Copper Ionic Diffusivity in a Copper Sulfide Scale," *Electrochem Soc, J*, Vol. 117, No. 7 (July 1970), pp. 870-4.

of the mixture in preparation for x-ray analysis transforms the $Cu_{1.75}S$ to $Cu_{1.8}S$ (digenite).[38] Digenite is believed to be a stable, low temperature phase only in the Cu-Fe-S system, when it contains a small amount of iron.

In addition to the copper sulfides, a small amount of Cu_5FeS_4 (bornite) was identified in the corrosion products, demonstrating the presence of dissolved iron in the steam.

An examination of the microstructure showed intergranular attack of the surface up to about 0.08 mm in depth (Figure 13). Intercrystalline corrosion in copper alloys have been observed previously in high pressure steam applications.[39] The precise cause of the intergranular corrosion in this circumstance was not established. Clearly, the grain boundaries were anodic with respect to the interior of the grain and perhaps also to the sulfide coating. Copper oxide particles within the metal, which are generally noble to it,[8] didn't appear to be concentrated along the grain boundaries, a situation that could have resulted in intercrystalline attack by galvanic corrosion cells.

In addition to intergranular attack, a small amount of uniform corrosion may have also taken place along the surface of the copper. This probably occurred early in the test cycle when the sulfide film was much thinner.

The electrochemical reactions have not been completely established for this test condition because the fluid chemistry is not definitely known. A simple reaction of copper with hydrogen sulfide is the most probable. However, other reactions can take place. Although copper does not react with nonoxidizing acids like dilute sulfuric acid, it readily reacts with those containing oxidizers such as oxygen or ferric and mercuric ions to form soluble compounds such as cupric sulfates.[26] Cupric sulfates, in turn, can react with hydrogen sulfide to form insoluble cupric sulfides.[30, v. 3] Once a layer of corrosion products forms on the copper, reactions may become controlled by diffusion processes. Corrosion products may also be cathodic to copper itself,[25] resulting in localized corrosion wherever the coating is porous, cracked or nonuniform.

---

[37] Eugene H. Rosenbloom. "An Investigation of the System Cu-S and Some Natural Copper Sulfides Between 25° and 700°C," *Econ Geol*, Vol. 61, No. 4 (June 1966), pp. 641-71.

[38] Nobuo Morimoto and Kichiro Koto. "Phase Relations of the Cu-S System at Low Temperatures: Stability of Anilite," *Amer Mineral*, Vol. 55, (January 1970), pp. 106-17.

[39] *Metals Handbook*, 8th ed., Vol. 1, Taylor Lyman, ed. Metals Park, Ohio, American Society for Metals, 1961.

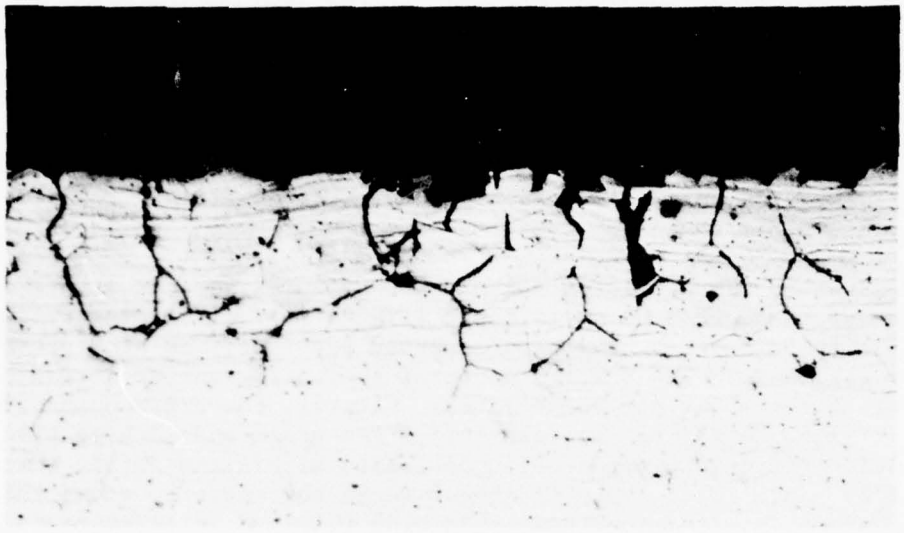

FIGURE 12. A Photomicrograph Showing Intergranular Corrosion Adjacent to a Welded Seam in the Sample Described in Figure 11. (200X)

FIGURE 13. A Photomicrograph Showing Intergranular Corrosion of a Copper Tube Exposed to an Anaerobic, Acid-Sulfate Steam. (200X)

The aerated segment of pipe was moderately to severely corroded, depending on the location. The upstream end adjacent to the anaerobic segment was perforated on the sides in many places and a deep groove was cut into the bottom of the junction between the anaerobic and aerated sections (Figure 14). The pipe was nearly filled with black corrosion products at this location that were analyzed as principally a mixture of copper sulfides (Table 2). It was not established whether the digenite found in this area was the stable (iron containing) or metastable variety. The volume of corrosion products gradually decreased toward the downstream end of the pipe, and a change from copper sulfides to basic copper sulfates (brochantite and langite) took place. The average corrosion rate also decreased toward the downstream end.

Basic copper sulfates form as a result of the hydrolysis of $CuSO_4$, or a reaction between $CuSO_4$ and either CuO, $Cu(OH)_2$, or a soluble base.[40] Copper sulfides readily oxidize in the presence of oxygen, which would produce $CuSO_4$ in the present circumstance.[41]

Corrosion appeared to be more uniform along the walls of the pipe, particularly at the upstream end. The condensate channel, particularly at the downstream end, contained numerous tiny pits (Figure 15). Pits up to 0.07 and 0.22 mm deep were found at the upstream and downstream ends, respectively. An increase in pitting depth toward the downstream end suggested that the sulfide corrosion products provided a more uniform coating than the sulfates. The increased corrosion rate at the upstream end was probably due mainly to a concentration of condensate in that area as the voluminous quantity of corrosion products would effectively block or limit its passage. Corrosion rates varied at the upstream end from 0.67 mm/year (26 mils/year) on the bottom of the condensate channel to greater than 1.6 mm/year (63 mils/year) on the walls (perforation). Comparable locations at the downstream end show 0.38 mm/year (15 mils/year) and 0.52 mm/year (21 mils/year). Fluid temperatures were also higher at the upstream end as was the quantity of dissolved gases.

Atomic absorption spectroscopy was used to analyze for the presence of mercury in two samples of corrosion products from the copper pipes (Table 3). A mercury concentration of 39 and 89 ppm was measured in corrosion products from the anaerobic and aerobic pipe, respectively. The chemical species present, however, was not known and so its effect on the corrosion process could not be determined. The transport of

---

[40] George Fowles. "Basic Copper Sulfates," *J Chem Soc*, (1926), pp. 1845-58.

[41] Motoaki Sato. "Oxidation of Sulfide Ore Bodies, II. Oxidation Mechanisms of Sulfide Minerals at 25°C," *Econ Geol*, Vol. 55 (1960), pp. 1202-31.

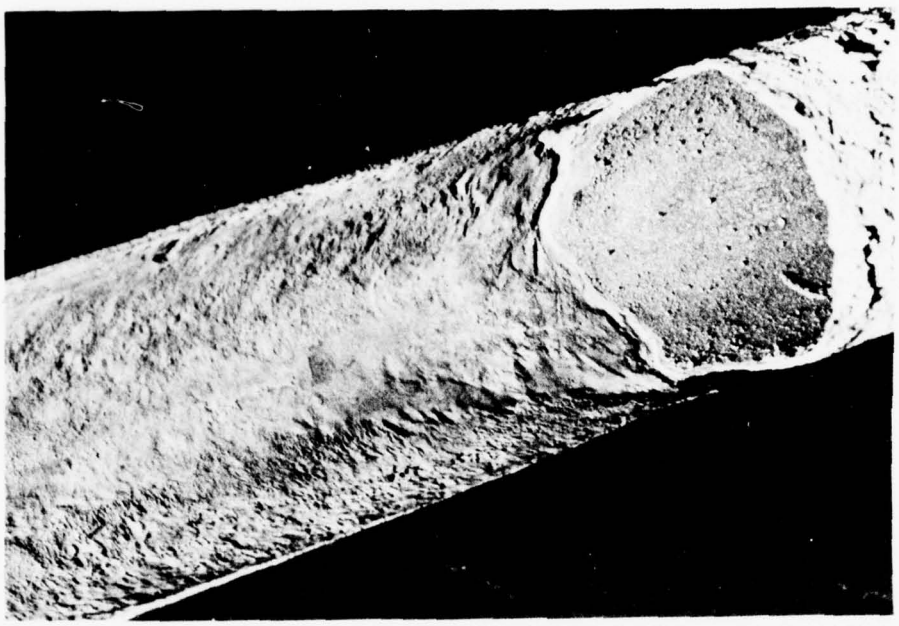

FIGURE 14. Inlet End of an Open Copper Pipe Exposed to an Aerated, Acid-Sulfate Steam, After Cleaning.

FIGURE 15. A Photomicrograph Showing Pitting Corrosion of an Open Copper Tube Exposed to an Aerated, Acid-Sulfate Steam. (200X)

TABLE 3. Mercury Content of Copper Corrosion Products.

Fluid	Location	Concentration, ppm
Acid sulfate	Anaerobic	39
Acid sulfate	Aerated	89
Diluted steam	Anaerobic	113
Alkaline water	Anaerobic	113
Alkaline water	Aerated	79

mercury in geothermal waters has been studied, although the chemical species present during transport remains a subject of debate.[42]

Extensive corrosion was observed on the exterior surface of the closed pipe adjacent to its downstream junction with the aerated segment. Exiting steam vapors condensed on this surface to form a thick coating of black-to-green-to-white hydrated and basic copper sulfates (chalcanthite and antlerite (Table 2)). These particular compounds were of interest insofar as they were not found elsewhere on the copper pipes. A recent publication contains a Pourbaix (potential-pH) diagram for the $Cu\text{-}SO_3\text{-}H_2O$ system at 25°C illustrating the conditions of formation for the basic copper sulfates as corrosion products.[43]

Corrosion products were also studied with the scanning electron microscope (SEM). Figure 16 shows a dendritic structure found in products removed from the inside of the aerated section. This specimen is reddish-black in color and has been tentatively identified as recrystallized copper. Figure 17 shows some sheet-like crystals found in some corrosion products taken from the same location. These may be bladed covellite crystals, although identification is very tentative.

PVC PLASTIC

The anaerobic fluid condition resulted in blistering of the surface, with the largest concentration of blisters being found on the ceiling of

---

[42] University of California. *Mercury and Antimony Deposits Associated With Active Hot Springs in the Western United States*, by Frank W. Dickson and George Tunnell. Los Angeles, 1967. (Institute of Geophysics and Planetary Physics, Publication No. 568.)

[43] Marcel Pourbaix. "Some Applications of Potential-pH Diagrams to the Study of Localized Corrosion," *Electrochem Soc, J*, Vol. 123, No. 2 (February 1976), pp. 25c-36c.

FIGURE 16. A Scanning Electron Microscope Photomicrograph of Dendritic Structure Found in Corrosion Products Removed From the Specimen Shown in Figure 14, Tentatively Identified as Recrystallized Copper. (1700X)

FIGURE 17. A Scanning Electron Microscope Photomicrograph of Sheet-Like Crystals Found in Corrosion Products Removed From the Specimen Shown in Figure 14, Tentatively Identified as Bladed Covellite, CuS. (330X)

the pipe. A ring cut from the pipe showed some discoloration (bleaching) of the inner half of the wall that contained a high density of voids. The void size increased toward the inside surface.

The formation of voids was probably due to the generation of some internal gas, as a result of prolonged exposure to elevated temperatures or ultraviolet radiation. The precise gas that was evolved was not identified. However, hydrogen chloride gas is commonly expelled from PVC compounds (dehydrochlorination) that have been heated or exposed to radiation.[44] Additives, if present, may migrate to the surface of the material at these temperatures. In addition, unreacted monomer in the structure would tend to volatilize under these conditions. Chlorine gas may be expelled if the plastic is exposed to SO_2 or NO_2 gases.[45]

In addition to being damaged by blistering, the plastic was judged to have been embrittled somewhat, although no precise measurements were made to verify this observation. Some embrittlement would be expected at these temperatures and under these exposed conditions due to the dehydrochlorination process.

Erosion damage to the surface of the closed pipe caused by these flow conditions was judged to be minimal. No evidence of impact craters was found on the surfaces, indicating that the steam was free of significant quantities of undissolved solids.

The aerated segment at the upstream end was covered with a high density of varying sized blisters (Figure 18). The bottom of the condensate channel contained a network of small surface cracks. In addition, the pipe in this region was spread and warped due to heat-induced softening of the plastic. Surface cracking or crazing commonly occurs in plastics under conditions of stress.[46]

Blistering of the surface gradually disappeared toward the downstream end along with evidence of softening. However, some embrittlement of the pipe was noticed along its entire length.

---

[44] A. Palma and M. Carenza. "Degradation of Poly(vinyl chloride) 1. Kinetics of Thermal and Radiation-Induced Dehydrochlorination Reactions at Low Temperatures," *J Appl Polymer Sci*, Vol. 14, No. 7 (1970) pp. 1737-54.

[45] H. H. G. Jellinek, F. Flajsman and F. J. Kryman. "Reaction of SO_2 and NO_2 With Polymers," *J Appl Polymer Sci*, Vol. 13, No. 1 (1969), pp. 107-16.

[46] H. A. Stuart. "Physical Causes of Aging in Plastics," *Angew Chem, Intern Ed*, Vol. 6, No. 10 (1967), pp. 844-51.

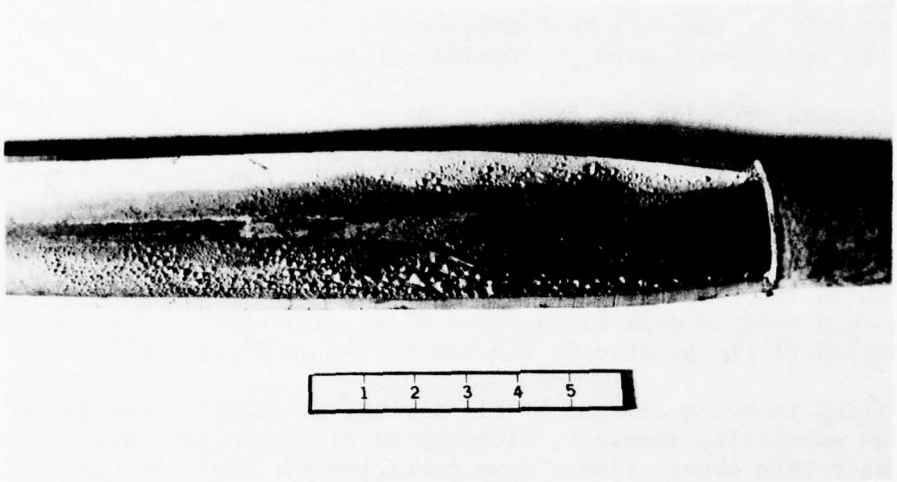

FIGURE 18. Inlet End of an Open PVC Pipe Exposed to an Aerated, Acid-Sulfate Steam, Showing Blistering of the Surface. Flow is from right to left. Scale in inches.

The condensate channel was stained a bright red-brown at the upstream end. Without being analyzed, this stain was believed to be mostly hematite. Rimming the hematite stain for a ways at its upstream boundary was a thin green deposit that was analyzed as FeS_2, marcasite. The walls above the condensate channel, at the downstream end, were stained a brown color. This stain was analyzed but was not identified. From its color and appearance it appeared to be a hydrated ferric oxide. This deposit probably resulted from the reaction of dissolved iron being carried in the steam with hydrogen sulfide that was also present, or else oxygen that was added by aeration.

No measurable amounts of channel erosion were found in the open pipe although the floor of the condensate channel was very smooth from the continual flow of water over it. The surface of the pipe showed some discoloration.

ABS PLASTIC

The closed pipe showed no apparent damage other than some possible embrittlement. No discoloration of the interior portion of the wall was observed. The exterior surface appeared dull where it was exposed to the atmosphere. This particular plastic may show some oxidation damage

as a result of prolonged exposure to elevated temperatures or radiation due to the presence of a butadiene in the structure.[47,48]

No noticeable erosion features were found on any part of the closed pipe contacted by the steam jet. No deposition of oxidation films on any surface appeared to have taken place.

The aerated pipe showed some spreading of the upstream end similar to that observed on the PVC specimen, only not as severe. Damage due to softening was restricted to about a 1-metre length, or less. The surface of the aerated channel did not appear to suffer any significant erosion damage. Some oxidation precipitates were found on the surface that were generally the same in appearance as found on the PVC specimen.

TRANSITE

A section of wall material from the closed pipe showed chemical attack of the cement binder to a depth of approximately 1 mm. Much of the cement in this zone had been leached out, although the matrix of asbestos fibers remained intact. Before cutting the wall open, the surface of the transite looked virtually undamaged. Damage to this material by chemical attack may be overlooked if inspection is confined to a casual view of the surface. Portland cement is subject to chemical attack by sulfate solution.[49] Insoluble reaction products often have a greater volume than the original compounds resulting in increased internal stresses.

Erosion damage to the closed pipe appeared to be minimal. Over long periods of time, however, erosion damage may increase as the wall becomes severely weakened by continual loss of the binder.

The aerated pipe showed about the same degree of deterioration as the closed one. Erosion damage over longer periods of time is difficult to predict in this situation, as effects due to the steam jet are reduced, although reduced pressures cause precipitation of solids which may increase damage in the condensate channel—particularly at the upstream end—where the exiting steam jet can act on the precipitates.

---

[47] J. Shimada and K. Kabuki. "The Mechanism of Oxidative Degradation of ABS Resin, Part I. The Mechanism of Thermooxidative Degradation," *J Appl Polymer Sci*, Vol. 12 (1968), pp. 655-69.

[48] Ibid, Part II, pp. 671-82.

[49] L. Heller and M. Ben-yair. "Effect of Sulfate Solutions on Normal and Sulphate-Resisting Portland Cement," *J Appl Chem*, Vol. 14 (January 1964), pp. 20-30.

GROUNDWATER-DILUTED STEAM RESULTS

STEEL

The anaerobic fluid condition resulted in the formation of a thick layer of loosely adherent, green-gray precipitates on the steel that smelled strongly of sulfur. An analysis of the coating identified a poorly crystallized hydrated ferric oxide (limonite) plus at least one additional nonmagnetic crystalline compound that could not be identified (Table 4). The unknown(s) had the same x-ray diffraction pattern as the unidentified corrosion product found in the steel specimen exposed to the anaerobic acid-sulfate fluid (Table 2). A chemical test identified a metal sulfide in the precipitate. An x-ray fluorescence analysis showed iron, silicon, and sulfur to be the major elements present. The coating was tested also for the presence of sulfates; none was found. Previous investigators have found free sulfur plus a variety of iron sulfides, stable, metastable, or amorphous in iron oxidation products, depending on the pH of the fluid, amount of hydrogen sulfide and oxygen present, and reaction time.[19,21,50,51] Iron sulfides mixed with other compounds are apparently very difficult to identify by x-ray diffraction methods, particularly if poorly crystallized.

Removing the deposit and examining the surface with a low-power binocular microscope showed corrosion to be relatively uniform and the rate to be low. An examination of the microstructure showed minor pitting of the surface to a depth of about 0.05 mm. Attack appeared to be heavier at both grain boundaries and near pearlite colonies. The presence of an iron sulfide in the layer of corrosion products, particularly one as loose and porous as this one seems to be, might serve as an additional source of galvanic corrosion because of its noble potential with respect to iron.[19]

No evidence of hydrogen infusion into the steel was found. Since the fluid pH is 5, and the hydrogen reduction reaction at the cathode becomes significant in steel only for acid solution with a pH below 4,[26] the amount of atomic hydrogen being generated may be insignificant in this situation.

---

[50] S. Takeno, H. Zôka, and T. Niihara. "Metastable Cubic Iron Sulfide - With Special Reference to Mackinawite," *Amer Mineral*, Vol. 55 (September 1970), pp. 1639-49.

[51] Robert A. Berner. "Iron Sulfides Formed From Aqueous Solution at Low Temperatures and Atmospheric Pressure," *J Geo*, Vol. 72 (1964), pp. 293-306.

TABLE 4. Corrosion Data From the Groundwater-Diluted-Steam Test Condition

Material	Aerated	Location		Precipitate	Name	Amount	Mode of attack	Maximum depth, mm	Maximum corrosion rate		Location of Maximum	Comments
									mm/yr	mpy		
Steel	No	Inlet	All	$FeOOH \cdot nH_2O$	Limonite	Medium	Pitting	0.05	0.05	2	Bottom	
Steel	No	Inlet	All	Iron sulfide	Unknown	Medium		...	...	...		Questionable
Steel	Yes	Inlet	Bottom	αFe_2O_3	Hematite	Medium		...	...	...		
Steel	Yes	Inlet	Bottom	Fe_3O_4	Magnetite	Medium		...	...	...		
Steel	Yes	Outlet	Bottom	$\alpha FeOOH$	Goethite	Medium	Channel	0.43	0.43	17	Bottom	
Steel	Yes	Outlet	Bottom	γFe_2O_3	Maghemite	Medium	Pitting	0.15	0.15	6	Side	
Cast iron	No	Inlet	All	Iron Sulfide	Unknown	Small	Uniform	0.8	0.8	31	Bottom	Rough surface
Cast iron	Yes	Inlet	Bottom	αFe_2O_3		Medium	Uniform	0.08	0.08	3	Bottom	Smooth surface
Cast iron	Yes	Inlet	Bottom	Fe_3O_4		Medium		...	...	...		
Cast iron	Yes	Outlet	Bottom	αFe_2O_3		Medium	Uniform	0.8	0.8	31	Bottom	Rough surface
Gal. steel	No	Inlet	Side	βZnS	Sphalerite	Small	Uniform	0.05	0.05	2	All	In zinc
Gal. steel	No	Inlet	Side	ZnO	Zincite	Trace		...	...	...		
Gal. steel	Yes	Inlet	Bottom	βZnS		Small	Uniform	0.05	0.05	2	All	In zinc
Gal. steel	Yes	Inlet	Bottom	ZnO		Trace		...	...	...		
Gal. steel	Yes	Inlet	Bottom	αFe_2O_3		Medium		...	...	...		
Gal. steel	Yes	Inlet	Bottom	Fe_3O_4		Medium		...	...	...		
Gal. steel	Yes	Outlet	Bottom	βZnS		Large	Uniform	0.05	0.05	2	All	In zinc
Gal. steel	Yes	Outlet	Bottom	ZnO		Small		...	...	...		
Gal. steel	Yes	Outlet	Bottom	αFe_2O_3		Small		...	...	...		
Gal. steel	Yes	Outlet	Bottom	γFe_2O_3		Small		...	...	...		
Aluminum	No	Inlet	Side	$Al_2O_3 \cdot 3H_2O$	Bayerite	Medium	Pitting	0.02	0.02	1	Side	
Aluminum	No	Inlet	Side	$Al_2O_3 \cdot 3H_2O$	Gibbsite	Medium		...	...	...		
Aluminum	Yes	Inlet	Side	$Al_2O_3 \cdot 3H_2O$	Bayerite	Medium	Pitting	0.03	0.03	1.2	Side	
Aluminum	Yes	Inlet	Side	$Al_2O_3 \cdot 3H_2O$	Gibbsite	Medium		...	...	...		
Aluminum	Yes	Inlet	Bottom	αFe_2O_3		Large		...	...	...		Fluid Precip.
Aluminum	Yes	Inlet	Bottom	γFe_2O_3		Medium		...	...	...		Fluid Precip.
Stainless steel	No	Inlet	Bottom	Fe_3O_4 deposit		Small	Grain boundary	0.02	0.02	1	Bottom	
Stainless steel	Yes	Outlet		αFe_2O_3 deposit			Grain boundary	0.03	0.03	1.2	Bottom	
Copper	No	Inlet	All	Cu_2S	Chalcocite	Trace	Pitting	Nil	...	...		
Copper	Yes	Inlet	All	$Cu_4(OH)_6SO_4$	Brochantite	Medium	Pitting	...	...	...		
Copper	Yes	Outlet	All	$Cu_4(OH)_6SO_4$	Brochantite	Medium	Pit	0.08	0.08	3	Side	Near water line
Copper	Yes	Outlet					Pitting	1.6	1.6	63	Side	Exterior
PVC	No	Inlet	All				Discoloration	4	...	...	All	Interior
PVC	Yes	Inlet	Bottom	Iron oxide stain		Small	Discoloration	4	...	...	All	Interior
PVC	Yes	Inlet					Channel	0.38	0.38	15	Bottom	Erosion
PVC	Yes	Inlet					Warping	...	...	...	Side	Heat induced
ABS	No	Inlet					Discoloration	1	...	...	All	Interior
ABS	No	Inlet					Blistering	...	...	...	Ceiling	Interior
ABS	Yes	Inlet	Bottom	Iron oxide stain			Discoloration	1	...	...	All	Interior
ABS	Yes	Inlet	Side	Iron sulfide			Blistering	...	...	...	All	Interior
ABS	Yes	Inlet					Crazing	...	...	...	Side	Interior
ABS	Yes	Inlet					Channel	0.46	0.46	18	Bottom	Erosion
ABS	Yes	Inlet					Warping	...	...	...		Heat induced
Transite	No	Inlet					Leaching	0.5	...	...	All	Cement gone
Transite	Yes	Inlet					Leaching	0.5	...	...	All	Cement gone

The aerated pipe was coated with a moderately thick layer of various ferric oxide corrosion products. Removal of these showed a corrosion groove cut into the bottom of the condensate channel, similar to the one found on the steel pipe tested in the acid-sulfate fluid, only not as deep. A maximum corrosion rate of about 0.43 mm/year (17 mils/year) was measured at the bottom of the groove. Some minor pitting was found on the sides of the open pipe, above the water line, at the downstream end. Pitting was probably the result of defects or breaks in the protective passivating oxide film found on the walls. Analysis of one sample of corrosion products from a copper tube exposed to the diluted steam found a quantity of chlorine. Significant amounts of the chloride ion in the fluid would tend to establish a greater level of pitting corrosion, rather than a more uniform attack.[5]

CAST IRON

The protective coating of tar was removed from the closed pipe, except for a small amount of residue in the condensate channel. A very thin film of corrosion products was found on the surface of the cast iron. Identification of the products was not attempted as not enough could be collected to run an analysis. However, the sulfurous smell from the film, plus prior analysis of this material in the acid-sulfate fluid suggested that the residue was the same as found on the steel pipe.

The surface showed fairly deep grooves, similar to those found on the cast iron tested in the sulfate fluid. The surface of this material was so uneven, initially, that it was difficult to tell whether the final surface pattern was due entirely to corrosion or partially to the casting process. If it was due entirely to corrosion, the corrosion rate was about 0.8 mm/year (31 mils/year).

The upstream end of the aerated pipe was noticeably free of the usual ferric oxide coating, and contained instead a residue of brittle tar on the bottom of the condensate channel and a thin coating on the walls of the sulfurous smelling residue found on the steel pipe. The surface of the cast iron was fairly smooth and corrosion appeared to be quite uniform. The rate of attack was estimated at 0.08 mm/year (3 mils/year).

The downstream end was covered with a moderately thick covering of ferric oxides (Table 4). Removing these showed extensive grooving of the surface in the flow direction (Figure 19). If this was due entirely to corrosion, the corrosion rate would be about the same as calculated for the anaerobic condition. An examination of the microstructure showed no noticeable leaching of the iron phase.

GALVANIZED STEEL

The anaerobic fluid condition resulted in nearly complete removal of the zinc coating by corrosion. The corrosion products were also sparse, either because of increased solubility in the corrodent or because they were not very adherent and were easily torn or abraded away by impacting water droplets. An analysis of the remaining products showed them to be a mixture of β-zinc sulfide and zinc oxide, with the former being the predominant species. Samples taken near the bottom of the pipe, in the condensate channel, showed the presence of the sulfurous-smelling deposit discussed previously, while the walls above the channel were stained a dark-brown from this same material. This unknown appeared to originate, at least in part, in the gathering system upstream from the test array or in the steam source itself. Contamination of the zinc corrosion products with this other residue could have resulted in it being less adherent. The possibility also existed for the initiation of galvanic corrosion between various parts of the film itself, particularly if it became highly contaminated. Zinc sulfide is soluble in acids,[52] although since it remained relatively intact in the presence of the stronger acid-sulfate fluid found at Devil's Kitchen, it wasn't expected to dissolve appreciably in the weaker, diluted steam found at the Coso resorts. Corrosion of the zinc coating appeared to be uniform and, while it was nearly completely gone, the steel underneath had not been attacked to any significant degree.

The aerated sample at the upstream end was covered with a thin coating of various ferric oxides plus zinc oxide and sulfide residues. The zinc plating was completely removed from the steel; however, corrosion of the latter was very slight. Attack appeared to be uniform, with material in the condensate channel showing slightly greater deterioration than the walls.

The zinc plating was nearly completely removed at the downstream end. The condensate channel was filled with a mixture of β-zinc sulfide, zinc oxide, and ferric oxides that formed an open botryoidal structure (Figure 20). Zinc sulfide was the main corrosion deposit found at the downstream end itself, while the amount of zinc oxide present appeared to increase toward the upstream end. Much of this residue appeared to be the remains of corrosion products that formed initially in upstream locations and were subsequently removed and transported downstream by the steam condensate. No significant corrosion of the steel pipe was found in the downstream areas. The zinc coating, however, was nearly completely removed as determined by an inspection of the microstructure.

---

[52] *Handbook of Chemistry and Physics*, 47th edition, R. C. Weast, ed. Cleveland, Ohio, The Chemical Rubber Company, 1966.

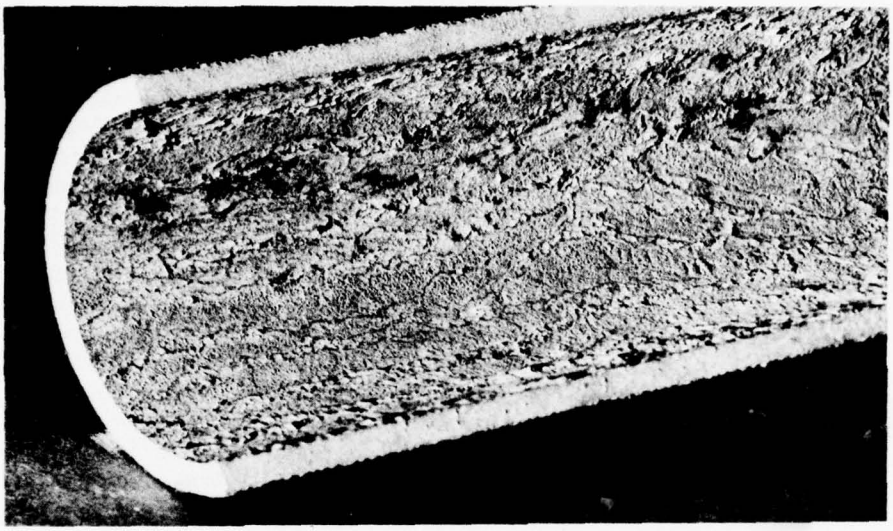

FIGURE 19. Outlet End of an Open Gray Cast Iron Pipe Exposed to Aerated Groundwater-Diluted Steam, After Cleaning, Showing Surface Grooves.

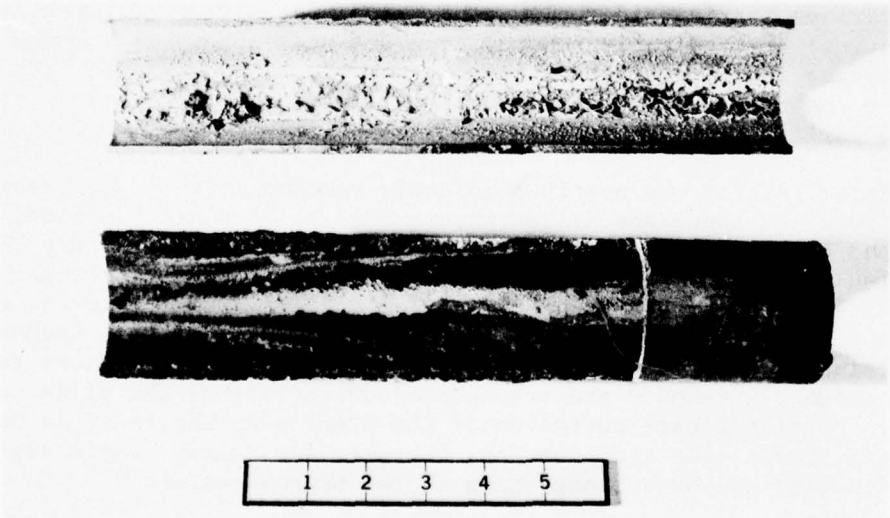

FIGURE 20. View of the Outlet (top) and Inlet (bottom) Areas of an Open, Galvanized Steel Pipe Exposed to a Groundwater-Diluted Steam. Flow is from right to left. Scale in inches.

ALUMINUM

The anaerobic fluid condition produced a thin, uneven film of white precipitates on the surface of the pipe in all locations other than the condensate channel which remained bare, except for a thin trail of black precipitate down the center. An x-ray diffraction analysis of the black residue showed it to be the hydrated iron oxide-sulfide mixture found in other pipes exposed to this fluid condition. Analysis of the white precipitate showed a mixture of two hydrated aluminum oxides, bayerite, and gibbsite[31,53] (Table 4) with the former being predominant. Both of these oxidation products are commonly found on aluminum exposed to a low temperature fluid with a pH of about 5.8. In fluids with a pH above that value, bayerite predominates, while in acid fluids, gibbsite forms. Where both form, the gibbsite may transform to bayerite with time.[53]

Corrosion of the aluminum was minor. An examination of its microstructure showed numerous tiny pits on the surface up to 0.02 mm deep. Pitting corrosion may have resulted from the nonuniform coating of hydrated oxides found in these areas. The possible presence of chloride ions in this steam as mentioned previously would tend to establish pitting corrosion as the dominant mode of attack, particularly on materials such as aluminum or stainless steel that form highly passivating, protective films on the surface.[26]

The walls of the aerated pipe at its upstream end were covered with a thick, uneven coating of bayerite and gibbsite in roughly equal proportions. This coating gradually disappeared toward the downstream end. The condensate channel at the upstream end contained a substantial deposit of ferric oxides, mainly hematite. This deposit was believed to initially be the sulfide-oxide mixture found in the closed pipes in this fluid system except that it had been gradually transformed to oxides in the hot, oxygenated condensate waters found in this location.

Corrosion of the aluminum occurred at the upstream end of the open channel only, and consisted mainly of numerous tiny pits up to 0.03 mm deep, in open spaces within the bayerite/gibbsite coating (Figure 21).

STAINLESS STEEL

The anaerobic fluid condition resulted in very minor corrosion of the closed pipe. An inspection of the microstructure showed some preferential attack to grain boundaries to a depth of about 0.02 mm.

---

[53] R. Schoen and C. Roberson. "Structures of Aluminum Hydroxide and Geochemical Implications," *Amer Mineral*, Vol. 55 (Jan. 1970), pp. 43-77.

A black deposit forming a thin narrow trail in the center of the condensate channel was analyzed as magnetite. This deposit was probably formed out of the sulfurous-smelling deposit found in this fluid system. The reason for its conversion to magnetite in this particular pipe was not established.

The surface of the aerated pipe was covered with a thin, reddish-brown film of ferric oxides. The walls above the condensate channel had a slight etched appearance in the direction of flow. A study of the microstructure showed minor corrosion to the surface, with attack concentrated at the grain boundaries. Grain boundary damage was less than 0.03 mm deep.

COPPER

Minor corrosion was found on the specimen exposed to anaerobic fluid conditions. The surface was covered with a very thin patchy tarnish of corrosion products. The tarnish was tentatively identified as Cu_2S, chalcocite, using the scanning electron microscope (Figure 22). No evidence of the sulfurous-smelling deposit was found in this pipe. An inspection of the microstructure showed very slight corrosion of the surface to a depth of about 0.005 mm.

The aerated specimen was covered with a moderately thick coating of blue-green corrosion products. These were identified principally as basic copper sulfates (Table 4). The presence of copper sulfides and oxides in the coating was suggested by the x-ray pattern, but could not be clearly verified. The corrosion products were thickest on the walls of the pipe, and at its upstream end. A thin coating of ferric oxides was also found on the bottom of the condensate channel on top of the sulfate deposits.

A study of the microstructure showed relatively minor corrosion within the condensate channel, up to 0.02 mm deep, and moderate to severe corrosion to the walls above, with the corrosion rate increasing toward the top edge of the open pipe and toward the upstream end. Attack was by pitting (Figures 23-25), and showed no apparent relation to the grain boundary network along the surface. The exterior surface of this specimen of pipe was severely pitted by condensing steam vapors (Figure 26) as the wooden insulating supports became soaked with moisture. Pitting corrosion of copper is fairly common in oxidizing environments, particularly when the corrosion products do not form a uniform protective coating on the metal or when debris is present on the surface allowing differential aeration or other concentration cells to form.[39]

One sample of corrosion products from the anaerobic pipe was analyzed for mercury. A concentration of 113 ppm was obtained using atomic absorption spectroscopy (Table 3).

FIGURE 21. A Photomicrograph Showing Pitting Corrosion in an Open Aluminum Pipe Exposed to Aerated Groundwater-Diluted Steam. (200X)

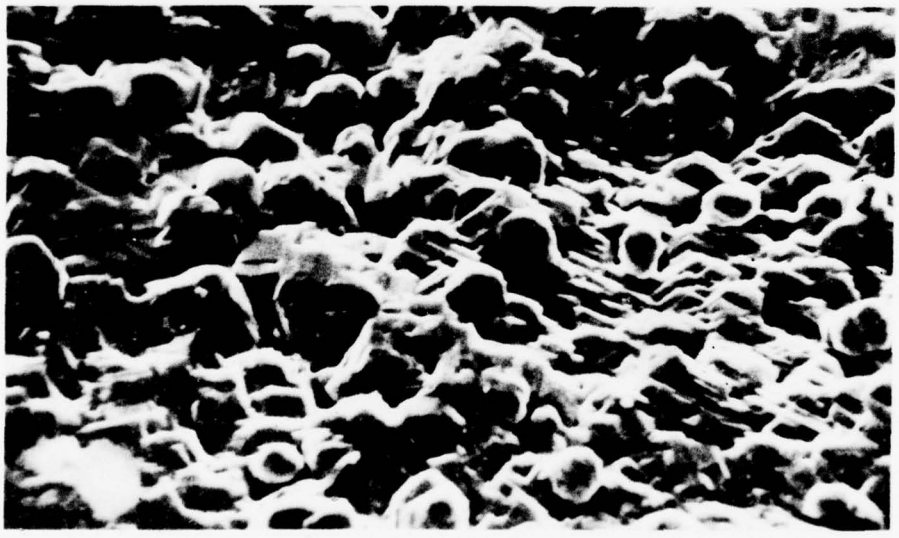

FIGURE 22. A Scanning Electron Microscope Photomicrograph of Silver-Gray, Plate-Like Sulfide Corrosion Products in a Closed Copper Tube Exposed to Anaerobic Groundwater-Diluted Steam, Identified as Cu_2S, Chalcocite. (320X)

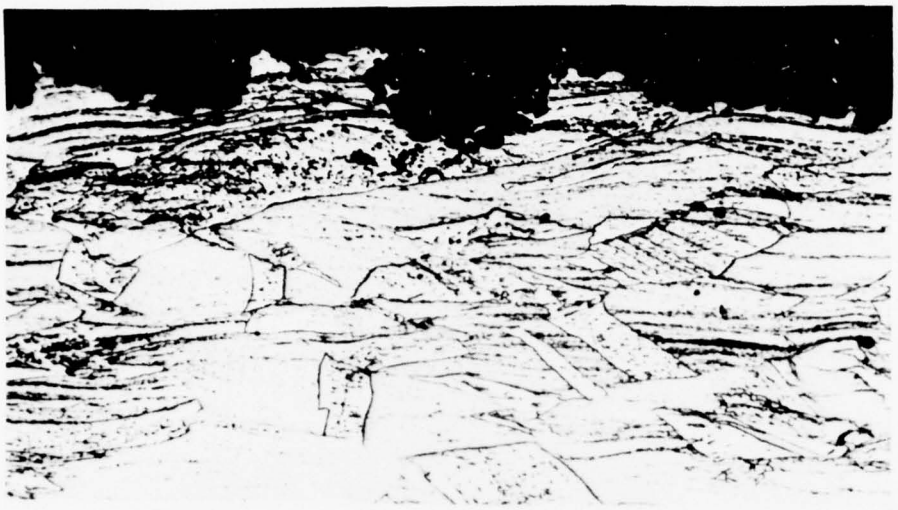

FIGURE 23. A Photomicrograph Showing Pitting Corrosion in an Open Copper Pipe Exposed to Aerated Groundwater-Diluted Steam. (200X)

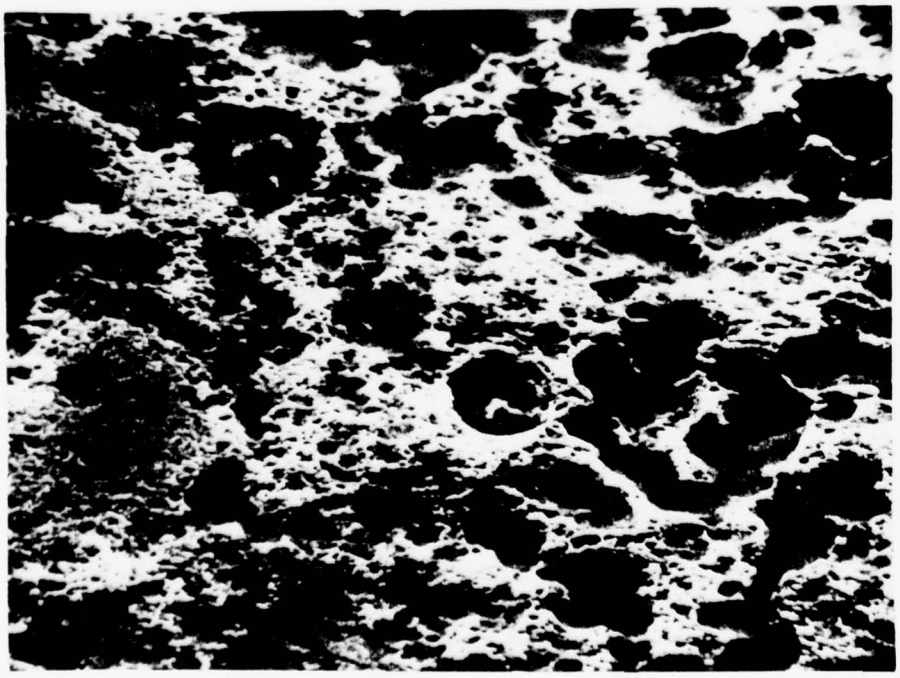

FIGURE 24. A Scanning Electron Microscope Photomicrograph Showing Pitting Corrosion of the Copper Specimen Described in Figure 23. (210X)

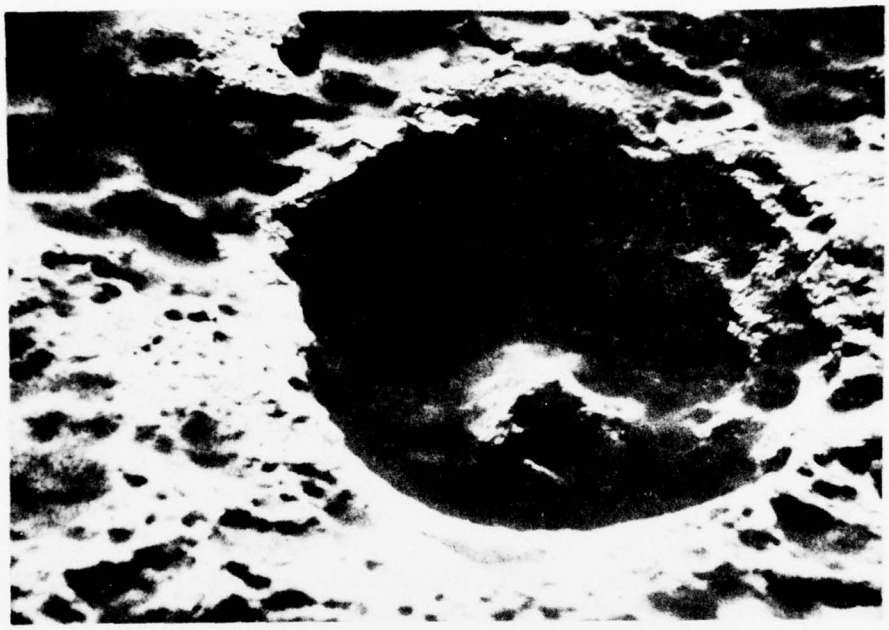

FIGURE 25. A Scanning Electron Microscope Photomicrograph Showing the Bottom of a Pit Viewed in Figure 24. (1060X)

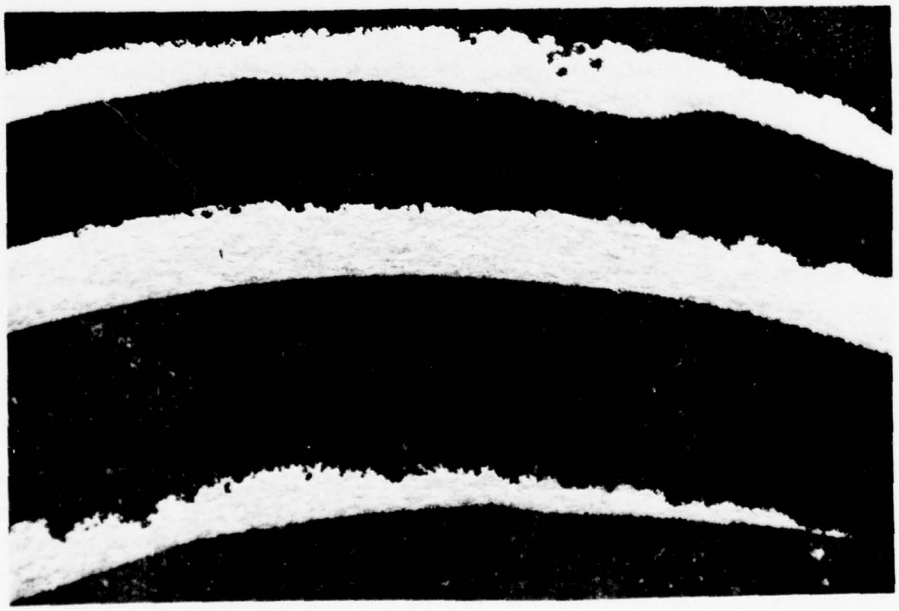

FIGURE 26. A Section View of the Specimen Described in Figure 23 Showing Pitting Corrosion of the External Copper Surface.

PVC PLASTIC

The anaerobic fluid resulted in appreciable bleaching of the wall and perhaps some embrittlement of the plastic. No voids were found within the bleached zone in contrast to the PVC specimen tested in the acid-sulfate fluid, which meant that there was probably no significant formation of volatiles in this situation, or that the volatiles formed were expelled before pressures built up sufficiently to cause voids to form. The first explanation is probably the more likely.

No erosion damage was found in the closed pipe as a result of steam flow through it. No precipitates were found in this specimen other than a slight stain on the bottom of the corrosion channel.

The aerated specimen at its upstream end showed about the same degree of softening (Figure 27) as found in the PVC sample tested in the acid-sulfate fluid. No evidence of surface cracks, blisters, or internal voids were found, however.

The open condensate channel was coated with a sequence of black-to-red-to-brown precipitates at the upstream end. Although not analyzed, the black precipitate appeared to be the sulfurous-smelling deposit found in the other pipes. The red and brown compounds were various ferric oxides probably derived from oxidation of the sulfide compound.

A depression in the center of the condensate channel, about 0.38 mm deep, was noticed at the upstream end of the open pipe and classified as an erosion feature. It was probably caused by scouring from precipitates that continually formed just above the area and were then swept downstream by the exiting steam jet.

ABS PLASTIC

The closed pipe showed some slight discoloring of the surface that had been in contact with the fluids. Numerous tiny blisters were found on this surface which indicated the formation of small quantities of gas, internally. Although this particular plastic is normally quite stable, some depolymerization of styrene may have taken place at elevated temperatures.

No evidence of surface erosion was found in the closed specimen. The interior surface was generally free of precipitation coatings, except for a thin trail of residue found on the bottom of the condensate channel.

The aerated pipe at its upstream end was discolored on the inner surface and showed some blistering identical to that found in the closed pipe. The pipe in this region showed some effects of softening similar

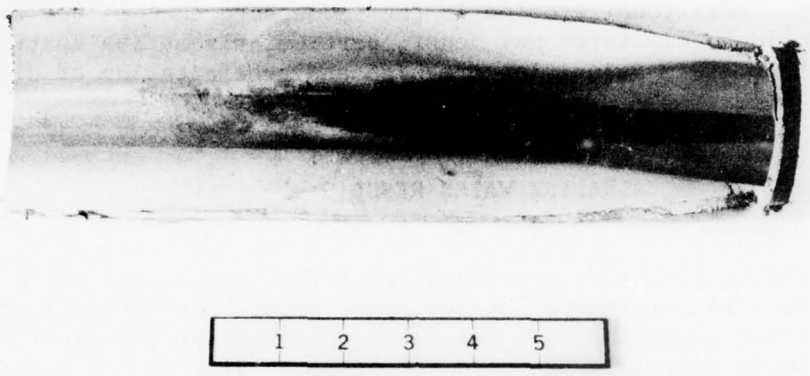

FIGURE 27. Inlet End of an Open PVC Pipe Exposed to Aerated Groundwater-Diluted Steam. Flow is from right to left. Scale in inches.

to those observed previously for this material. In addition to blistering, some crazing of the surface was observed on the walls above the condensate channel in areas covered with a thin film of gray precipitates. The precipitate was not identified, although it appeared to be primarily an iron sulfide-oxide mixture.

Some erosion of the condensate channel was observed. The contour of the eroded surface generally coincided with the deposition of a coating of iron oxidation products identical to those found on the PVC specimen. The erosion mechanism was probably the motion of iron oxidation products through the channel. A maximum erosion depth of 0.45 mm was measured about 15 cm downstream from the inlet.

Discoloration, softening effects, and surface crazing rapidly declined toward the downstream end of the pipe. However, some embrittlement of the material was felt to have occurred throughout its length.

TRANSITE

A section of wall material from the closed pipe showed about 0.5 mm of penetration by chemical attack. Virtually all of the cement in this zone had been leached out. The asbestos fiber matrix remained essentially intact, although the load-bearing capacity of the wall had been reduced. The erosion rate should begin to increase as the surface layer weakens, although no appreciable erosion had occurred in this particular test.

The aerated specimen showed essentially the same degree of deterioration as the closed pipe. Erosion effects due to steam impingement should be less over a larger time frame because of the reduced pressures in this region. Additional erosion in the condensate channel due to scouring by solid precipitates may occur, particularly at the upstream end where exiting steam velocities are high and precipitation of dissolved solids occur.

ALKALINE WATER RESULTS

The analyses of corrosion processes resulting from contact with this fluid condition were complicated by the added presence of several additional crystalline compounds that deposited on the pipes in significant quantities. These generally produced strong x-ray diffraction patterns that often masked those produced by corrosion products and made identification of the latter more difficult. Their presence on the surface of the samples also resulted in more complex corrosion conditions, primarily by restricting the flow of dissolved oxygen to parts of the surface and by modifying flow conditions.

One of the contaminants was a light-brown clay mineral that collected in great abundance on the bottom of the water channel in all locations of the pipe. This clay mineral, illite, which was identified using differential thermal analyses techniques, produced a very noisy, complex x-ray diffraction pattern. Since clay minerals consist of tiny light particles that stay in suspension in liquids for long periods of time, some success was achieved using simple gravity separation in water to remove the clay from the corrosion products.

A second contaminant, sodium chloride, precipitated out along the walls above the water line in the open aerated pipes (Figure 28). Its high solubility allowed it to be easily separated from the corrosion products most of the time. Some feldspar minerals were also found mixed in with the corrosion products. Although these could not be physically separated from the corrosion products, their x-ray patterns were readily identified.

In general, corrosion products found on the zinc and copper specimens could be usually identified by x-ray diffraction analyses, while those on the iron and steel samples were very difficult to identify as the diffraction patterns were noisy. Magnetic iron oxides could be separated from the other products and usually identified by color and streak. Metal sulfides were found using simple chemical identification techniques. The x-ray diffraction patterns of samples taken from below the water line were generally very noisy, complex, and showed the presence of additional compounds that could not be readily identified. The process of dissolving contaminants may also have inadvertently introduced some extraneous compounds.

STEEL

The anaerobic fluid condition resulted in the deposition of a thin uneven layer of corrosion products composed mainly of magnetite on surfaces above the water line, and a loose coating of a hydrated ferric oxide plus one or more ferric oxides on surfaces below the water line (Table 5), as determined by x-ray diffraction analysis. The hydrated ferric oxide identified (lepidocrocite) commonly forms in alkaline solutions containing chloride ions.[54,55] Chemical analyses also verified the presence of a metal sulfide on all surfaces. A study of the microstructure showed localized pitting corrosion to be the dominant mode of attack (Figure 29). Corrosion below the water line appeared to be more severe, with pits up to 0.25 mm in depth being found in these areas. Pits tend to grow larger, generally, in the direction of gravity.[5] Additionally, the loose hydrated oxide film found below the water line would tend to be less protective. No relation was found between microstructural features and pitting locations. However, pitting corrosion of steel in a chloride solution containing hydrogen sulfide has been observed previously[56] and attributed to the presence of mill scale (magnetite) on the surface of the steel. A separate study attributed localized corrosion in acidic hydrogen sulfide-sodium chloride solutions containing an oxidant to the formation of H_2S_2.[57]

Magnetite was the only corrosion product identified on the aerated specimen at the upstream end while magnetite and/or maghemite were found at the downstream end. From the appearance of the coatings, other ferric oxides and hydrated oxides may have been present, but were not readily identified by x-ray diffraction analyses. The oxide layers did not appear to be either very uniform or adherent.

Corrosion was more severe on the aerated surface than on the one exposed to anaerobic fluids. Again, the attack was generally localized with the size of the major pits increasing toward the downstream end and also toward the bottom of the water channel. The density and size of tiny pits was about the same for the aerated and anaerobic conditions.

---

[54] J. Bernal, D. Dasgupta and A. Mackay. "The Oxides and Hydroxides of Iron and Their Structural Interrelations," *Clay Minerals Bull*, Vol. 4 (1959), pp. 15-30.

[55] R. T. Foley. "Role of the Chloride Ion in Iron Corrosion," *Corrosion*, Vol. 26, No. 2 (February 1970), pp. 58-70.

[56] L. M. Dvoracek. "Pitting Corrosion of Steel in H_2S Solutions," *Corrosion*, Vol. 32, No. 2 (February 1976), pp. 64-8.

[57] P. R. Rhodes. "Corrosion Mechanisms of Carbon Steel in Aqueous H_2S Solutions," *Electrochem Soc, J*, Vol. 123, No. 8 (August 1976), p. 247c (abstract only).

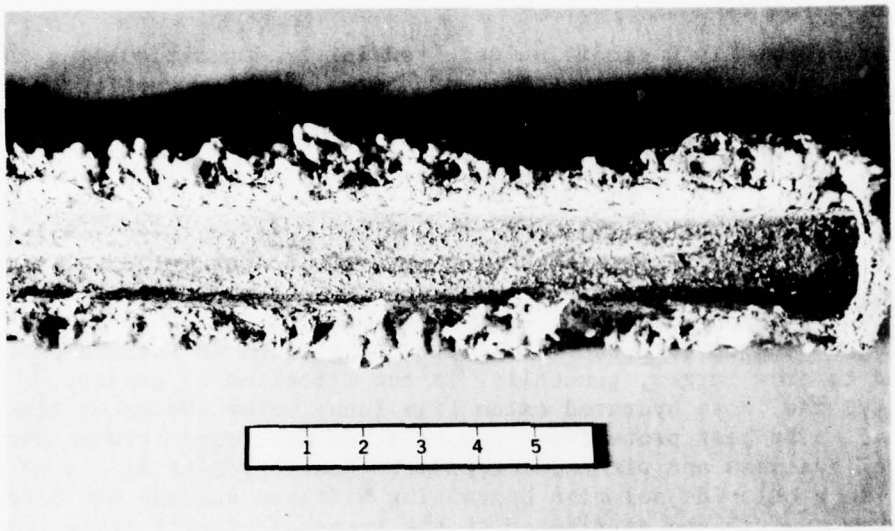

FIGURE 28. Inlet End of an Open Aluminum Pipe Exposed to Hot Aerated Alkaline Water Showing Sodium Chloride Precipitation. Flow is from right to left. Scale in inches.

FIGURE 29. A Photomicrograph Showing Pitting Corrosion in a Closed Steel Pipe Exposed to Hot, Anaerobic Alkaline Fluids. (200X)

TABLE 5. Corrosion Data From the Alkaline Water Test Condition.

Material	Aerated	Location		Precipitate	Name	Amount	Dominant mode of attack	Maximum depth, mm	Maximum corrosion rate		Location of Maximum	Comments
									mm/yr	mpy		
Steel	No	Inlet	Side	Fe_3O_4	Magnetite	Small		...	...	...		
Steel	No	Inlet	Side	Iron sulfide	Unknown	Trace		...	...	...		
Steel	No	Inlet	Bottom	$\gamma FeOOH$	Lepidocrocite	Small	Pitting	0.25	1.3	51	Bottom	
Steel	No	Inlet	Bottom	Fe_3O_4		Small		...	...	...		
Steel	No	Inlet	Bottom	γFe_2O_3	Maghemite	Small		...	...	...		
Steel	Yes	Inlet	Bottom	Fe_3O_4		Small		...	...	...		
Steel	Yes	Outlet	Bottom	Fe_3O_4		Small	Pitting	1.0	5.2	205	Bottom	Perf. in 1 year
Steel	Yes	Outlet	Bottom	γFe_2O_3				...	...	...		
Cast iron	No	Inlet	Side	Fe_3O_4		Small	Uniform	0.2	1.04	41	Bottom	
Cast iron	No	Inlet	Side	Iron sulfide	Unknown	Trace		...	...	...		
Cast iron	Yes	Outlet					Uniform	0.15	0.78	31	Bottom	
Gal. steel	No	Inlet	Side	ZnO	Zincite	Medium	Pitting	0.05	0.26	10	Bottom	In zinc
Gal. steel	No	Inlet	Side	βZnS	Sphalerite	Medium		...	...	...		
Gal. steel	No	Outlet	Bottom	$Zn_4(OH)_2Si_2O_7 \cdot H_2O$	Hemimorphite	Medium		...	...	...		
Gal. steel	Yes	Inlet	Bottom	ZnO		Small		...	...	...		
Gal. steel	Yes	Outlet		$Zn_5(OH)_8Cl$	Basic zinc chloride	Trace	Pitting	0.05	0.26	10	Bottom	In zinc
Aluminum	No	Inlet	Bottom	Amorphous		Medium	Pitting	2.0	10.4	410	Bottom	Perf. in 20 weeks
Aluminum	Yes	Outlet					Pitting	1.0	5.2	205	Bottom	Perf. in 1 year
Stainless steel	No	Inlet					Pitting	0.03	0.16	6	Bottom	
Stainless steel	Yes	Inlet					Pitting	0.05	0.26	10	Bottom	
Stainless steel	Yes	Inlet					Transgranular	4	...	...	Side	
Copper	No	Inlet	Bottom	Cu_2O	Cuprite	Medium	Pitting	0.05	0.26	10	Bottom	
Copper	No	Inlet	Bottom	Cu_2S	Chalcocite	Medium		...	...	...		
Copper	No	Inlet	Bottom	Cu_5FeS_4	Bornite	Trace		...	...	...		
Copper	No	Inlet	Side	Cu_2O		Large		...	...	...		
Copper	No	Inlet	Side	Cu_2S		Small		...	...	...		
Copper	No	Inlet	Ceiling	Cu_2O		Medium		...	...	...		
Copper	No	Inlet	Ceiling	CuO	Tenorite	Medium		...	...	...		
Copper	No	Inlet	Ceiling	$Cu_4(OH)_6SO_4$	Brochantite	Trace		...	...	...		
Copper	Yes	Inlet	Bottom	Cu_2O		Small	Pitting	0.04	0.21	8	Bottom	
Copper	Yes	Inlet	Bottom	$Cu_2(OH)_3Cl$	Atacamite Paratacamite	Small		...	...	...		
Copper	Yes	Inlet	Bottom	Cu_2S		Trace		...	...	...		
Copper	Yes	Outlet					Pitting	0.05	0.26	10	Bottom	
PVC	No	Inlet					Discoloration	2	...	...	All	Interior
PVC	Yes	Inlet					Discoloration	2	...	...	All	Interior
PVC	Yes	Inlet					Warping	...	...	...		Heat induced
ABS	Yes	Inlet					Warping	...	...	...		Heat induced
Transite	No	Inlet						...	...	...		Cement not attacked
Transite	Yes	Inlet						...	...	...		Cement not attacked

However, the aerated pipe also contained a scattering of some very large pits, up to 1 mm in depth in the bottom of the water channel (Figure 30). These tended to increase in size and number toward the downstream end. Since the amount of dissolved oxygen in the water should have been greater at the downstream end where temperatures were lower, the formation of these large pits may have required the presence of larger quantities of oxygen, in addition to chloride ions. Pitting of metals in aerated chloride solutions is fairly common.[5,58]

CAST IRON

A very thin coating of corrosion products was found on the surface of the closed pipe above the water line that was tentatively identified as being mostly magnetite. Below the water line, corrosion products appeared to include several ferric oxides and hydrated oxides. Oxide products were identified from x-ray diffraction patterns that were of poor quality. The identification of magnetite was aided by its magnetic property, color, and streak. In addition to the oxides, the corrosion products in all areas contained a metal sulfide which was identified by chemical analysis alone. The corrosion products generally did not provide a uniform adherent coating. The protective coating of tar was completely removed by the hot waters.

The anaerobic fluid condition resulted in fairly uniform corrosion of the cast iron. Pitting of the surface was judged to be slight. Corrosion did not appear to follow surface irregularities as noticed on the cast iron specimens tested in the other fluid systems. The corrosion rate was estimated to be less than 1.0 mm/year (41 mils/year).

Corrosion products found on the aerated pipe appeared to be ferric oxides and hydrated oxides. In general, they were poorly adherent, flaking off easily, and did not appear to provide any protection to the metal. Corrosion of the surface was generally uniform, particularly at the upstream end, and the rate was judged to be about the same as for the anaerobic condition. A study of the microstructure showed essentially no leaching of the iron phase.

GALVANIZED STEEL

The anaerobic fluid condition resulted in the formation of a thin, white coating on the zinc above the water line that was identified as a

---

[58] Jose R. Galvele. "Transport Processes and the Mechanism of Pitting of Metals," *Electrochem Soc, J*, Vol. 123, No. 4 (April 1976), pp. 464-74.

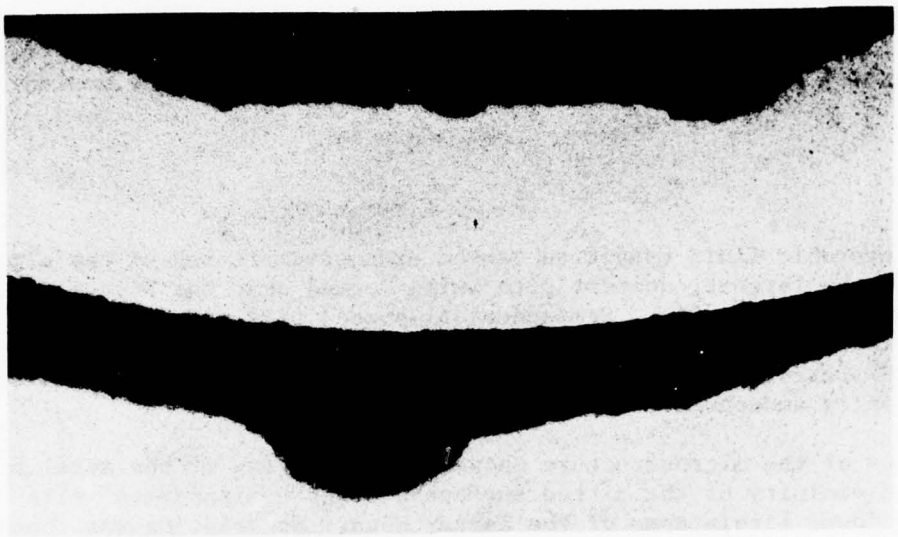

FIGURE 30. A Section View of an Open Steel Pipe Exposed to Hot, Aerated Alkaline Fluids Showing Pitting Corrosion.

mixture of β-zinc sulfide and zinc oxide in roughly equal proportions. The thicker, brown-white corrosion products found below the water line were identified as a hydrated zinc silicate, hemimorphite.

An inspection of the surface using a low-powered binocular microscope showed the presence of numerous, tiny pits beneath the covering of corrosion products. A study of the microstructure showed that although the zinc was nearly gone in most locations, the steel underneath had not been attacked to any degree. Pitting appears to have been confined essentially to the zinc. Zinc commonly pits in aerated chloride solutions.[58]

The aerated specimen initially appeared to have suffered extensive corrosion. Numerous large, shallow pits were observed on the walls and floor of the pipe, both above and below the water line. An inspection of the microstructure showed the pits to be confined to the zinc itself, while the steel remained untouched. No appreciable corrosion of the steel took place even where the pit had exposed the bare metal. Much of the zinc coating remained intact in areas some distance from pit locations.

An analyses of the corrosion product on the aerated zinc specimen showed it to be principally zinc oxide. A small amount of basic zinc chloride was found also at the downstream end. The presence of chloride ions in solutions at these temperatures is believed to suppress the

reversal of potential that occurs between the zinc and the iron due to the presence of the oxide corrosion product.[26] The solubility of oxygen, which promotes this reversal, is also reduced as the chloride content is increased.

ALUMINUM

The anaerobic fluid condition caused extensive pitting of the aluminum, with the largest, deepest pits being formed near the bottom of the water channel (Figure 31). Hemispherical-shaped pits, up to 2 mm in depth were found in these areas covered over with white solid products. An x-ray diffraction analysis of the corrosion products showed them to be essentially amorphous compounds.

A study of the microstructure showed some cracking of the metal on and in the vicinity of the pitted surfaces. Tiny hemispherical pits were also found within some of the larger ones. No relation was found between the initiation sites for the pits and the location of secondary phases or grain boundaries in the metal.

Chloride ions stimulate pitting corrosion in aluminum,[26] particularly in areas where solid matter has collected and differential aeration of the surface occurs. The accumulation of clay minerals on the floor of the water channel may serve to create conditions favorable for the initiation of oxygen cell corrosion. The abundance of oxide corrosion products on most of the pipes exposed to this particular anaerobic fluid condition demonstrates the presence of dissolved oxygen in the fluid. Dissolved oxygen may also oxidize ferrous ions in the fluid to ferric ions, which in turn react with aluminum to deposit iron on the surface, which then initiates localized corrosion.

The aerated sample suffered extensive pitting; however, the pits were typically irregular in shape rather than hemispherical and were much shallower within the water channel (Figure 32). Above the water line, under an extensive covering of sodium chloride precipitate, some large, generally irregularly shaped pits up to 1.4 mm deep, were observed. The reason for the change in shape of the pit in the aerated specimen was not established. However, the extensive precipitation of sodium chloride that occurs in this region and subsequent reduction in its solution concentration may influence the pitting process somewhat. The increased oxygen content in the water may also be a factor. The shape of a corrosion pit is believed to be a function of the current density in the pit and properties of the metal.[59]

---

[59] Z. Szklarska-Smialowska. "Review of Literature on Pitting Corrosion Published Since 1960," *Corrosion*, Vol. 27, No. 6 (June 1971), pp. 223-33.

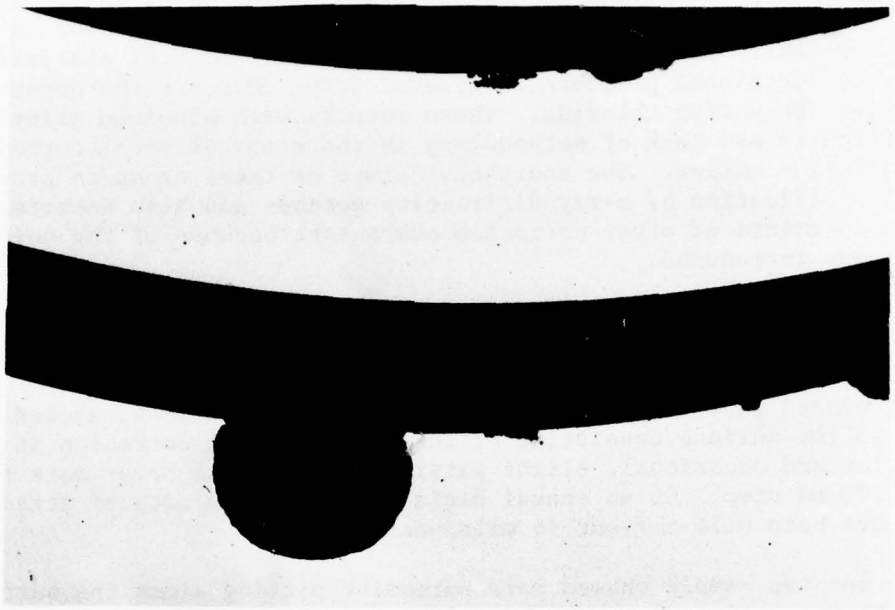

FIGURE 31. A Section View of a Closed Aluminum Pipe Exposed to Hot, Anaerobic Alkaline Fluids, Showing *Pitting Corrosion*.

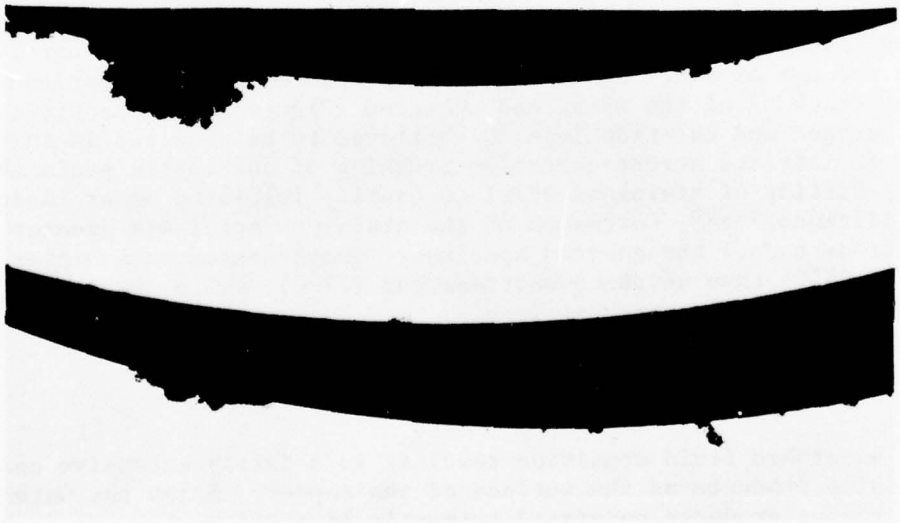

FIGURE 32. A Section View of an Open Aluminum Pipe Exposed to Hot, Aerated Alkaline Fluids, Showing Pitting Corrosion.

The salt deposits found on the aerated aluminum specimen proved difficult to remove, in contrast to those found on other specimens which flaked off easily or readily dissolved in water. An x-ray analysis showed the additional presence of gypsum, $CaSO_4 \cdot 2H_2O$, in the deposit, along with the sodium chloride. These results with aluminum illustrate the difficulty and lack of methodology in the study of metal corrosion in an alkaline medium. The amorphous nature of these products prevents ready identification by x-ray diffraction methods and also interferes with measurements of other corrosion components because of the noisy backgrounds introduced.

STAINLESS STEEL

The closed pipe, exposed to anaerobic fluid conditions, showed minor attack to the surface consisting of some preferential corrosion at grain boundaries and occasional, slight pitting. Attack was never more than about 0.03 mm deep. On an annual basis, however, the rate of attack would have been 0.16 mm/year (6 mils/year).

The aerated sample showed more extensive pitting along the surface below the water line than was observed under anaerobic conditions, particularly at the upstream end. An inspection of the surface using a low-powered binocular microscope showed clusters of tiny, shallow pits on the surface below and above the water line. Examination of the microstructure showed these to be about 0.05 mm deep. Some preferential attack to the grain boundaries was noticed. Deeper corrosion pits up to 0.38 mm in depth were observed near the upper boundary of the open pipe, in areas where the sodium chloride had precipitated out. At the upper boundary itself, where plastic deformation of the pipe had occurred during the process of slitting it to form the open channel, extensive transgranular cracking of the metal had occurred (Figure 33). The presence of both oxygen and chloride ions is believed to be required in an electrolyte to initiate stress corrosion cracking of austenitic stainless steel.[2] Pitting of stainless steel is usually initiated under these same conditions.[26,58] Corrosion of the stainless steel was greater at the upstream end of the aerated specimen. Temperatures were higher at this end (94°C) than at the downstream end (77°C), while the degree of aeration was probably somewhat less.

COPPER

The anaerobic fluid condition resulted in a fairly extensive coating of corrosion products on the surface of the copper. Below the water line corrosion products consisted primarily of a 3:1 mixture of Cu_2O and Cu_2S, and a small amount of Cu_5FeS_4 (bornite). Approximately midway up the wall, Cu_2O plus a small amount of Cu_2S were identified. On the ceiling of the pipe, products consisted of equal proportions of Cu_2O and

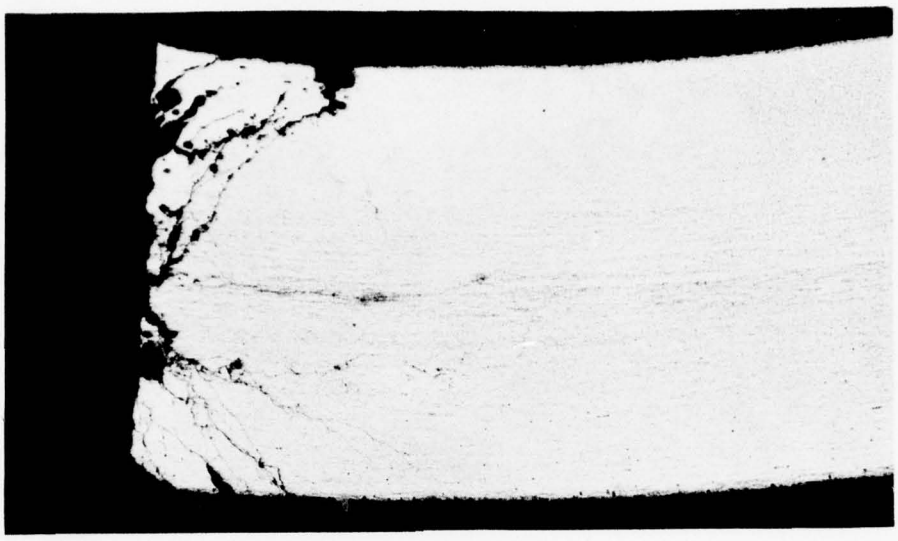

FIGURE 33. A Section View of an Open Stainless Steel Pipe Exposed to Hot, Aerated Alkaline Fluids, Showing Transgranular Stress-Corrosion Cracking.

CuO plus a small amount of basic copper sulfate, brochantite. Corrosion of the surface, however, was modest with preferential attack generally taking place at grain boundaries (Figure 34). Some minor pitting to a depth of 0.05 mm was noticed at lower portions of the surface that appeared to initiate at grain boundaries.

Corrosion to the aerated sample was approximately the same as for the closed, anaerobic condition except for an increased density of pits on the surface below the water line (Figure 35). Their average depth was approximately the same as for the other specimen. Attack again was concentrated at grain boundaries.

A thin coating of corrosion products was found on the aerated surface. It consisted mainly of Cu_2O, $Cu_2(OH)_3Cl$, and a small amount of Cu_2S (at the upstream end only). Cuprous oxide is normally noble to copper itself, which can result in pitting of the metal under conditions where the coating is not uniform and the electrolyte is aggressive.[8] The basic cupric chloride, atacamite (and/or paratacamite) is a common corrosion product in aerated sea water environments.[60]

---

[60] J. Sharkey and S. Lewin. "Conditions Governing the Formation of Atacamite and Paratacamite," *Amer Mineral*, Vol. 56 (January 1971), pp. 179-92.

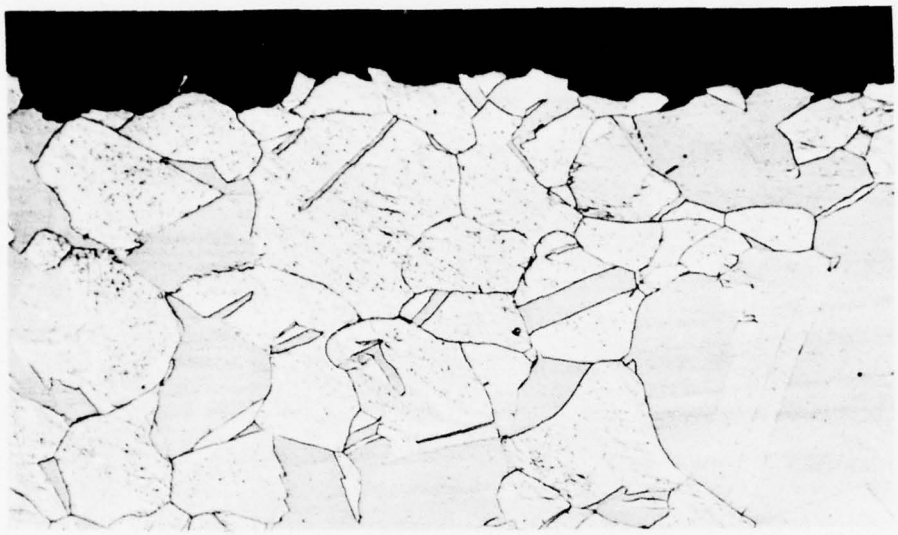

FIGURE 34. A Photomicrograph Showing Surface Corrosion of a Closed Copper Tube Exposed to Hot, Anaerobic Alkaline Fluids. (200X)

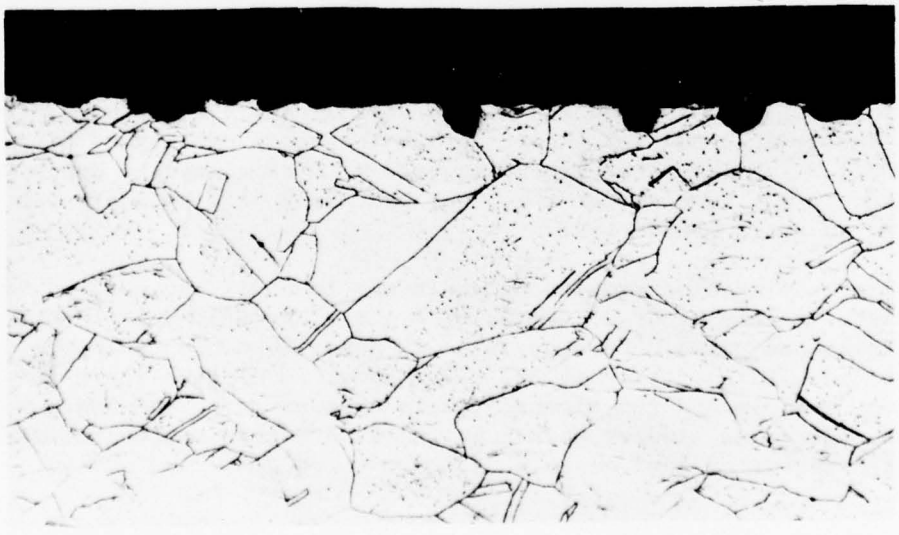

FIGURE 35. A Photomicrograph Showing Pitting Corrosion of an Open Copper Tube Exposed to Hot, Aerated Alkaline Fluids. (200X)

Two samples of corrosion products (one from each fluid condition) were analyzed for mercury. The sample from the anaerobic fluid condition was found to contain 113 ppm of mercury while that from the aerated pipe contained 79 ppm.

PVC PLASTIC

The closed pipe suffered no apparent damage other than some discoloration of the inside surface. No significant erosion of the wall occurred and no blistering was observed. Some embrittlement of the plastic may have occurred.

The aerobic pipe showed some bleaching of the inside surface and spreading of the walls at the upstream end due to heat-induced softening of the material. No measurable erosion of the channel was found.

ABS PLASTIC

The closed pipe suffered no observable damage other than some possible embrittlement. The open, aerated pipe showed no damage other than heat-induced softening of the upstream end resulting in spreading of the walls.

TRANSITE

A sample of wall material from the closed pipe showed no evidence of chemical attack to the cement binder. Some chloride solutions will attack portland cement.[61] In the present circumstance, however, mechanical erosion processes from contact with the fluid may be the major removal mechanism. No erosion features were found on the surface.

The aerated pipe also showed no damage during this brief time frame. The presence of large amounts of clay minerals in the water may lead to increasing levels of erosion over a larger span of time.

COMPARISON OF RESULTS

Comparing results from the two steam installations was a relatively straightforward task as the fluids were chemically similar and so were

---

[61] L. Heller and M. Ben-yair. "Effect of Chloride Solutions on Portland Cement," *J Appl Chem*, Vol. 16 (August 1966), pp. 223-26.

the flow conditions. Exposure times were also identical and were long enough to establish a yearly corrosion rate for each material with some measure of confidence. The accuracy of any value was limited somewhat by the number of measurements taken, but was believed to be adequate for comparison purposes.

Comparisons with the alkaline fluid were not as easily made because the mode of attack was often markedly different. In addition, corrosion rates in this situation were established from a relatively short test period and may not be directly comparable to those obtained over significantly longer periods of time. Corrosion rates for situations involving uniform attack are not often linear, but usually decrease with time as corrosion products build up on the surface and rates become diffusion dependent.[4] The appearance of breaks in the protective film, however, may periodically accelerate attack in localized areas and change the mode of attack from uniform to pitting. Pitting rates are quite variable, as an individual pit may become inactive and stabilize at a small size for extended periods of time, then grow very rapidly over a short time interval. This expansion process, once initiated, becomes self-sustaining i.e., autocatalytic.[5] Stress corrosion cracking may aid the growth process.[62] Pitting corrosion rates determined over one span of time may be substantially in error, then, when used to predict the degree of damage over considerably different time intervals.

Figure 36 compares corrosion rates for all of the materials studied in the three environments at the Coso Thermal Area, and under aerated and anaerobic test conditions. The comparisons that follow should be viewed for the most part as a rough guide when used for evaluating the performance of materials in the three Coso geothermal environments.

CORROSION PRODUCT CONTAMINATION

Corrosion products found on the specimens were generally contaminated with additional elements as shown by x-ray fluorescence analysis. Of 16 samples examined, 13 contained significant quantities of silicon. Large amounts of silica (opal) in the coatings might lead to possible scaling problems over longer periods of time. Approximately 50% of the samples from the alkaline test condition contained chlorine and bromine, while copper corrosion products from the acid sulfate test condition contained barium. Other common elements found included aluminum, iron, potassium, calcium and sulfur. The effects that these additional elements had on the properties of the coatings were not established.

---

[62] A. Goldberg and L. Owen. "Pitting Corrosion in Plain Carbon Steel Exposed to Geothermal Brine," *Electrochem Soc, J*, Vol. 123, No. 8 (August 1976), pp. 248c-49c (abstract only).

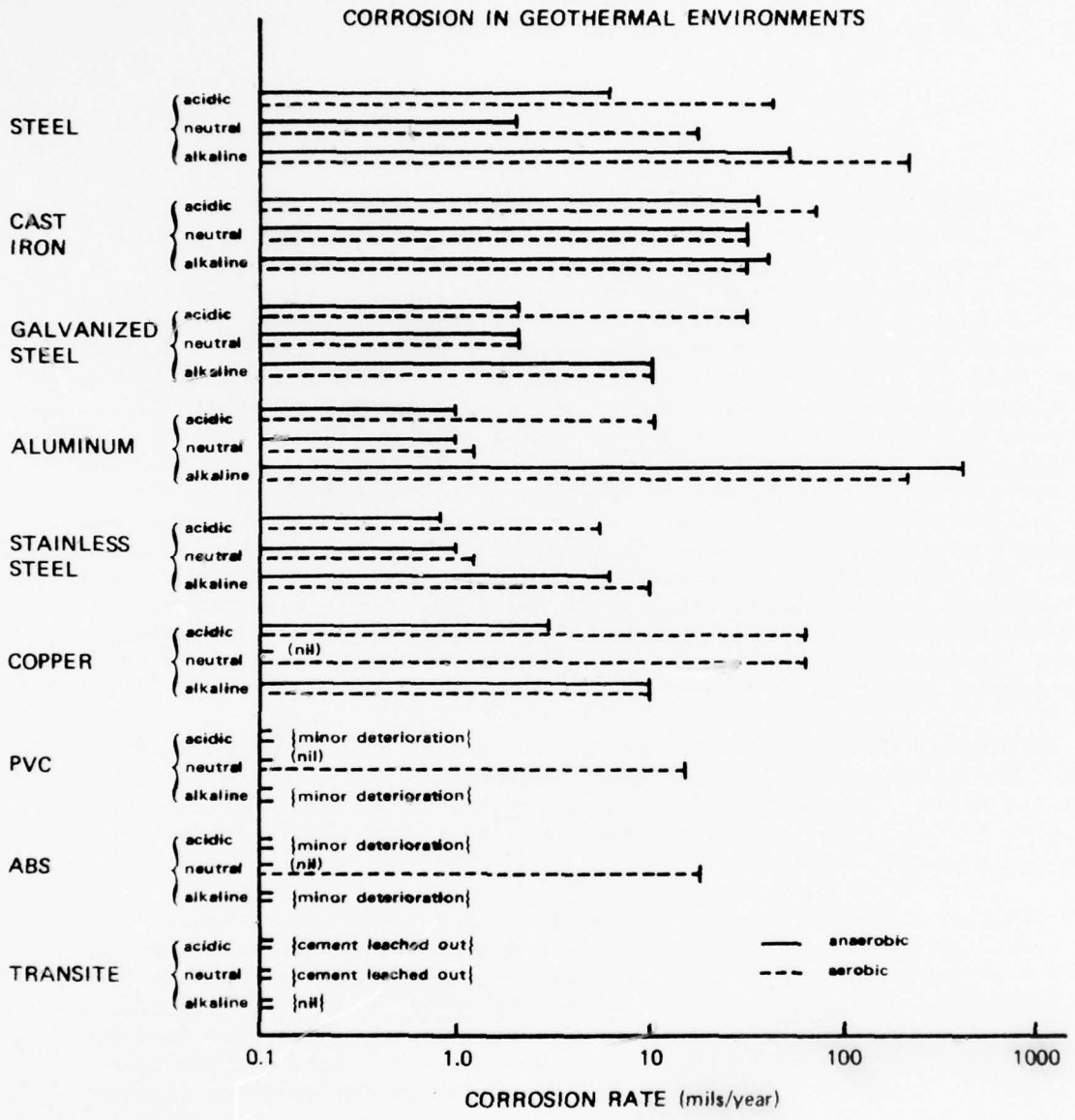

FIGURE 36. A Comparison of Corrosion Rates for Various Materials in Three Geothermal Fluids Found at the Coso Thermal Area.

Chloride ions are known to influence the characteristics of oxide coatings formed on copper, leading to the growth of less protective coverings.[63]

STEEL

The most corrosive anaerobic fluid condition toward the steel was the hot, alkaline water followed by the acid sulfate steam and groundwater steam. This result is probably a valid one as corrosion rates for steel are generally greater in an oxygenated fluid, in the absence of protective films,[26] and the alkaline fluid, as pumped from the ground, was found to contain an appreciable amount of dissolved oxygen. Within a pH range of 4 to 10, the rate of reduction of oxygen at cathodic areas is a principal factor in determining the corrosion rate of steel. The considerable amount of chloride ions in the alkaline fluids tend to readily break down any passivating or protective film formed on the steel allowing corrosion to proceed at nearly a linear rate with time. Corrosion rates in steel, where protective coatings are absent or have been broken down, tend to increase with flow velocity in fluids containing oxidizers, although trace amounts of oxygen in very dilute acids or larger amounts in more concentrated acids are found to increase cathodic polarization and inhibit corrosion within a small range of flow velocities. Corrosion rates also increase continuously with temperature if the system is closed to prevent oxygen from escaping.

The corrosion rate in the acid sulfate steam environment measured about 6 mils/year, which was slightly higher than the rate found in the diluted steam. A somewhat higher rate for the former would be expected in view of the slightly greater level of acidity and higher concentration of hydrogen sulfide.

The rate of reduction of hydrogen ions at cathodic areas generally controls the corrosion rates in steel in nonoxidizing acid environments with a pH less than about 4.[26] Corrosion rates in these situations increase directly with an increase in the degree of cold-working, surface roughness, impurity levels, temperature, or any other mechanism that decreases the hydrogen overvoltage at cathodic areas. The reaction rate is normally insensitive to flow velocity, although the addition of oxidizing agents to the fluid introduces flow dependency.

---

[63] D. J. G. Ives and A. E. Rawson. "Copper Corrosion, IV, The Effect of Saline Additions," *Electrochem Soc, J*, Vol. 109, No. 6 (June 1962), pp. 462-66.

The absence of strongly acid conditions in the groundwater-diluted steam, combined with a very low concentration of oxygen, other oxidizers, and hydrogen sulfide results in a very low rate of corrosion in the steel. Increased levels of corrosion in the presence of the acid sulfate steam, which contained virtually no oxygen but substantially more hydrogen sulfide may be accounted for partly by added quantities of the latter and possible additions of oxidizing ferric ions. Both of the steam conditions were judged to be very dilute acids and as a result, infusion of hydrogen into the steel was not expected to be significant.

The localized form of corrosion that appeared in all the specimens may be typical in these fluid environments. The characteristics of the sulfide deposits formed by the acid fluids may be largely responsible for establishing a pitting mode of corrosion. In the alkaline fluid, chloride ions promote this type of corrosion.[5] Pitting in steel commonly initiates at sulfide inclusions.[24] Maximum corrosion rates averaged less than about 50 mils/year for the samples tested, which is a satisfactory rate for many noncritical applications.[26]

The aerated, alkaline fluid was tentatively judged to be the most corrosive of the environments toward the steel, followed again by the acid-sulfate steam and groundwater-diluted steam. This result is predicated on the successful extrapolation of the pitting corrosion data from the alkaline fluid test conditions, which may not be valid. However, since the maximum pitting depth was about the same for a 10-week period in the alkaline fluid, as the maximum channel depth was for a one-year test period in the acid-sulfate steam, it seemed likely that some additional enlargement of the pits would occur over the next 42 weeks, particularly for the large ones that appeared to have become autocatalytic. If the extrapolation was correct, perforation of the steel would have occurred in about one year.

The principal cathodic reaction in all three fluids should be the reduction of oxygen. A possible alternate or additional cathode reaction would be the reduction of ferric ions. The dissolution rate of metal inside of an individual pit in steel exposed to a chloride-rich fluid is increased as chloride ions migrate to these anodic areas and combine with the ferrous ions to form ferrous chlorides that, in turn, hydrolyze to form hydrochloric acid. Hydrogen and chloride ions both act to increase the dissolution rate of the metal.[5] The corrosion rate of steel in an open, aerated fluid is generally a maximum at about 80°C[8] which may explain the presence of the larger pits at the downstream end of the open channel only, where temperatures averaged about 77°C.

The development of the deep, corrosion channel in the steel when exposed to the acid-sulfate fluid might have resulted simply from the formation of cathodic areas near the water line, where oxygen would be more abundant, and anodic areas at the bottom of the condensate channel where oxygen would be more sparse. A sluggish motion or pooling of the

condensate in the open channel due to the presence of precipitate barriers would also allow for additional acidification of the fluids as noted in standing pools of water on the ground within this region, and a subsequent increase in the rate of corrosion, although highly acid fluids tend to result in soluble corrosion products[31] which were not observable in this situation. Corrosion rates within the condensate channel would be diffusion-controlled as a result of the thick covering of corrosion products and should be lower than those in the alkaline fluid where the corrosion products are not as protective. For the acid steam environments, corrosion rates within the condensate channel appear to correlate with the degree of acidity of the fluid, although since the fluid chemistries are not precisely known, the presence of additional oxidizers such as ferric ions in solution may also contribute to a higher rate of corrosion in the more acid environment.

CAST IRON

No significant difference was observed in the corrosion rate of cast iron in the three anaerobic fluid environments. Measuring errors as a result of the inherent roughness of these surfaces may have partly (or entirely) accounted for these results. However, a close inspection of the surfaces indicated that some of the irregularities that appear to follow flow patterns may have been due to corrosion processes and not to casting conditions. The presence of thin, uneven coatings of iron oxides and sulfides on the surface of the metal, and uneven removal of the protective coating of tar may have combined to produce very uneven corrosion of the specimens. Graphite flakes and iron carbides within the cast iron plus magnetite and iron sulfide deposits on the surface can all be noble to iron and form galvanic cells with it.[25]

Corrosion rates in the open, aerated cast iron pipes were similar to those measured for the closed ones, although the appearance of the surface was quite different on various specimens. Excluding the graphitized zone found in the specimen exposed to the acid sulfate steam (which clearly needs additional study), average rates were less than 50 mils/year. This is stated to be an upper bound for materials that are used in noncritical applications, e.t., tanks, piping, etc.[26] For critical parts, e.g., impellors, springs, etc., a rate of 5 mils/year or less is advised.

GALVANIZED STEEL

Corrosion rates in all three anaerobic fluids appeared to be similar. Corrosion was essentially confined to the zinc coating in all conditions while the steel underneath showed no significant deterioration. Based on these results, the useful life of a steel pipe in these three environments would appear to be extended by about one year or more

with the addition of a zinc coating no more than 0.050 mm thick on the steel.

The most corrosive aerated fluid condition, based on measurements, was probably the acid sulfate fluid due to the apparent potential reversal of the zinc coating with respect to the steel. The pitting rate in the steel, however, was only about 28 mils/year in this situation. Projecting this rate into the future might not be prudent for reasons discussed earlier. Over longer periods of time, the specimen exposed to the alkaline fluid would be expected to be the most severely corroded. Once the sacrificial coating of zinc was gone in a year or so, pitting corrosion of the steel would be expected to initiate.

The open pipe exposed to the diluted steam generally showed the least amount of deterioration. Corrosion was confined entirely to the zinc. This specimen would normally have been expected to corrode in a similar or worse fashion than the one exposed to the acid sulfate steam. For one thing, sulfate ions normally suppress the potential reversal associated with the high-temperature oxide coating that forms on the zinc.[26] The concentration of this ion should have been higher in the acid sulfate steam. Either a sufficient quantity of chloride ions was present in the diluted steam to suppress the reversal (which is possible since chloride ions were discovered in one sample of corrosion products taken from a copper pipe exposed to this fluid), or else the presence of the unknown iron sulfide-oxide deposit found in this steam influenced the corrosion process in some inexplicable fashion.

ALUMINUM

The anaerobic alkaline fluid was clearly the most corrosive toward the aluminum. The specimen exposed to this condition would probably have perforated in about a 20-week period of time. In contrast, the samples exposed to the acid steams deteriorated at a very low rate (1 mil/year).

Pitting corrosion of aluminum in the alkaline fluid may have been initiated at sites where ferric ions, which were being carried in solution, had plated out. Aluminum is sensitive to pitting corrosion in oxygenated chloride solutions containing heavy metal ions.[26] The presence of a heavy deposit of clay minerals on the floor of the pipe in this situation could also have resulted in the formation of local differential aeration cells. This alkaline fluid appeared to contain appreciable amounts of dissolved oxygen, based on the number of oxide coatings found on the inside surfaces of closed specimens exposed to this environment. The pitting corrosion reaction is probably the same as described for the aerated steel pipe exposed to this fluid, involving the formation of hydrochloride acid within the pit and the reduction of oxygen and possibly ferric ions around the periphery, although the

nature of the fluid within the aluminum pit has been a subject of debate.[58]

Very slight pitting corrosion was observed on the samples exposed to the anaerobic acid steam conditions. When aluminum corrodes in an acid environment, hydrogen is believed to evolve at both anodic and cathodic areas.[26] The formation of hydrogen at anodes may be responsible for increased localized corrosion. Aluminum is amphoteric and corrodes in acid and basic solutions. However, the corrosion rate within a pH range of 4.5 to 7 at elevated temperatures is generally quite low in the absence of the heavy ions of copper and iron, mercury or its salts, and chloride ions. Aluminum does not appear to react with hydrogen sulfide.[64]

The aerated, alkaline fluid caused severe pitting corrosion and associated cracking of the open aluminum pipe. This specimen would have probably failed in about one year. The mechanism of corrosion was generally the same as discussed for the anaerobic fluid condition, except that the shape of the pits was more irregular and the fluid chemistry was slightly different (fewer chloride ions and generally more oxygen).

Slight pitting corrosion was also found on the specimens exposed to the aerated acid steam conditions although the corrosion rate again was quite low (1 mil/year). The cathodic reactions in these situations consist primarily of the reduction of oxygen. The deposition of a layer of ferric oxides on the downstream walls of the pipe in the acid sulfate steam environment resulted in pitting corrosion in these areas (up to 12 mils/year). Whether the oxide coating served as a cathode or simply initiated differential aeration conditons was not established.

STAINLESS STEEL

The anaerobic alkaline fluid was slightly more corrosive than the other fluids, although corrosion rates were very low (less than 6 mils/year) in all situations. The grain boundaries were attacked preferentially in all three samples. In addition, minor amounts of pitting were found in the sample exposed to the alkaline fluid. Pitting corrosion is common in this stainless steel when exposed to hot aerated sodium chloride solutions[26] and occurs by the same mechanism as described for the aerated aluminum and steel specimens.[58]

The aerated specimens generally corroded at about the same rate as the closed ones, and in the same fashion. In addition, intergranular

---

[64] I. L. Rozenfeld. *Atmospheric Corrosion of Metals*, Houston, National Association of Corrosion Engineers, 1972.

corrosion near a weld was found in the sample exposed to the acid sulfate steam, while transgranular stress corrosion cracking was found on the upper surface of the specimen exposed to alkaline water where the material had been cut open. Intergranular corrosion is caused if the material is sensitized during welding and not properly heat-treated afterward. Post welding treatment involves heating the sample to 1050° - 1100°C, followed by rapid cooling.[26] Stress corrosion cracking in austenitic stainless steel can be eliminated by protecting it cathodically, eliminating chloride ions in acid media or oxidizers in neutral media, and by avoiding high concentrations of hydroxyl ions.

COPPER

Corrosion rates were generally quite low (less than 10 mils/year) in all three anaerobic fluid conditions. The alkaline water resulted in the highest rate due to the presence of dissolved oxygen in the fluid. Corrosion was by pitting in this instance; a consequence perhaps of defective cuprous oxide corrosion products which are cathodic to copper[8] combined with the sodium chloride solution that served as a good electrolyte.[63,65] Also, the mixture of oxide and sulfide corrosion products found in this instance is believed to result in a less protective coating than one composed entirely of the former.[66]

The anaerobic acid sulfate fluid caused intergranular corrosion of the surface layers of the copper tubing plus a slight amount of uniform corrosion. The reactions that caused intergranular attack and also resulted in the formation of insoluble copper sulfides on the surface of the metal, in this instance, have not been definitely established as the fluid chemistry is not precisely known. A direct reaction between hydrogen sulfide and copper in the absence of oxidizers seems to be very slow.[35] The reduction of ferric ions at cathodic areas would result in the dissolution of copper. Dissolved copper would then combine with sulfuric acid to form soluble cupric sulfates.[30, vol. 3] These, in turn, readily react with hydrogen sulfide to precipitate cupric sulfides. Once the film of corrosion products is established, corrosion rates become diffusion-dependent. This coating is noble to copper and could form a galvanic cell with it.[25] Intergranular corrosion needs to be studied in more detail.

---

[65] M. F. Obrecht and M. Pourbaix. "Corrosion of Metals in Potable Water Systems," in *Proceedings of Third International Congress on Metallic Corrosion, Moscow, 1966, Vol. 4* (Moscow, 1969), pp. 228-45.

[66] J. F. Bates and J. M. Popplewell. "Corrosion of Condenser Tube Alloys in Sulfide Contaminated Brine," *Corrosion*, Vol. 31, No. 8 (August 1975), pp. 269-75.

The copper specimen exposed to the anaerobic diluted acid steam was not appreciably attacked. The corrosion rate was estimated to be less than 1 mil/year. The aerated, acid sulfate steam was the most corrosive fluid toward the copper resulting in perforation of the walls of the tube at the upstream end, and pitting corrosion of the floor, particularly at the downstream end. Corrosion rates greater than 63 mils/year were found where perforation had taken place.

Somewhat lower corrosion rates were measured on the sample exposed to the diluted acid steam, although the exterior portions of the walls were severely corroded. Corrosion was generally by pitting attack. The lowest rate was measured on the specimen exposed to the alkaline fluid. Copper is fairly resistant to corrosion by quiescent or low velocity (less than 1 metre/second) saline waters.[26,39] Resistance is predicated on the formation of insoluble oxide films that reduce the flow of oxygen to the surface of the metal. Highly acid fluids prevent the formation of protective oxide coatings leading to an accelerated rate of attack.[31]

PVC PLASTIC

It was difficult to compare results for the plastic specimens as variations in material quality may have accounted for most of the observed differences, and not the fluid environments themselves. The PVC plastic was not expected to be particularly sensitive to any of the fluids in which it was tested. Deterioration of the material should result largely from elevated temperatures that caused softening, loss of volatile additives, and formation of hydrogen chloride gases. Temperatures were expected to be substantially identical in all three fluid systems, and so these effects would be similar. Exposure to sunshine would also result in photooxidation damage by ultraviolet radiation. The major damage that the fluids themselves could cause would be due to mechanical abrasion, e.g., erosion by solid particles and water droplets, plus cavitation processes.

The specimen exposed to the anaerobic acid sulfate fluid showed severe blistering on the inner surface. The wall itself was found to contain numerous voids, apparently caused by the formation of some gas, internally. Samples tested in the other environments showed no such effect although all showed discoloration along the inner portion of the wall and an undetermined amount of embrittlement due to some loss of additives. Blistering may have resulted from the volatilization of excess, unreacted monomer in this particular sample. No significant amount of surface erosion was observed in any of the samples.

Aerated specimens all showed some softening of the material at the upstream end, resulting in an outward spreading of the walls in this area. Effects rapidly diminished toward the downstream end. Some embrittlement of the material appeared to have taken place in all of the

samples. Erosion of the floor within the condensate channel was noticed at the upstream end of the sample exposed to the diluted acid steam caused by the precipitation of iron oxidation products from the steam in this area that scoured the surface as they were swept downstream by the exiting steam jet.

Severe blistering was found at the upstream end of the specimen exposed to the aerated acid sulfate steam. Its origin remains unknown, but may be explained also as due to the presence of unreacted monomer in the structure.

This plastic should probably not be used in an acid sulfate environment until the origin of the blisters can be established. Thermal softening effects may also limit its usefulness in high-pressure, high-temperature environments.

ABS PLASTIC

Those exposed to anaerobic fluids all showed possible oxidation damage to the interior surface and an undetermined amount of embrittlement. No measurable amount of erosion damage to the inside surfaces was observed. The specimen exposed to the diluted acid steam contained numerous tiny blisters on the interior surface that appeared to be the result of the formation of gas within the wall. Depolymerization of styrene could account for this effect. The inner portion of the wall was also slightly bleached on this occasion.

The aerated samples all showed some spreading of the walls at the upstream end as a result of thermal softening of the material. Thermal effects were generally less severe than observed for the PVC plastic. The specimen exposed to the diluted acid steam showed some blistering at the upstream end along with minor crazing of the upper walls. A narrow erosion channel on the floor of the pipe was found in this area that was formed in the same fashion as on the PVC pipe.

This plastic needs additional testing to establish the origin of the blisters. Although thermal degradation was less than on the PVC material, its use in higher pressure geothermal environments may be limited.

TRANSITE

As transite consists of a matrix of relatively inert asbestos fibers held together with a cement binder, chemical attack by fluids on the cement was expected to be the primary damage mechanism, followed by mechanical abrasion damage to the weakened structure by the high-velocity steam jet. Chemical leaching of cement to a depth of about 1 mm was observed on all inside surfaces of the specimen exposed to the acid sulfate

fluid. Similar damage to a depth of about 0.5 mm was found on the specimen exposed to the diluted acid steam, while the sample exposed to the alkaline fluid showed no damage. Erosion damage appeared to be minor on all samples, although loose asbestos fibers were found in scattered areas on the floor of the open channels exposed to the acid steam conditions. Damage due to leaching was often deceptive, as the surfaces appeared to be undamaged when viewed with the unaided eye.

This material might also be subject to damage by thermal shock due to its relatively poor conductivity, limiting the usefulness in application where thermal gradients are large or temperatures cyclical.

MATERIAL SELECTION AT COSO THERMAL AREA

As a result of this study, low carbon steel, galvanized steel, gray cast iron, 304 stainless steel, transite, and possibly copper were found to be suitable for handling (internally) the low pressure, low velocity, anaerobic acid-sulfate and groundwater diluted steam conditions found at the Coso Thermal Area, assuming they were not subject to external tensile stresses, cyclic loads (also thermal cycling), or else coupled to other materials or to each other. The study did not attempt to examine such considerations as galvanic or coupling effects between these materials, their susceptibility to stress corrosion, corrosion fatigue, or fretting corrosion, all of which may have an important bearing on the ultimate usefulness of these materials in geothermal environments. For example,

(1) Aluminum and copper alloys are subject to stress corrosion cracking when embrittled by mercury.[16,26]

(2) Steel is subject to stress corrosion cracking in acid fluids, particularly those containing hydrogen sulfide.[2]

(3) Corrosion fatigue is generally related to the metal's corrosion resistance rather than to its strength.[26] The concept of a fatigue limit, below which failure does not occur, doesn't apply when the material is exposed to a corrosive medium. The damage tends to be synergistic, i.e., is greater than that from corrosion or fatigue acting separately.

(4) The presence of cupric or ferric cations in the fluids can initiate pitting corrosion in aluminum.[26]

(5) Coupling PVC to zinc can result in dechlorination of the former due to a reaction between chlorine and zinc.

Steel, galvanized steel, gray cast iron, stainless steel, and transite were found to be generally resistant to external condensates and noncondensible gases found in these two steam environments, assuming the condensates were not allowed to form pools of water in contact with the material, or else permeate a porous structure (like wood) that was in contact with the material. None of the materials was tested while buried in the ground, and in view of the moist acid or alkaline soil conditions

in these locations, external corrosion to the metals would, in general, be expected to be severe. Leaching of the cement binder in the transite should be rapid in a highly acid environment, while its behavior in an alkaline soil appears at present to be less predictable.

If metals were to be buried, they would have to be coated with an inert impermeable substance and/or possibly also be protected by a galvanic couple (either using a sacrificial anode, or external current source). The plastics tested should be more suitable for burial in these soil conditions than the metals. However, in view of their behavior in the test fluids, their longevity under these environments cannot be predicted based on the data obtained to date. Stress cracking and embrittlement of plastic pipes in geothermal environments have been observed.[2]

If steel in a stressed condition is used in an anaerobic acid fluid thermal environment containing hydrogen sulfide, the probability of stress corrosion cracking can be lowered by reducing the strength of the material. Recommendations have been made to keep strength levels for carbon and low-alloy steels below about $6.06 \times 10^8 N/m^2$ and below 7.58×10^8 to $8.28 \times 10^8 N/m^2$ for high chromium steels in these circumstances.[2] Higher strength steels may possibly be tolerated for steam conditions but are not suitable for carrying cold, geothermal condensates as delayed fracture has been observed under this condition. Hydrogen sulfide can generally be removed by aeration. However, the oxidizers and oxidation products present a new set of corrosion conditions that can be equally troublesome.

The cast iron, aluminum, stainless steel, and transite appeared to be generally suitable for use in the aerated acid sulfate and diluted steam conditions, assuming the absence of coupling and stress conditions as discussed for the anaerobic fluid conditions. The steel and galvanized steel might be suitable in the aerated diluted steam but were judged unsuitable for handling aerated acid-sulfate condensates.

Only transite handled the hot aerobic alkaline fluids in a completely satisfactory manner, although galvanized steel, cast iron, copper and stainless steel appeared to be satisfactory within the test period. Steel was also marginally satisfactory. Using any of the materials other than transite in this environment requires careful thought because of dissolved oxygen in the water. The fairly low corrosion rate of copper, for example, is predicated on the retention of the oxide deposit formed on its surface in this environment. Increasing the velocity of the water significantly may loosen this protective coating and increase the corrosion rate.[39] Austenitic stainless steels are subject to both pitting corrosion and stress corrosion cracking in hot water containing chloride ions and dissolved oxygen.[26] Gray cast iron is subject to graphitization over long periods of time in sodium chloride fluids.

The corrosion rate of steel was only marginally satisfactory at 51 mils/year and once the zinc plating was removed, galvanized steel would be expected to corrode at a similar rate. Successful use of the low carbon steels in this fluid condition would require a more protective coating of oxides on the metal than was formed during the brief testing period. Over longer periods of time, the corrosion rate might reduce some as the coating of corrosion products increased in thickness, although thicker coatings are not always more protective.[63] Additional testing is required to study the protectiveness of various thicknesses of oxidation coatings.

The elimination of oxygen from the alkaline fluids would be one way to substantially reduce corrosion rates. It was not established whether the oxygen was present in the water before being pumped from the ground or whether it was introduced into the pumping/distribution installation by leakage from the atmosphere through joints, fittings, or seals. It may be possible to eliminate the oxygen by sealing the installation more tightly. If not, the introduction of oxygen scavengers such as sodium sulfite into the system might effectively reduce or eliminate the undesired oxygen. Treatment with sodium sulfite is effective up to temperatures of about 260°C (4.48×10^6 N/m^2 pressure), where acid decomposition products begin to form.[26]

Removal of sodium chloride by separation techniques would also reduce corrosion rates by eliminating the major contaminant responsible for breaking down passive coatings on metals and initiating pitting corrosion. Salt solutions containing dissolved hydrogen sulfide are also believed to cause severe corrosion fatigue of metals.[2] The presence of sulfide corrosion products in samples exposed to the hot alkaline fluids at the Coso Resort Area demonstrates the presence of hydrogen sulfide in this fluid. Removal of dissolved salts may then extend the fatigue life of materials exposed to this environment.

The transite was the only material that appeared to withstand the aerated hot alkaline fluids in a completely satisfactory fashion. The steel and aluminum were unsatisfactory and the galvanized steel would become so after the zinc plating was dissolved away. The stainless steel was subject to stress corrosion cracking along its upper edge and also pitting corrosion above the water line. The copper and cast iron seemed to perform well during the test period, although over larger periods of time, both materials may suffer deterioration from causes mentioned previously.

In general, hot, aerated salt solutions are one of the more corrosive environments toward ordinary metallic construction materials. Exterior surfaces exposed to aerated salt sprays can be rapidly corroded in the case of iron and steel, or else may fail by stress corrosion cracking, in the case of the austenitic stainless steels.[2] Aluminum alloys may suffer both modes of attack, particularly the 2,000 and 7,000

series of precipitation hardening alloys.[67] A few additional comments can be advanced about material useage in geothermal environments. These are mostly taken from reference 2, which is an excellent source of information on this subject as are the other articles in the same publication.

At higher pressures and flow velocities, the wetness of the steam becomes an important consideration when using materials that are subject to erosion-corrosion damage. For example, steam with a wetness of 20 to 30 percent can severely damage well casings.[68] To prevent excess erosion of turbine blades, an upper limit of 9% wetness and 274 m/s operating speed is recommended.[2]

The pressure of hot, aerated thermal groundwater in contact with the casing at the wellhead can result in severe corrosion. The use of multiple casings at the surface and careful grouting of the spaces between provides protection in this circumstance.[2] Thermal expansion of pipelines can produce significant stresses resulting in stress corrosion cracking of materials such as stainless steels that are exposed additionally to hot salt sprays.

Installations that are shut down for long periods of time may suffer corrosion from pools of water remaining in pipelines and other containers that mix with air leaking in from the atmosphere. Systems should be either drained of water or else allowed to remain filled with steam to prevent admittance of atmospheric oxygen.[2]

The corrosiveness of cooling tower water appears to depend largely on the ratio of ammonia to hydrogen sulfide in the fluids.[2] The pH of these fluids in existing geothermal plants ranges from about 3 to 7. The choice of materials for use in a geothermal cooling tower should be based on prior experiments that have determined the fluid chemistry in this location.

The use of mechanical/electrical instruments in geothermal environments should be done with care. For example, steel or copper alloy springs are subject to stress corrosion cracking and may have to be replaced.[2] Silver or copper electrical contacts tarnish in hydrogen sulfide atmospheres in which case more noble metals (gold, platinum) may have to be used instead.

---

[67] Markus O. Speidel. "Stress Corrosion Cracking of Aluminum Alloy," *Met Trans A*, Vol. 6A, No. 4 (April 1975), pp. 631-51.

[68] Keiji Matsuo. "Drilling for Geothermal Steam and Hot Water," *Geothermal Energy (Earth Sciences, 12)*, UNESCO, Paris (1973), pp. 73-83.

SUMMARY AND CONCLUSIONS

Reported here are results from a preliminary testing program on corrosion of selected engineering materials in various geothermal environments. Samples of nine different types of commercial pipe were exposed up to one year to three different geothermal fluids under anaerobic and aerobic conditions. The resulting corrosions were then examined by several techniques including ordinary microscopy, scanning electron microscopy and x-ray diffraction. Results were documented by a series of photographs, many of which are included in this report. A comprehensive summary of observed corrosion rates is presented graphically (Figure 36).

The wealth of information obtained in this investigation is pertinent to the local geothermal situation (as for a possible geothermal power plant), but also can be very useful for many other geothermal areas. Two general conclusions reached during this study are:

(1) Geothermal corrosion is highly specific and depends greatly on the nature of the engineering materials involved, on the nature of the geothermal fluid, and on the conditions of exposure.

(2) It appears quite possible that such geothermal corrosion problems can well be combatted by proper choice of materials and conditions. However, considerable additional experimental testing and further theoretical studies are needed in order to obtain reliable information suitable for engineering design purposes.

RECOMMENDATIONS

Future work should include the following:

(1) Detailed analyses of fluid chemistries, including anions, cations and gases present.

(2) Analyses for other toxic metals, including arsenic, antimony, lead, and cadmium.

(3) Additional study of the cast iron to establish corrosion modes and rates more accurately, and to examine the graphitization mechanism in more detail.

(4) Further analysis of the unknown iron sulfide compound found in the diluted acid steam environment and its influence on corrosion processes.

(5) Study of additional materials in these environments, particularly those with inert or sacrificial coatings.

(6) Study of chemical inhibitors and scavengers for use in geothermal environments.

(7) Study of materials, as by potentiostatic methods, under controlled laboratory conditions using synthetic and natural geothermal fluids.

(8) Study of materials under loads to establish threshold conditions for initiation of stress corrosion cracking.

(9) Analyses of "plumber's nightmare" galvanic corrosion test specimens.

ACKNOWLEDGEMENT

Acknowledgement is gratefully made to Kenneth Graham of the Navy Postgraduate School at Monterey for performing the scanning electron microscopy, x-ray fluorescence analysis, and atomic absorption spectroscopy. Recognition is also extended to J. Kenneth Pringle of the Detonation Physics Division for consultations and providing the author with information on x-ray diffraction procedures used in establishing the identity of corrosion products.

REFERENCES

1. Lawrence Livermore Laboratory. *Possibilities for Controlling Heavy Metal Sulfides in Scale From Geothermal Brines*, by D. D. Jackson and John H. Hill. Livermore, Calif., 19 January 1976. (UCRL-51977, publication UNCLASSIFIED.)

2. T. Marshall and W. R. Braithwaite. "Corrosion Control in Geothermal Systems," *Geothermal Energy (Earth Sciences, 12)*, UNESCO, Paris (1973), pp. 151-60.

3. Bureau of Mines. *Corrosion Resistance of Metals in Hot Brines: A Literature Review*, by Lloyd H. Banning and Laurance L. Oden. Washington, D.C., August 1973. (BuMines IC 8601, publication UNCLASSIfied.)

4. Idaho National Engineering Laboratory, ERDA. *Corrosion Engineering in the Utilization of the Raft River Geothermal Resource*, by Richard L. Miller. Idaho Falls, Idaho, August 1976. (ANCR-1342, publication UNCLASSIFIED.)

5. Mars D. Fontana and Norbert D. Greene. *Corrosion Engineering*. New York, McGraw-Hill, 1967.

6. J. A. Collins. "Effect of Design, Fabrication and Installation on the Performance of Stainless Steel Equipment," *Corrosion*, Vol. 11 (1955), pp. 11t-18t.

7. C. M. Hudgins, and others. "Hydrogen Sulfide Cracking of Carbon and Alloy Steels," *Corrosion*, Vol. 22 (August 1966), p. 238.

8. G. Butler and H. C. K. Ison. *Corrosion and Its Prevention in Waters*. New York, Reinhold Publishing Corp., 1966.

9. R. S. Bolton. "Management of a Geothermal Field," *Geothermal Energy (Earth Sciences, 12)*, UNESCO, Paris (1973), pp. 175-84.

10. E. Tolivia. "Corrosion Measurements in a Geothermal Environment," *Geothermics*, Special Issue 2, Vol. 2, Part 2, Pisa, Italy (Sept. 1970). United Nations, New York, pp. 1596-1601.

11. Donald E. White. "Thermal Waters of Volcanic Origin," *Bulletin of the Geologic Society of America*, Vol. 68 (Dec. 1957), pp. 1637-57.

12. Naval Weapons Center. *Geologic Investigations at the Coso Thermal Area*, by Carl F. Austin and J. Kenneth Pringle. China Lake, Calif., NWC, June 1970. (NWC TP 4879, publication UNCLASSIFIED.)

13. Bureau of Mines. *Bucket-Drilling the Coso Mercury Deposit, Inyo County, California,* by Leon W. Dupuy. Washington, D.C., 1948. (BuMines Report Invest. 4201, publication UNCLASSIFIED.)

14. Thomas D. Brock, and Jerry L. Mosser. "Rate of Sulfuric-Acid Production in Yellowstone National Park," *Bulletin of the Geological Society of America,* Vol. 86 (February 1975), pp. 194-8.

15. Thomas D. Brock, and others. "Biogeochemistry and Bacteriology of Ferrous Iron Oxidation in Geothermal Habits," *Geochimica et Cosmochimica Acta,* Vol. 40 (1976), pp. 493-500.

16. R. J. H. Wanhill. "Cleavage of Aluminum Alloys in Liquid Mercury," *Corrosion,* Vol. 30 (October 1974), pp. 371-8.

17. C. F. Austin and J. K. Pringle. "Geothermal Corrosion Studies at the Naval Weapons Center," University of Michigan, Ann Arbor, Mich., July 1974. *Preliminary Reports, Memoranda and Technical Notes of the Materials Research Council Summer Conference, La Jolla, Calif.* (ARPA Report 005020, publication UNCLASSIFIED.)

18. C. J. Cron, J. H. Payer, and R. W. Staehle. "Dissolution Behavior of Fe-Fe_3C Structures as a Function of pH, Potential, and Anion - An Electron Microscope Study," *Corrosion,* Vol. 27 (January 1971), pp. 1-25.

19. J. S. Smith and J. D. A. Miller. "Nature of Sulphides and Their Corrosive Effect on Ferrous Metals: A Review," *Brit Corrosion J,* Vol. 10, No. 3 (1975), pp. 136-43.

20. R. T. Foley. "Complex Ions and Corrosion," *Electrochem Soc J,* Vol. 122, No. 11 (November 1975), pp. 1493-94.

21. E. C. Greco and J. B. Sardisco. "Reaction Mechanisms of Iron and Steel in Hydrogen Sulfide," Proceedings of the Third International Congress on Metallic Corrosion, Moscow, 1966. Vol. 1 (1969), pp. 130-8.

22. S. E. Traubenberg and R. T. Foley. "The Influence of Chloride and Sulfate Ions on the Corrosion of Iron in Sulfuric Acid," *Electrochem Soc J,* Vol. 118, No. 7 (July 1971), pp. 1066-70.

23. R. Bartonicek. "Corrosion of Steel in Solutions of Chlorides and Sulphides," Proceedings of the Third International Congress on Metallic Corrosion, Moscow, 1966, Vol. 1 (1969), pp. 119-29.

24. Gösta Wrangleń. "Electrochemical Properties of Sulfides in Steel and the Role of Sulfides in the Initiation of Corrosion," *Sulfide Inclusions in Steel,* American Society for Metals, Metals Park, Ohio (1975), pp. 361-79.

25. Gösta Wrangleń. *An Introduction to Corrosion and Protection of Metals.* New York, Halsted Press, 1972.

26. Herbert H. Uhlig. *Corrosion and Corrosion Control.* New York, John Wiley and Sons, 1971.

27. Asahi Kawashima, Koji Hashimoto, and Saburo Shimodaira. "Hydrogen Electrode Reaction and Hydrogen Embrittlement of Mild Steel in Hydrogen Sulfide Solutions," *Corrosion,* Vol. 32, No. 8 (August 1976) pp. 321-31.

28. P. K. Foster, T. Marshall, and A. Tombs. "Corrosion Investigations in Hydrothermal Media at Wairakei, New Zealand," *UN Conference on New Sources of Energy,* Rome, 1961. United Nations, N.Y. (E/Conf. 35G47).

29. *Gray and Ductile Iron Castings Handbook,* ed. by C. F. Walton. Cleveland, Ohio, The Gray and Ductile Iron Founders' Soc., Inc., 1971.

30. J. W. Mellor. *A Comprehensive Treatise on Inorganic and Theoretical Chemistry* (16 volumes). New York, Longmans Green and Company, published 1922-1937.

31. Marcel Pourbaix. *Atlas of Electrochemical Equibria in Aqueous Solutions.* New York, Pergamon Press, 1966.

32. P. T. Gilbert. "The Nature of Zinc Corrosion Products," *Electrochem Soc, J,* Vol. 99, No. 1 (January 1952), pp. 16-19.

33. G. R. Foster, S. G. Lee, and J. R. Myers. "Stress Corrosion of Eta-Phase, Hot-Dip-Zinc Alloy in Potable Hot Water," *Corrosion,* Vol. 30, No. 7 (July 1974), pp. 239-41.

34. A. Joshi and D. F. Stein. "Chemistry of Grain Boundaries and Its Relation to Intergranular Corrosion of Austenitic Stainless Steel," *Corrosion,* Vol. 28, No. 9 (September 1972), pp. 321-30.

35. Per Backlund. "The Influence of Oxygen Pressure on the Reaction of Hydrogen Sulphide With Copper," *Acta Chemica Scandinavica,* Vol. 23, No. 5 (1969), pp. 1541-52.

36. A. Etienne. "Electrochemical Method to Measure the Copper Ionic Diffusivity in a Copper Sulfide Scale," *Electrochem Soc, J,* Vol. 117, No. 7 (July 1970), pp. 870-4.

37. Eugene H. Rosenbloom. "An Investigation of the System Cu-S and Some Natural Copper Sulfides Between 25° and 700°C," *Econ Geol,* Vol. 61, No. 4 (June 1966), pp. 641-71.

38. Nobuo Morimoto and Kichiro Koto. "Phase Relations of the Cu-S System at Low Temperatures: Stability of Anilite," *Amer Mineral*, Vol. 55 (January 1970), pp. 106-17.

39. *Metals Handbook*, 8th ed., Vol. 1, Taylor Lyman, ed. Metals Park, Ohio, American Society for Metals, 1961.

40. George Fowles. "Basic Copper Sulfates," *J Chem Soc*, (1926), pp. 1845-58.

41. Motoaki Sato. "Oxidation of Sulfide Ore Bodies, II. Oxidation Mechanisms of Sulfide Minerals at 25°C," *Econ Geol*, Vol. 55 (1960), pp. 1202-31.

42. University of California. *Mercury and Antimony Deposits Associated With Active Hot Springs in the Western United States*, by Frank W. Dickson and George Tunnell. Los Angeles, 1967. (Institute of Geophysics and Planetary Physics, Publication No. 568.)

43. Marcel Pourbaix. "Some Applications of Potential-pH Diagrams to the Study of Localized Corrosion," *Electrochem Soc, J*, Vol. 123, No. 2 (February 1976), pp. 25c-36c.

44. A. Palma and M. Carenza. "Degradation of Poly(vinyl chloride) 1. Kinetics of Thermal and Radiation-Induced Dehydrochlorination Reactions at Low Temperatures," *J Appl Polymer Sci*, Vol. 14, No. 7 (1970), pp. 1737-54.

45. H. H. G. Jellinek, F. Flajsman and F. J. Kryman. "Reaction of SO_2 and NO_2 With Polymers," *J Appl Polymer Sci*, Vol. 13, No. 1 (1969), pp. 107-16.

46. H. A. Stuart. "Physical Causes of Aging in Plastics," *Angew Chem, Intern Ed*, Vol. 6, No. 10 (1976), pp. 844-51.

47. J. Shimada and K. Kabuki. "The Mechanism of Oxidative Degradation of ABS Resin, Part I. The Mechanism of Thermooxidative Degradation," *J Appl Polymer Sci*, Vol. 12 (1968), pp. 655-69.

48. J. Shimada and K. Kabuki. "The Mechanism of Oxidative Degradation of ABS Resin, Part II. The Mechanism of Thermooxidative Degradation, *J Appl Polymer Sci*, Vol. 12 (1968), pp. 671-82.

49. L. Heller and M. Ben-yair. "Effect of Sulfate Solutions on Normal and Sulphate-Resisting Portland Cement," *J Appl Chem*, Vol. 14 (Jan. 1964), pp. 20-30.

50. S. Takeno, H. Zôka, and T. Niihara. "Metastable Cubic Iron Sulfide - With Special Reference to Mackinawite," *Amer Mineral*, Vol. 55 (September 1970), pp. 1639-49.

51. Robert A. Berner. "Iron Sulfides Formed From Aqueous Solution at Low Temperatures and Atmospheric Pressure," *J Geo*, Vol. 72 (1964) pp. 293-306.

52. *Handbook of Chemistry and Physics*, 47th edition, R. C. Weast, ed. Cleveland, Ohio, The Chemical Rubber Company, 1966.

53. R. Schoen and C. Roberson. "Structures of Aluminum Hydroxide and Geochemical Implications," *Amer Mineral*, Vol. 55 (January 1970), pp. 43-77.

54. J. Bernal, D. Dasgupta and A. Mackay. "The Oxides and Hydroxides of Iron and Their Structural Interrelations," *Clay Minerals Bull*, Vol. 4 (1959), pp. 15-30.

55. R. T. Foley. "Role of the Chloride Ion in Iron Corrosion," *Corrosion*, Vol. 26, No. 2 (February 1970), pp. 58-70.

56. L. M. Dvoracek. "Pitting Corrosion of Steel in H_2S Solutions," *Corrosion*, Vol. 32, No. 2 (February 1976), pp. 64-8.

57. P. R. Rhodes. "Corrosion Mechanisms of Carbon Steel in Aqueous H_2S Solutions," *Electrochem Soc, J*, Vol. 123, No. 8 (August 1976), p. 247c (abstract only).

58. Jose R. Galvele. "Transport Processes and the Mechanism of Pitting of Metals," *Electrochem Soc, J*, Vol. 123, No. 4 (April 1976), pp. 464-74.

59. Z. Szklarska-Smialowska. "Review of Literature on Pitting Corrosion Published Since 1960," *Corrosion*, Vol. 27, No. 6 (June 1971), pp. 223-33.

60. J. Sharkey and S. Lewin. "Conditions Governing the Formation of Atacamite and Paratacamite," *Amer Mineral*, Vol. 56 (January 1971), pp. 179-92.

61. L. Heller and M. Ben-yair. "Effect of Chloride Solutions on Portland Cement," *J Appl Chem*, Vol. 16 (August 1966), pp. 223-26.

62. A. Goldberg and L. Owen. "Pitting Corrosion in Plain Carbon Steel Exposed to Geothermal Brine," *Electrochem Soc, J*, Vol. 123, No. 8 (August 1976), pp. 248c-49c (abstract only).

63. D. J. G. Ives and A. E. Rawson. "Copper Corrosion, IV, The Effect of Saline Additions," *Electrochem Soc, J*, Vol. 109, No. 6 (June 1962), pp. 462-66.

64. I. L. Rozenfeld. *Atmospheric Corrosion of Metals*, Houston, National Association of Corrosion Engineers, 1972.

65. M. F. Obrecht and M. Pourbaix. "Corrosion of Metals in Potable Water Systems," in *Proceedings of the Third International Congress on Metallic Corrosion, Moscow, 1966, Vol. 4* (Moscow, 1969), pp. 228-45.

66. J. F. Bates and J. M. Popplewell. "Corrosion of Condenser Tube Alloys in Sulfide Contaminated Brine," *Corrosion*, Vol. 31, No. 8 (August 1975), pp. 269-75.

67. Markus O. Speidel. "Stress Corrosion Cracking of Aluminum Alloy," *Met Trans A*, Vol. 6A, No. 4 (April 1975), pp. 631-51.

68. Keiji Matsuo. "Drilling for Geothermal Steam and Hot Water," *Geothermal Energy (Earth Sciences, 12)*, UNESCO, Paris (1973), pp. 73-83.

INITIAL DISTRIBUTION

1 Director of Navy Laboratories
4 Naval Air Systems Command
  AIR-30212 (2)
  AIR-954 (2)
7 Chief of Naval Operations
  OP-03E6 (2)
  OP-05 (1)
  OP-098 (1)
  OP-0986, CAPT Fulk (1)
  OP-413
    CDR. R. D. Furiga (1)
    LCDR. R. Owens (1)
4 Chief of Naval Material
  MAT-03 (2)
  MAT-032 (1)
  MAT-03Z, CAPT Vincent M. Skrinak (1)
10 Naval Facilities Engineering Command
  FAC-03, CDR. R. P. Cope (1)
  FAC-032F, Walter Adams (1)
  FAC-044, H. G. Lewis (1)
  FAC-0441, L. V. Irvin, Jr. (1)
  FAC-0442, S. Z. Bryson III (1)
  FAC-09, CAPT W. Daniel (1)
  FAC-09B, CAPT C. Courtright (1)
  FAC-102, CDR. E. J. Peltier, Jr. (1)
  FAC-1023, M. E. Carr (1)
  FAC-203, CDR. E. W. Thomas (1)
1 Naval Facilities Engineering Command, Pacific Division (Utilities Division)
1 Naval Facilities Engineering Command, Western Division, San Bruno (Utilities Division)
5 Naval Sea Systems Command
  SEA-033 (3)
  SEA-09G32 (2)
2 Chief of Naval Research, Arlington
  ONR-102 (1)
  ONR-473 (1)
2 Assistant Secretary of the Navy (Research and Development)
  Dr. P. Waterman, Special Assistant (Energy) (1)
1 Commandant of the Marine Corps
1 Civil Engineering Laboratory, Port Hueneme (Technical Library, Mike Slaminski)

2 Naval Academy, Annapolis
  Library (1)
  Mechanical Engineering Department, *Professor Chin Wu* (1)
2 Naval Postgraduate School, Monterey
1 Naval Research Laboratory
1 Office of Naval Research Branch Office, Boston
1 Office of Naval Research Branch Office, Chicago
1 Office of Naval Research Branch Office, New York
1 Office of Naval Research Branch Office, Pasadena
1 Office of Naval Research Branch Office, San Francisco
1 Headquarters, U. S. Army
1 Headquarters, U. S. Air Force
1 Air Force Academy (Library)
1 Air University Library, Maxwell Air Force Base
2 Assistant Secretary of Defense
  Dr. W. C. Christensen (1)
  RADM W. A. Myers III (1)
12 Defense Documentation Center
1 Assistant Commissioner for Minerals, Anchorage, AK
1 Bureau of Mines, El Centro (Don H. Baker, Jr.)
1 Bureau of Reclamation, Boulder City, NV
1 California Assembly Office of Research, Sacramento, CA
1 California Department of Conservation, Sacramento, CA
1 California Department of Water Resources, Sacramento, CA
1 California Division of Mines and Geology, Sacramento, CA
1 California Energy Resources Conservation and Development Commission, Sacramento, CA
1 California State Land Division, Sacramento, CA
7 Energy Research and Development Administration
  Division of Geothermal Energy (1)
  John A. Belding (1)
  Louis V. Divone (1)
  Martin Gutstein (1)
  George M. Kaplan (1)
  Gerald S. Leighton (1)
  Henry H. Marvin (1)
1 Energy Research and Development Administration, Division of Geothermal Energy, Idaho Operations, Idaho Falls, ID
1 Energy Research and Development Administration, Division of Geothermal Energy, Nevada Operations, Las Vegas, NV
1 Idaho Bureau of Mines and Geology, Moscow, ID
1 National Academy of Engineering, Alexandria, VA (W. F. Searle, Jr.)
1 National Academy of Sciences (Dr. Robert S. Shane, National Materials Advisory Board)
2 Applied Physics Laboratory, Johns Hopkins University, Laurel, MD
1 Associated Universities, Inc., Upton, NY (Brookhaven National Laboratory)
1 Battelle Memorial Institute, Pacific Northwest Laboratory, Richland, WA

1 Case Western Reserve University, Cleveland, OH (Department of Metallurgy and Materials Science)
1 Colorado Energy Research Institute, Golden, CO
1 EG&G Idaho, Inc., Idaho Falls, ID
1 Electric Power Research Institute, Menlo Park, CA
1 Franklin Institute, Philadelphia, PA (Library, Miriam Padusis)
1 Geothermal Energy Institute, New York, NY
1 IIT Research Institute, Chicago, IL (Document Librarian)
1 Jet Propulsion Laboratory, CIT, Pasadena, CA
1 Lawrence Berkeley Laboratory, Berkeley, CA
2 Los Alamos Scientific Laboratory, Los Alamos, NM
  Jacobo R. Archuleta (1)
  Reports Library (1)
1 Massachusetts Institute of Technology, Cambridge, MA (Michael Batzle)
1 Oak Ridge National Laboratory, Oak Ridge, TN
1 Ohio State University, Columbus, OH (Department of Metallurgical Engineering)
1 Oregon State University, Corvallis, OR (Department of Mechanical Engineering)
1 Pennsylvania State University, University Park, PA (Department of Geosciences)
1 Princeton University, Forrestal Campus Library, Princeton, NJ
1 Purdue University, West Lafayette, IN (Library)
1 Sandia Corporation, Albuquerque, NM (Leonard E. Baker)
1 Stanford Corporation, Santa Monica, CA (Technical Library)
1 Stanford Research Institute, Menlo Park, CA (Robert W. Bartlett)
1 Tetra Technology, Inc., Pasadena, CA (J. J. Reed)
1 University of California, Lawrence Radiation Laboratory, Livermore, CA (Metallurgy Division)
1 University of California at Los Angeles, Los Angeles, CA (Prof. Kenneth L. Lee)
1 University of Denver, Denver Research Institute, Denver, CO
1 University of Hawaii, Honolulu, HI
1 University of South Dakota, Vermillion, SD (South Dakota Geological Survey Science Center)
2 University of Southern California Law Center, Los Angeles, CA
  John J. McNamara (1)
  Professor Christopher D. Stone (1)
2 University of Utah, Salt Lake City, UT
  College of Engineering (1)
  Geology and Geophysics Library (1)
1 University of Utah, Research Institute, Salt Lake City, UT
1 University of Utah, Research Institute, Earth Sciences Group, Salt Lake City, UT